DISSERTATION

# MARKERS AND MECHANISMS OF RESISTANCE TO TOCERANIB PHOSPHATE (PALLADIA®) IN CANINE CUTANEOUS MAST CELL TUMOR

Submitted by

Charles H.C. Halsey

Graduate Degree Program in Cell and Molecular Biology

In partial fulfillment of the requirements

For the Degree of Doctor of Philosophy

Colorado State University

Fort Collins, Colorado

Summer 2014

Doctoral Committee:

Advisor: Daniel Gustafson

Douglas Thamm
EJ Ehrhart
Deanna Worley

ABSTRACT

MARKERS AND MECHANISMS OF RESISTANCE TO TOCERANIB PHOSPHATE (PALLADIA®) IN CANINE CUTANEOUS MAST CELL TUMOR

Mast cell tumors (MCTs) are one of the most common skin tumors in dogs, accounting for up to 21% of all canine cutaneous tumors, and exhibit extremely variable biologic behavior. Mutations in the juxtamembrane, kinase and ligand binding domains of the *c-kit* proto-oncogene have been associated with the tumorigenesis of canine MCTs, resulting in growth factor-independent and constitutive phosphorylation of the KIT receptor tyrosine kinase (RTK). Approximately one-third of canine MCTs carry a *c-kit* mutation. As such, small molecule inhibitors of KIT are an attractive therapeutic strategy for MCTs in dogs.

Toceranib (TOC) phosphate (Palladia®) is one such RTK inhibitor of KIT that has biological activity against canine MCTs. Despite its clinical benefit in the treatment of MCT, the vast majority of dogs eventually develop resistance to TOC. Therefore, there is a need to identify distinctive clinical and molecular features of resistance in this population. The overarching hypothesis of this dissertation is that understanding the mechanisms of TOC-resistance in canine MCT will allow us to develop rational second line and combination therapies that will overcome or prevent drug resistance.

In order to begin to study the mechanisms that confer resistant to TOC in canine MCT, TOC-resistant MCT sublines were generated from the *c-kit*-mutant canine C2 mastocytoma cell line. By chronically exposing C2 cells to TOC, three TOC-resistant (TR) sublines were established over a period of seven months and designated TR1, TR2, and TR3. While TOC

inhibited KIT phosphorylation and cell proliferation in a dose-dependent manner in the treatment-naïve, parental C2 line ($IC_{50}$ <10 nM), the three sublines were resistant to growth inhibition by TOC ($IC_{50}$ > 1,000 nM) and phosphorylation of the KIT receptor was less inhibited compared to the TOC-sensitive C2 cells. Additionally, sensitivity to three structurally distinct KIT RTK inhibitors (imatinib, masitinib, and LY2457546) was variable among the sublines. All 3 sublines retained sensitivity to the cytotoxic agents vinblastine and lomustine. Through sequencing efforts of canine *c-kit*, secondary point mutations in the juxtamembrane and tyrosine kinase domains of the resistant sublines were identified.

To explore the impact of these mutations on the TOC-resistant phenotype, we constructed four *in silico* homology models of the cytoplasmic region of TOC-sensitive and -resistant canine KIT to predict the consequent structures of the drug binding site. Utilizing computational-based small molecule docking techniques, we calculated the predicted binding energies and orientations of TOC and the three other KIT inhibitors within the KIT mutant homology models to determine the structural basis of TOC resistance *in vitro* in the context of canine MCT. Each of the three TOC-resistant mutants was predicted to induce a conformational change in the region of the binding site to a greater or lesser degree. The TR1 mutation, however, was predicted to have only minor effects on the binding of masitinib and imatinib while both TR2 and TR3 mutations induced a substantial decrease in predicted binding affinity. To evaluate the utility of the *in silico* homology model and small molecule docking methodologies in predicting response to novel KIT inhibitors, we docked ponatinib into the intracellular domain of the TOC-sensitive and each of the three TOC-resistant KIT mutant protein structures, followed by binding energy calculations. Ponatinib was predicted to bind favorably to TOC-sensitive KIT, but exhibited a substantial decrease in the favorability of the predicted binding to each of the three

TOC-resistant mutants. In concordance with the predicted binding energies, ponatinib inhibited the growth of the TOC-sensitive C2 cells in a dose-dependent manner and failed to inhibit growth of the TOC-resistant cells.

Lastly, we developed an immunohistochemical-based assay to directly measure activated (phosphorylated) KIT (pKIT) in canine MCT. This assay was used to investigate whether pKIT provides a pharmacodynamic marker for monitoring response to TOC in canine MCTs in order to potentially identify patients that respond to TOC and those that are refractory and therefore might benefit from an alternative treatment. MCTs from 4/7 (57.1%) patients demonstrated a partial response to TOC therapy, 2/7 (28.6%) patients showed stable disease, and one patient demonstrated progressive disease. Of the four patients that had a partial response, 3/4 (75%) demonstrated a reduction in pKIT 6 hours after the first dose of TOC. The utility of measuring pKIT in MCT as a predictor of biological aggressiveness was determined retrospectively in a set of MCTs in order to investigate its association with two commonly used prognostic grading systems as well as other established prognostic markers (KIT localization, Ki67 expression, mitotic index, and *c-kit* mutation status) for MCT. Expression of phosphorylated KIT was significantly ($p<0.05$) correlated with mitotic index, Ki67, *c-kit* mutation status, and grade by the 2-tier grading system.

We have described mechanisms of resistance to targeted therapy in the context of TOC and its use in the treatment of canine MCT. The combination of studies presented herein provide evidence that canine MCTs and their acquired resistance to the TKI TOC demonstrate an excellent model of acquired resistance to targeted therapy. In summary, we have developed an *in vitro* model of canine MCT to study TOC resistance, identified novel secondary mutations in the target kinase of TOC-resistant MCT sublines, characterized these mutations for the first time in

veterinary medicine by computational modeling, and developed a clinically-relevant immunohistochemical-based assay to monitor response to TOC therapy in MCT. This model may be better utilized to study the molecular basis of and strategies to circumvent drug resistance.

# ACKNOWLEDGEMENTS

This work could not have been completed without the contribution and support of numerous people. I would first like to thank my advisor and mentor, Dr. Daniel Gustafson, for his guidance, encouragement and support during the course of my PhD training. I was fortunate to identify Dan as a mentor very early in my combined training and he has taught me self-discipline in the laboratory. In addition, he embraced my desire to leverage my pathology training to pursue various extraneous projects without objection, despite the fact that these efforts may have slowed progress on the work presented herein. My time in the Gustafson Lab has no doubt made me a better comparative pathologist.

I am equally indebted to Dr. Doug Thamm, who exemplifies the kind of clinician-scientist I would like to become. His excitement towards clinical research is infectious and his insightful discussions about the translational research were tremendously helpful throughout this project.

I would not be the pathologist I am today without Dr. EJ Ehrhart. From training as a first year resident to navigating the job market, EJ has provided intuitive direction in my career and is the reason I am pursuing a career in molecular pathology and cancer research. He is a well-respected colleague and close friend.

It should be a requirement before granting of the PhD degree for all PhD candidates to have a “defunct” PhD project in their research repertoire. I entered this program with an eagerness to study the lymphatic system as it relates to cancer. Funding avenues did not share my interest, but Dr. Deanna Worley did. In addition to her helpful guidance and discussions with the current project, she has championed efforts towards successfully advancing investigations into

the lymphatic system and I am grateful to her including me in these efforts.

Thank you to Barb Rose and Dr. Amber Wolf-Ringwall for their assistance in generating the cells lines, Drs. Anne Avery and Robert Burnett for their assistance with the sequencing efforts, Janna Yoshimoto for her assistance with the flow cytometry, Dr. Dawn Duval for her assistance with the cloning technique. Thank you to Drs. Philip Reigan and Donald Backos for conducting the homology modeling and critical review of the manuscript. Thank you to Brad Charles for his technical assistance with immunohistochemical staining of tumor sections. Funding was provided by an NIH NCRR T32 Fellowship and a grant from the College Researh Council (CRC).

My most sincere thanks to the faculty and staff at the Animal Cancer Center. Working at this incredible institution even for a short time is something of which I will be most proud throughout my career. A very special thanks to Barb Rose for all of her technical support and teaching.

Many thanks to my resident mates and friends, too numerous to name, but a special acknowledgement is warranted for Drs. Karen Fox and Brett Webb. They made residency training one of the most enjoyable chapters of my career.

Finally, thank you to my family, whose love and support is unmatched; to my children Austin, Ella, and Charlie who help keep things in proper perspective; and lastly to my wife, Day, whom I could not live without and makes everything else in my life so easy.

# DEDICATION

This dissertation is dedicated to my wife, Day Halsey, for whose unconditional and tireless support through veterinary school, residency, and now PhD I will be forever grateful.

TABLE OF CONTENTS

LIST OF TABLES

**Chapter Two**



**Chapter Three**



**Chapter Four**

LIST OF FIGURES

**Chapter One**



**Chapter Two**

**Chapter Three**

**Chapter 4**

# Chapter One

## Literature Review

## MAST CELL TUMOR: DISEASE REVIEW

Mast cell tumor (MCT) is the most common skin tumor in dogs, accounting for up to 21% of canine cutaneous tumors, and one of the most malignant tumors in this species [1]. MCTs are commonly found in older dogs, with a mean age of 9, although they are reported in younger dogs [1,2]. Several breeds are reported to be overrepresented for MCTs including Boxers, Boston Terriers, English Bulldogs, Labrador and Golden Retrievers, Cocker Spaniels, Schnauzers, Chinese Shar-pei, Rhodesian ridgebacks, Weimaraners, Beagles, and Staffordshire terriers [2]. This overrepresentation in certain breeds may indicate a genetic component to the etiopathogenesis of MCT [1]. There is no sex predilection. MCTs most commonly arise from the skin of the trunk and perineal region (50%) followed by the limbs (40%), and head and neck (10%). Less frequently, MCTs present as primary tumors in the oral cavity, nasopharynx, larynx, and gastrointestinal tract [1,2]. Clinical appearance can vary widely ranging from a single, well-circumscribed, raised, nodule to multifocal to coalescing, ulcerated nodules, with erythema of the surrounding skin due to rapid and robust degranulation, a phenomenon known as Darier's sign. Mast cells are distinct in that they are characterized by the presence of abundant cytoplasmic granules. These granules represent vasoactive amines, such as histamine and heparin, as well as various proteolytic enzymes such as chymase and tryptase. While these cytoplasmic granules are important in the normal physiological function of mast cells, in MCTs they can often lead to

complications upon rapid and robust degranulation such as gastrointestinal tract ulceration (35-83%), hemorrhage, intraoperative hypotension, and delayed wound healing [1,2].

Histologically, MCTs are generally characterized by a poorly-demarcated, unencapsulated infiltrative mass that effaces and replaces normal dermal collagen and subcutaneous adipose tissue, often extending deep to the subjacent skeletal muscle and elevating the overlying epidermis (Figure 1.1). These masses are composed of tightly packed sheets and rows of discreet rounds cells with abundant basophilic cytoplasmic granules (Figure 1.2).

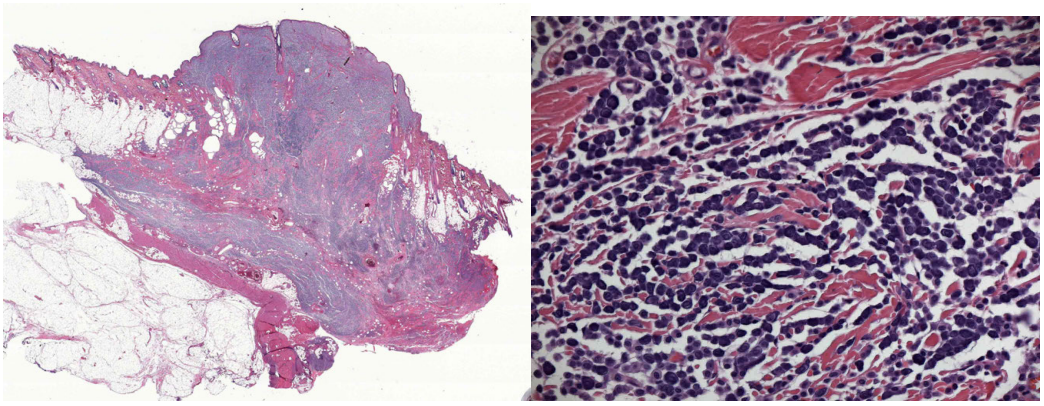

**Figure 1.1 (left) and 1.2 (right):** Haired-skin; mast cell tumor.

## MOLECULAR PATHOGENESIS

Aberrantly regulated receptor tyrosine kinases (RTKs) have been implicated in human and canine cancer. Mechanisms of dysregulation include activating mutations, overexpression, and autocrine/paracrine loops of activation. The tumorigenesis of 30-50% of MCT is driven by activating mutations in the juxtamembrane, kinase, and ligand-binding domains of the *c-kit* proto-oncogene. *c-kit* encodes the RTK KIT, a 145-kDa type III receptor protein-tyrosine kinase, which is comprised of an extracellular ligand binding domain composed of five immunoglobulin-like loops, encoded by exons 1-9, a transmembrane domain, encoded by exon 10, and a split cytoplasmic kinase domain, encoded by exons 11-21, including a negative

regulatory juxtamembrane (exon 11), an ATP-binding domain (exon 13), and a phosphotransferase domain (exon 17) [3-6]. The *c-kit* proto-oncogene was first identified as the normal cellular homolog of the feline sarcoma viral oncogene *v-kit*, which induces feline fibrosarcoma [7]. The KIT receptor shares structural similarity with other Type III RTKs such as FMS-like tyrosine kinase-3 (Flt-3), platelet derived growth factor receptor (PDGFR), and colony-stimulating factor-1 receptor (CSF-1R) [8]. KIT signaling plays a role in erythropoiesis, lymphopoiesis, mast cell development and function, megakaryopoiesis, gametogenesis, and melanogenesis [9]. KIT is expressed in hematopoietic stem cells, erythroid, megakaryotic, dendritic, and myeloid progenitor cells [10]. While KIT expression is commonly lost during cell differentiation, mature mast cells, melanocytes, and the intestinal pacemaker cells (interstitial cells of Cajal) maintain KIT expression throughout differentiation [4].

The ligand for KIT, stem cell factor (SCF), also termed mast cell growth factor (MGF), KIT ligand (KL), or steel factor, promotes the development of mast cells from hematopoietic precursors upon binding to the KIT receptor [11]. KIT/SCF interactions promote the proliferation, survival, and differentiation of mast cells [3,12,13]. In addition, KIT has been shown to be important for fibronectin adhesion, chemotaxis, degranulation, chemotaxis, and secretory activity of mast cells [3,14-16]. Indeed, mice lacking germline mutations in either *c-kit* ($Kit^{W}/Kit^{W\text{-}v}$) or SCF ($Msf^{Sl}/Msf^{Sl\text{-}d}$) are phenotypically characterized by a tissue-wide deficiency in mast cells [7,17,18]. SCF binds to two KIT monomers promoting KIT dimer formation [4,14]. This results in receptor autophosphorylation at specific tyrosine residues within the cytoplasmic domain. Sequences containing these phosphotyrosine residues subsequently serve as docking sites for critical signal transduction molecules containing SH2 and other phosphotyrosine-binding domains [19-21]. These molecules include the adaptor molecules Grb2 (pY703 and

pY936) and Shc, the Src kinases Lyn and Fyn (pY568 and pY570, respectively), phospholipase C (pY936), and phosphoinositide 3-kinase (PI3K) (pY721) [22,23]. In the canine KIT receptor, pY721 becomes phosphorylated in response to SCF and mediates the docking of PI3K [24]. Downstream signaling through the PI3K/Akt/mTOR pathway is the main signaling cascade for proliferation and survival of canine mast cells [25]. While crosstalk between PI3K and Ras/Raf/ERK MAPK pathways is common in many malignancies, downstream ERK1/2 modulation does not correlate with KIT inhibition in canine MCT [25,26].

Three common mechanisms of KIT activation in tumors have been described. These include paracrine and/or autocrine stimulation of the receptor by SCF, activation by other kinases and/or loss of inhibitory mechanisms, and, most commonly, activating mutations in the *c-kit* gene [27,28]. The KIT receptor ligand, SCF, has recently been shown to be overexpressed in canine MCT independent of activating mutations in KIT. Furthermore, production of SCF has been demonstrated in Ki67-positive MCT by immunohistochemistry suggesting that autocrine/paracrine production of SCF contributes to the growth and survival of canine MCT [29,30]. Mutated forms of *c-kit* have been implicated in the tumorigenesis of gastrointestinal stromal tumor (GIST) and acute myelogenous leukemia as well as mast cell disease in humans [31,32]. Similarly, activating mutations in *c-kit* have been identified in canine MCT. Most commonly, an internal tandem duplication (ITD) has been identified in exon 11 of canine *c-kit* [3,5,7]. Exon 11 encodes the juxtamembrane domain of the KIT receptor, which has an inhibitory function in regulating KIT kinase activity. This inhibitory function is lost in oncogenic forms of KIT harboring an ITD in exon 11 [33]. Less frequently, mutations in the *c-kit* gene occur in exons 8 and 9, which encode the extracellular domains of KIT. Mutations are characterized by ITD (exon 8) and amino acids substitutions and insertions (exons 8 and 9) and

exon 17, which encodes the kinase domain [5,34,35]. Indeed, these mutations are associated with ligand-independent autophosphorylation of the KIT receptor and self-sufficient growth of neoplastic mast cells. Up to 40% of histologically intermediate or high-grade MCTs harbor ITDs in the juxtamembrane domain of KIT. Mutated KIT is significantly associated with increased incidence of recurrent disease, metastasis, and death in canine MCT [2,3,5,36-38].

## HISTOLOGIC GRADING AND PROGNOSTIC FACTORS

Several histologic grading systems have been assessed for the prognostic evaluation of canine cutaneous MCTs. Histologic grading by the Patnaik system has been the gold standard and has provided a strong foundation in the grading of canine cutaneous MCTs; however, certain criteria within the grading system require subjective interpretation and significant inter-pathologist variability exists [39,40]. This has presented challenges for clinicians in determining clinical behavior from tumor grade and thus the decision for adjuvant therapy, especially for "intermediate grade" MCTs. Recently, additional grading schemas have been explored; however, regardless of the grading system used, grade is considered as only one prognostic factor and in conjunction with the overall clinical picture: size and site of the MCT, whether single or multiple tumors exist, presence of metastases (stage), completeness and quality of surgical margins, prognostic molecular markers, and emerging molecular markers.

Histologic grading by the Patnaik grading scheme is currently the primary method by which therapeutic decisions and prognoses are made [41]. This scheme divides MCTs into one of three grades according to histologic parameters such as mitotic index (MI), differentiation, depth of invasion, granularity, stromal reaction, edema, and necrosis. Statistically significant differences in survival times between groups/grades, as determined by these specified

histological features, were present. The Patnaik grading scheme has inherent weaknesses characterized by subjective criteria and interobserver variability. As a result, the challenge with grading canine cutaneous MCTs using this scheme has been the frequency at which grade II MCTs are diagnosed and further complicated by the observation that some grade II MCTs are fairly benign while others are biologically aggressive. Therefore, this traditional and widely accepted grading system has failed to reliably differentiate between these aggressive and non-aggressive grade II MCTs. As such, alternative grading schemes have recently emerged to better prognosticate MCTs and improve concordance among pathologists. These grading schemes include 1) a 2-tiered grading system, separating MCTs into "low" and "high" grade based on specific histological parameters, and 2) a grading system that includes the significance of mitotic index (MI) as a single prognostic factor regardless of grade.

The 2-tier system attempts to address the predominance of Patnaik grade II MCTs and the ambiguity and biologic variability within this group. Additional goals of this novel grading scheme are to evaluate consistency in grading of canine cutaneous MCT between multiple pathologists at multiple institutions and to improve concordance among pathologists and prognostic significance. The 2-tier system divided MCTs in to "high" or "low" grade, in which tumors were classified as high grade if any one of the following criteria existed: 7 or more MFs / hpf, at least 3 multinucleated cells (at least 3 nuclei) / 10hpf, at least 3 "bizarre" nuclei (characterized as highly atypical with marked indentations, segmentation, and irregular shape), or karyomegaly (nuclear diameters of at least 10% of tumor cells vary by at least two-fold). High grade MCT by the proposed 2-tier system had a significant association between Patnaik high-grade MCTs, increased mortality, and increased risk of developing additional tumors and metastatic disease. The MST for high grade was < 4 months while the MST for low grade was >

2 years. Overall, the authors concluded that the 2-tiered grading system is a better predictor of survival than Patnaik [42]. Moreover, the authors demonstrated improved concordance among pathologists and prognostic significance via the development of this novel 2-tier grading system. However, the criteria by which tumors are classified still introduce subjectivity (i.e. karyomegaly and “bizarre nuclei”).

A common parameter in all grading schemes is the evaluation of the mitotic index (MI) as a measure of proliferation. Indeed, a study by Romansik and co-workers [43], and later validated by Elston and co-workers [44], offers the most compelling evidence for the prognostic importance of MI. The purpose of these studies was to evaluate the utility of MI as a predictor of biologic behavior and survival in dogs with cutaneous MCTs. The authors demonstrated prognostic significance of MI, regardless of grade, with stratification into two groups: MI of 0-5 (low) and MI >5 (high). Furthermore, they demonstrated the ability to differentiate aggressive and less aggressive grade II MCTs via MI with this method of stratification. Grade II MCTs with MI <5 had a MST of 80 months compared to grade II MCTs with MI >5 which had a MST of 3 months [43].

Significant differences were present between grades I and III and II and III, but no significant differences in distribution of MI were identified between grades I and II. Significant differences between MI and rate of metastatic disease were described, however no significant differences between MI and local recurrence were identified. The authors concluded that MI may help identify subsets of aggressive grade II MCTs and may be a more sensitive prognostic indicator than grade [43]. Elston and co-workers also explored MI as a single prognostic parameter, yet described stratification into 3 groups: MI=0 in which reach MST was not reached, MI=1-7 had a MST of 18 months, MI >7 had a MST of 3 months [44]. This study

corroborates the significance of MI as a prognostic factor in canine cutaneous MCT as demonstrated by Romansik. MI as a parameter significantly reduces subjectivity and interobserver variability. The challenge still lies with identifying appropriate cutoffs (“5” as Romansik reports, or further stratification as Elston suggests). Further studies will be necessary to determine this. Finally, while MI is a single, objective variable, regions of mitotic activity within a tumor sample vary and subjectivity is introduced upon selection of regions of highest mitotic activity.

Regardless of grading schema, there exists a subset of MCTs that exhibit more aggressive biologic behavior. This uncertainty, in addition to a high degree of interobserver variability, necessitates the need for additional prognostic and therapeutic indicators. Histologic features of MCTs alone do not provide a comprehensive representation as it relates to biological aggressiveness and guidance of therapeutic decisions. Indeed, MCT tumorigenesis is driven by molecular mechanisms and signaling pathways that do not manifest via routine light microscopy. As such, identification of concurrent molecular characteristics will likely prove to play a significant role. To date, molecular investigations of MCT biomarkers include Ki67, AgNOR, KIT expression, and *c-kit* mutation status [3,7,45,46].

MCT behavior is partially dependent on aberrant signaling of certain proteins, which cannot be detected on routine histopathological evaluation. Activating mutations in the juxtamembrane, kinase and ligand binding domains of the *c-kit* proto-oncogene have been associated with the pathogenesis and aggressiveness of canine MCTs, resulting in growth factor-independent constitutive phosphorylation of the KIT receptor tyrosine kinase (RTK) [3,5,37,47]. Approximately one-third of canine MCTs carry a *c-kit* mutation and the majority of MCTs with *c-kit* mutations are histologically intermediate or high grade [7]. London and co-workers first

showed that *c-kit* mutations, particularly internal tandem duplications in the juxtamembrane domain of exon 11, are associated with an increased incidence of recurrent disease, metastasis, and death [7,37]. Such mutations in *c-kit* have been associated with aberrant KIT protein localization; however, there is not a 1:1 correlation between KIT localization and *c-kit* mutation status, suggesting the possibility of alternate mechanisms of receptor activation, such as KIT overexpression or autocrine/paracrine production of stem cell factor, the growth factor ligand for KIT. While the majority of gain-of-function mutations of *c-kit* have been identified in exon 11 of canine MCTs, exons 8 and 9, and less commonly exon 17, also acquire activating mutations [5]. Differential patterns of KIT staining by immunohistochemistry (IHC) in MCTs, associated with mutations in the *c*-kit proto-oncogene, are indicators of biologic behavior [45]. Kiupel and co-workers showed that mast cells exhibiting benign biologic behavior demonstrated membrane-associated KIT expression while mast cells associated with malignant transformation and aggressive biologic behavior demonstrate a cytoplasmic redistribution of KIT. Furthermore, Webster and co-workers demonstrated that MCTs with aberrant KIT localization or internal tandem duplication in exon 11 of *c-kit* are associated with increased cellular proliferation as measured by Ki67 and AgNOR, suggesting a role for KIT in the tumorigenesis and aggressiveness of canine MCTs. Markers of cellular proliferation such as Ki67, PCNA, and AgNOR have been shown to be significantly associated with progression of canine MCT. These studies demonstrate that markers of proliferation, *c-kit* mutation status, and KIT protein localization are useful markers of tumor aggressiveness in canine MCT.

Anatomic and microanatomic location of MCT has been shown to be associated with clinical aggressiveness. MCTs located at the subungual, inguinal, preputial, and scrotal areas, or a mucocutaneous junction such as the perineum or oral cavity carry a guarded prognosis [48-51].

More recently, MCTs arising from the subcutaneous tissue have been shown to have a more favorable prognosis [52,53]. In a retrospective analysis of 306 dogs diagnosed with subcutaneous MCT, only 27 (9%) died from their disease [52]. Finally, the presence of multiple cutaneous MCTs on the impact of prognosis is somewhat contradictory in the literature. Kiupel and co-workers showed that dogs with multiple synchronous cutaneous MCTs at the time of diagnosis had a worse prognosis compared with dogs with single tumors [54]. In contrast, Mullins and co-workers reported that multiple cutaneous MCTs are associated with a low rate of metastasis and an overall good prognosis for long-term survival [55].

Clinical stage of canine MCT has been shown to be a prognostic indicator, albeit plagued with some controversy. While several studies have indicated the presence of metastatic disease in regional lymph nodes as a negative prognostic indicator [56-58], others have shown that with excision of positive lymph nodes followed by adjuvant chemotherapy and/or radiation therapy long-term survival can be achieved [59-61]. These disparities might be due in part to a lack of consensus as to what defines a lymph node positive for metastatic disease coupled with sampling techniques of varying sensitivity (i.e. fine-needle aspirate, histologic evaluation, sentinel lymph node mapping) [62].

## TREATMENT OF CANINE MAST CELL TUMOR

The prognostic indicators outlined above serve to aid in the approach to treating MCT. The vast majority of dogs with low to intermediate grade MCTs experience longer survival times with complete surgical excision alone compared to those with high grade MCTs [55,63]. While lateral margins of 3 cm of normal tissue and one facial plane have traditionally been adequate to achieve complete excision and local control, more recent evidence suggests that 1 cm margins

might achieve similar long term survival times [2,64-66]. Furthermore, incomplete excision of low grade MCTs does not preclude the possibility that local control will be achieved. Indeed, only 20-30% of incompletely excised low grade MCTs recurred in one study [64]. In cases in which surgical excision with adequate margins is not feasible and/or poor prognostic factors such as histologic intermediate to high grade MCTs are encountered, radiation therapy and/or systemic chemotherapy is indicated. Commonly used cytotoxic agents for the treatment of canine MCT include vinblastine (VBL) and lomustine (CCNU) [1]. In addition, systemic corticosteroids have been shown to have clinical efficacy against canine MCT. Indeed, the reported response rate to prednisone is 20% and reported remission times range from 10 to 20 weeks [1,67]. In a recent study, the use of adjuvant systemic therapy (corticosteroids, lomustine (CCNU), and vinblastine (VBL)) following surgical excision of intermediate grade MCT with evidence of local-regional lymph node metastasis, the median survival time was 1359 days [68]. In another study investigating the use of VBL and prednisone following surgical excision +/- radiation therapy, 100% of dogs with "high-risk" intermediate grade MCT were alive at 3 years and those with high grade MCT had an overall survival time (OS) of 1374 days [60]. High grade MCTs, *c-kit*-mutant MCTs, and MCTs with diffuse cytoplasmic labeling for KIT were similarly shown to benefit from postoperative vinblastine and prednisone [69].

## PHARMOCOLOGIC TARGETING OF MAST CELL TUMOR

Targeted therapy involves the use of small compounds that interfere with specific molecules involved in tumor growth and progression. Demonstration of the antiproliferative properties of small molecule tyrosine kinase inhibitors (TKIs) was first described by Yaish and co-workers in 1988 [70]. In this seminal paper, a series of low molecular weight TKIs were

synthesized and demonstrated increasing affinity over a 2500-fold range to the kinase domain of epidermal growth factor receptor (EGFR). These TKIs potently inhibited EGFR kinase activity as well as EGF-dependent autophosphorylation of the receptor [70]. The importance of tyrosine kinases at critical regulators of cell proliferation and survival led the development of this class of compounds for the treatment of cancer and other proliferative disorders [71]. Krystal and co-workers characterized the ability of six indolinone TKIs to inhibit KIT kinase activity. These included SU5416, SU5614, SU6668, SU6597, SU6663, and SU6561 [72]. These compounds were shown to inhibit SCF-induced KIT activation in H526 SCLC cells and induce apoptosis and growth arrest in a dose-dependent manner [72]. Liao and co-workers explored the efficacy of three additional indolinones (SU11652, SU11654, and SU11655). All three act as competitive inhibitors of ATP, binding to several members of the split kinase family of RTKs, including VEGFR2, FGFR, PDGFR, and KIT. Several MCT cell lines expressing either wild-type (WT) KIT, a point mutation in the JM domain, an internal tandem duplication in the JM domain, or a point mutation in the catalytic domain were used to examine KIT inhibition by these compounds. All three small molecules inhibited SCF-induced phosphorylation KIT as well as autophosphorylation of both KIT mutants in a dose- and time-dependent manner [73]. Results of these studies demonstrated the therapeutic potential for the use of this class of compounds in KIT-driven tumors. Further investigations into the clinical efficacy of TKIs in canine MCT are discussed below.

## RECEPTOR TYROSINE KINASE INHIBITORS OF MAST CELL TUMOR

The ideal small molecule tyrosine kinase inhibitor is therapeutic at the nanomolar range, orally bioavailable, highly specific with minimal toxicity. TKIs are ATP-mimetics that block the

ATP-binding site of kinases in a competitive approach. As outlined above, oncogenic mutations involving the *c-kit* gene are intimately involved in the tumorigenesis of canine MCT. These activating mutations result in ligand-independent kinase activity, subsequent autophosphorylation of tyrosine residues, and stimulation of downstream signaling pathways. Most notably, mutations within exon 11, encoding the juxtamembrane domain, account for the majority of the oncogenic mutations in canine MCT. This juxtamembrane domain is critical in KIT signal transduction in both its interactions with adapter proteins and phosphatases as well as through regulation of KIT catalytic activity. Furthermore, the vast majority of canine MCTs express the KIT receptor tyrosine kinase and mutated forms confer growth factor-independent growth. As such, KIT represents a logical and attractive therapeutic target in the treatment of recurrent, non-resectable canine cutaneous MCT.

The clinical efficacy of three small molecule KIT tyrosine kinase inhibitors have been tested in canine MCT. Imatinib mesylate (Gleevec®) is a small molecule inhibitor of KIT and the cytoplasmic kinase Abl that has shown clinical efficacy against GIST harboring KIT mutations and chronic myleogenous leukemia positive for Bcr-Abl rearrangements [74-76]. Isotani and co-workers demonstrated biologic activity of imatinib against canine MCTs with demonstrable exon 11 mutations in *c-kit* [77]. Imatinib was administered to 21 dogs with MCT. Within two weeks, 10 of 21 dogs (48%) had a measurable response to imatinib treatment. All dogs with a confirmed *c-kit* mutation in exon 11 (N=5) responded to imatinib (1 complete response, 4 partial responses). In another study, dogs diagnosed with MCT and bone marrow involvement were treated with either CCNU (N=9) or imatinib (N=3). Treatment with CCNU induced a partial response in 1 of 8 dogs with a median survival time of 43 days. In contrast, all three dogs treated with imatinib experienced complete responses [78].

Masitinib mesylate (Masivet®, Kinavet®), another potent KIT TKI, has clinical efficacy against canine MCTs [79,80]. In addition to activity against KIT, masitinib also demonstrated inhibition of PDGFRα/β and Lck/Lyn tyrosine kinase activity, and weaker inhibition of FGFR3 and FAK [81]. Hahn and co-workers demonstrated in a randomized phase III clinical trial that dogs with non-resectable or recurrent grade II or III nonmetastatic MCTs benefited from masitinib with an increase in the median time to tumor progression from 75 to 253 days versus placebo regardless of *c-kit* mutation status [80]. In a subsequent study, this group of investigators similarly showed a significant increase in 1- and 2-year overall survival in dogs with unresectable intermediate and high grade MCTs treated with masitinib versus placebo. The 12- and 24-month median overall survival time was 322 and 617 days, respectively [82]. Finally, Smrkovski and co-workers similarly showed clinical efficacy of masitinib as a rescue agent in metastatic and non-resectable MCTs demonstrating an overall response rate of 50%. Despite the a high rate of mild and self-limiting toxicity (61.5%), the median survival time for responding dogs was 630 days versus 137 days for non-responders [83].

Toceranib phosphate (Palladia®) is the most widely used TKI that is approved for the treatment of canine MCT. Toceranib (TOC) was initially developed as SU11654, one of the multitargeted indolinones screened by SUGEN described above. This orally bioavailable small-molecule multikinase inhibitor potently inhibits a wide spectrum of kinases including KIT, VEGFR2, PDGFR, and Flt-3 [29,84]. Similar to other TKIs, TOC exerts its effect by binding to the ATP-binding site of the catalytic domain of KIT thereby blocking cross-phosphorylation of intracellular tyrosine residues. This results in cessation of downstream intracellular signaling required for growth and survival of malignant mast cells, followed by cell death via apoptosis and cell cycle arrest [26,29,73,84,85]. In addition, TOC is expected to have anti-angiogenic

properties due to VEGFR2 inhibition. Pryer and co-workers demonstrated the ability of SU11654/TOC to effectively inhibit activated KIT in MCT 8 hours after a single oral dose [26]. More recently, London and co-workers showed in a multi-center, double-blind randomized trial that TOC, demonstrated clinical efficacy against recurrent intermediate and high grade mast cell tumor [85]. In this study, 42.8% of patients receiving TOC experienced an objective response. Furthermore, dogs with tumors harboring an ITD in exon 11 of *c-kit* were more likely to respond to TOC treatment than those negative for the mutation [85].

## PHARMACOKINETIC PROPERTIES OF TOCERANIB PHOSPHATE

Toceranib phosphate is chemically designated as (Z)-5-[(5-Fluoro-2-oxo-1,2-dihydro-3H-indol-3-ylidene)methyl]-2,4-dimethyl-N-(2-pyrrolidin-1-ylethyl)-1Hpyrrole-3-carboxamide phosphate. The chemical structure is shown in Figure 1.3. The molecular formula is $C_{22}H_{25}FN_4O_2$ with a molecular weight of 396.46g/mol. The pharmacokinetic (PK) profile of TOC phosphate has been evaluated in clinical studies in healthy laboratory dogs and dogs with MCT [86,87]. TOC is administered at a target dose of 3.25 mg/kg every other day (EOD), based on previously established data exploring effective inhibition of phosphorylated KIT, and clinical efficacy in mice with xenograft tumors and MCT-bearing dogs [26,85,88]. In these studies, plasma concentrations were greater than or equal to 40 ng/ml over the 48-hr dosing interval [85]. Yancey and co-workers demonstrated in healthy Beagle dogs that this dose given EOD achieved plasma concentrations of 40 ng/ml for 6 to 33 hours of a 48-hour dosing interval [86]. Because dosing intervals of 24-hours led to unacceptable toxicities in these early studies, an EOD dosing schedule was adopted yielding trough plasma concentrations below the therapeutic window and safeguarding tolerability [88]. Absolute oral availability of TOC is 77% administered as tablets

to fasted dogs, however, there were no significant effects of food on PK parameters evaluated [86]. Following a single oral dose, peak plasma concentrations ($C_{max}$) ranging from 68.6 ng/mL to 112 ng/mL were reached between 5.3 hr and 9.3 hr ($t_{max}$) [86]. TOC is highly protein bound, ranging from 90.8% to 92.8% [87]. Distribution is widespread throughout the body with detectable levels of drug in numerous tissues for 168 hours after a single oral dose [87]. Elimination occurs through the hepatobiliary system as the vast majority of [$^{14}$C]-labeled TOC is excreted in the feces (92%) versus only 7% eliminated in the urine [87]. TOC is metabolized to toceranib *N*-oxide in the liver by the cytochrome P450 isoenzyme or flavin monooxygenase systems [87]. Changes in TOC metabolism or plasma concentrations may occur as a result of interactions between TOC and inducers or inhibitors of these enzyme systems. Overall, TOC has a favorable pharmacokinetic profile.

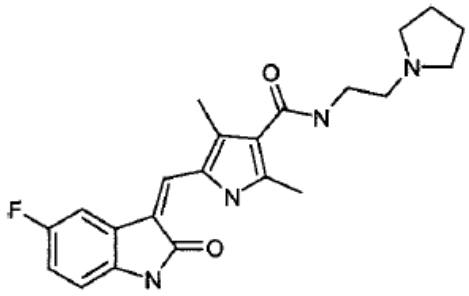


**Figure 1.3:** Chemical structure of toceranib (TOC).

## RESISTANCE TO TARGETED THERAPY

The discovery of molecular and genetic alterations driving the tumorigenesis of numerous malignancies has led to the development of targeted therapies. Indeed, a tumor that is driven by “oncogene addiction” such as mutations, gene translocations, or gene amplification is exquisitely sensitive to therapies targeting those addictions. Despite these initial benefits, the

success of targeted therapy is largely mitigated by the nearly inevitable development of resistance and disease progression. As the burden of clinical resistance increases, so does the requisite to understand the mechanisms of resistance to targeted therapies, which often times are as complicated and heterogeneous as the tumor population they are deployed to treat. The following sections focus on a review of common pathway-dependent and –independent mechanisms of resistance, common experimental approaches to studying mechanisms of acquired resistance, and strategies to overcome or prevent the development of resistance.

Pathway-dependent Mechanisms of Resistance:

Almost in parallel with studying mechanisms of resistance, it is equally important to understand the mechanism by which tumor growth and survival is maintained. That is, the identification of the signaling pathway to which a tumor is "addicted" and, therefore, the intended drug target. Not only does the discovery of these pathways facilitate the development of the therapy and patient selection, they are commonly the focus of potential hotspots for exposing resistance mechanisms [89,90]. There are three common pathway-dependent mechanisms of resistance. These include reactivation of the target kinase, activation of downstream effectors, and activation of a bypass pathway. Each of these is discussed individually below.

One of the most common mechanisms by which a tumor becomes resistant to a given targeted therapy is through reactivation of the target kinase. This can occur either through secondary mutations in the kinase or amplification of the target gene [90]. Secondary point mutations are the most mechanism by which this occurs [91]. This occurs most often in the target kinase domain, significantly altering drug binding affinity by perturbing contact point between the drug and target or altering the amino acids surrounding the binding site thereby decreasing

the ability of the drug to reach its target [92,93]. The “gatekeeper” mutation is among the most common point mutations in drug targets that impedes drug binding and leads to resistance. The gatekeeper is a single amino acid residue located in the ATP-binding pocket of protein kinases and has been shown to control sensitivity to a wide range of small molecule inhibitors by regulating access of the drug to the ATP-binding site [93]. Typically, mutations of the gatekeeper to a larger amino acid impedes drug access and is responsible for clinical resistance [94]. Examples of gatekeeper mutations involved in resistance to targeted therapies include T790M in EGFR of erlotinib- and gefitinib-resistant NSCLC [95,96], T670I in KIT of imatinib-resistant GIST [97], T315I in BCR-ABL rearranged imatinib-, dasatinib-, and nilotinib-resistant CML [98-100], and L1196M in ALK-rearranged crizotinib-resistant NSCLC [101]. The specific mechanism by which these gatekeeper mutations confer resistance varies between tumor type. For example, the T315I in ABL causes steric hindrance within the drug-binding site precluding the ability of imatinib to effectively bind [100]. Interestingly, the T790M mutation in EGFR causes increase affinity for ATP compared to the inhibitor thereby prohibiting the ability of erlotinib or gefitinib to dislodge ATP from the binding site [102]. Still other secondary mutations alter the conformational state of the target kinase thereby prohibiting drug binding while simultaneously assuming a more active conformation. This has been demonstrated in imatinib- and sunitinib-resistant GIST. Secondary KIT mutations occur in the kinase activation loop, most commonly a D816V point mutation. This causes a shift in conformational equilibrium in favor of the active state despite initial KIT inhibition by imatinib or sunitinib [103]. A more recently described secondary mutation conferring resistance to targeted therapy is the V600E mutation in BRAF in vemurafenib-resistant melanoma resulting from alternative splicing [104]. As a result, BRAF lacks the RAS binding domain and produces enhanced dimerization with other RAF

family members ultimately circumventing RAF inhibition [104]. Target reactivation also occurs through gene amplification. This occurs following selective pressure of the drug which drives increased expression of the target gene and therefore overexpression of the target protein [91]. Ultimately this leads to a shift in the drug-target stoichiometry in favor of the target and culminating in inadequate target inhibition. This has been described in imatinib-resistant CML for which resistance was associated with progressive BCR-ABL gene amplification [100]. Similarly, Ercan and co-workers showed focal amplification of T790M-containing allele of EGFR in NSCLC resistant to a novel EFGR inhibitor (PF00299804) [105].

A second commonly reported mechanism by which tumors circumvent inhibition by targeted therapy is through the activation of alternative or bypass signaling pathways. These are pathways that effectively work around the effect of the kinase inhibitor by engaging a parallel signaling cascade independent of the original target kinase culminating in similar oncogenic output and ultimately relapse. Engelman and co-workers demonstrated maintenance of EFGR signaling in NSCLC in the presence of erlotinib and gefitinib by sustained activation of the PI3K/Akt signaling cascade [89]. Similarly, engagement of MET signaling can bypass EGFR inhibition by gefitinib in NSCLC [98,99]. In yet another study, imatinib-resistant GIST cells demonstrated upregulation of Axl for which Akt is a downstream target [106,107]. In both imatinib- or nilotinib-resistant CML, both Mahon and co-workers and Ito and co-workers demonstrated activation of the Src kinase Lyn as a bypass mechanism to BCR-ABL inhibition [108,109].

A final reported pathway-dependent mechanism of resistance is the activation of downstream signaling molecules. That is, members of the pathway downstream of the target kinase are reactivated. Following RAF inhibition in BRAF-mutant melanoma, Wagle and co-

workers describe attenuation of the initial dramatic patient response by the activation of a downstream kinase, MEK1. Following sequencing, an activating mutation in codon 121 of the *MEK1* gene was identified that was absent in the pre-treatment samples [110]. In another study, NSCLC with gefitinib-sensitizing EGFR mutations became resistant to the inhibitor following activation of Ras. These studies suggest that activation of targets immediately downstream of EGFR confer secondary resistance to gefitinib [111].

Regardless of the pathway-dependent mechanism of resistance, all of the broad categories outlined above eventually culminate in pathway reactivation and sustained downstream signaling leading to growth and survival of tumor cells.

Pathway-independent Mechanisms of Resistance:

While TKI resistance is most often attributed to reactivation of the target pathway through one of the mechanisms described above, it is not uncommon for tumors to fail to response to a given inhibitor even in the face of sustained signaling inhibition. The following section summarizes the common pathway-independent mechanisms of resistance responsible for this phenomenon. These include enhanced drug efflux, drug plasma sequestration, differential induction of apoptosis, and altered drug metabolism.

Ineffective intracellular drug concentrations lead to cessation of any tumor response and ultimately disease progression. One of the most commonly reported mechanism by which this occurs is enhanced drug efflux/transport. The expression or overexpression of multidrug resistant (MDR) proteins plays a pivotal role in treatment failure in cancer patients [91,104,108,111-114]. MDR proteins are ATP-driven transmembrane pumps responsible for the transport of a broad range of proteins. They are members of the ATP-binding cassette (ABC) transporter family and present in normal tissue, such as testes, placenta, and brain serving as a protective barrier, and

kidney, liver, and intestine, playing a role in systemic detoxification [104]. P-glycoprotein (P-gp), is one of the most well-studied transmembrane efflux protein, for which a broad range of structurally diverse substrates exists. P-gp is encoded by *ABCB1*, or *MDR1*, genes [104,115,116]. Indeed, these drug transporters have emerged as key regulators of intracellular drug concentrations and a source of drug resistance. Overexpression of P-gp has been demonstrated in CML cells resistant to imatinib [112]. Furthermore, several investigators have demonstrated a reversal of the resistant phenotype in numerous models by pharmacological inhibition [104,117] or gene silencing [118,119] of P-gp. Widmer and co-workers demonstrated that inhibition of P-gp by RNAi silencing of imatinib-resistant was associated with increased intracellular levels of imatinib and restored sensitivity [119]. Another drug transporter, BCRP, encoded by *ABCG2*, has also been reported to be an active transporter for mitoxantrone, topotecan, and flavopiridol. Furthermore, its overexpression has been described in several drug-resistant tumor scenarios [120]. Elkind and co-workers described BCRP-mediated protection of EGFR inhibition by gefitinib following transport of the drug out of A431 cells leading to a reduction in effective intracellular drug concentrations. Furthermore, this was reversed following co-treatment with a ABCG2-specific inhibitor [121]. Another method by which tumor cells effectively decrease intracellular concentrations of inhibitors is by sequestration by plasma proteins. Perhaps the most well-studied of these proteins is plasma protein-1 acid glycoprotein (AGP) [91]. Indeed, AGP has been shown to bind imatinib and effectively alter its pharmacokinetics, plasma concentrations, and intracellular distribution in CML patients [122-124]. Recently, a novel mechanism of resistance to targeted therapy was described by Gotink and colleagues involving lysosomal sequestration of sunitinib, thereby similarly decreasing the effective intracellular concentrations of drug. In multiple *in vitro*, xenograft, and patient tumor model systems,

intracellular drug concentrations were measured in sunitinib-resistant cells and tumors. Fluorescent microscopy demonstrated intracellular sunitinib distribution in lysosomes, which were significantly higher expressed in resistant cells. Lysosomal sequestration correlated with a 1.7- to 2.5-fold higher intracellular concentration; however, this precluded the ability of the drug to effectively inhibit its target. Indeed, key downstream signaling proteins, phospho-Akt and phospho-ERK were unchanged and comparable to untreated samples [125].

The evasion of apoptosis is a unique hallmark of cancer [126]. Indeed, apoptosis is often the result of a shift in the balance of key components of the intrinsic apoptotic pathway that are critical to the cell's growth and survival [127]. The intrinsic, or mitochondrial, apoptotic pathway has emerged as a critical link between targeted inhibition of kinases and cell death [128]. This pathway is regulated by Bcl-2 family members comprised of pro-apoptotic and anti-apoptotic proteins, the balance of which shifts the fate of the cell towards survival or death. The pro-apoptotic BH3-only BIM is unique in its ability to bind with high affinity to all Bcl-2 family members, including Bax and Bak, which are directly activated by BIM. BIM consistently mediates a critical role in TKI-induced apoptosis. As such, it is a reasonable candidate to study when investigating differential induction of apoptosis following targeted therapy [128]. Indeed, Nakagawa and co-workers described a BIM deletion polymorphism precluding the transcription of the proapoptotic isoform required for gefitinib- and erlotinib-induced apoptosis in NSCLC. As a result, this inability to induce apoptosis despite adequate inhibition of the signaling pathway conferred an inherent drug-resistant phenotype [129]. Similarly, Paraiso and co-workers demonstrated that loss of PTEN contributes to resistance to the BRAF inhibitor, PLX4720, via suppression of BIM-mediated apoptosis [130]. Differential induction of apoptosis as a mechanism of resistance has likewise been associated with the overexpression of survivin, a

negative regulator of apoptosis, as it is known to inhibit caspase activation [131]. As such, overexpression of survivin has been shown to mediate resistance to lapatinib in breast cancer both *in vitro* and *in vivo* [132].

Studying Resistance to Targeted Therapy:

One of the simplest and most common methods to studying drug resistance is the development of drug-resistant cell lines from a parental line after continuous and stepwise exposure to the drug in question [95,98,133]. Cells with predefined drug-sensitizing mutations are exposed to increasing amounts of the targeted compound until resistant subpopulations emerge. These resistant sublines continue to proliferate even in the presence of high concentrations of drug. Following the establishment of a drug-resistant subline, extensive studies can be performed comparing the resistant sublines to the drug-sensitive parental line to uncover novel mutations, pathway alterations, or other genomic alterations that may confer the resistant phenotype. In order to uncover the mechanisms of resistance to gefitinib in non-small cell lung cancer (NSCLC), Ogino and co-workers continuously exposed NSCLC cells to gefitinib. The resistant cells that emerged harbored a secondary mutation, T790M, in EGFR [95]. Similarly, imatinib-resistant and nilotinib-resistant melanoma sublines were established by Todd and co-workers following chronic exposure of M230 cells to these receptor tyrosine kinase inhibitors. The emergence of several secondary mutations in *c-kit* were identified and further shown to confer the observed resistance to these compounds [133].

A second commonly used approach to studying resistance to targeted therapy is through the use of random mutagenesis of the intended drug target. This involves the construction of mutagenesis libraries using an expression vector containing the target cDNA, which are

subsequently packaged into viral delivery systems and incubated with drug-sensitive cell lines. These cell lines are grown in the presence of efficacious doses of the query compound followed by the selection of resistant clones. This method was used to identify several mutations in the BCR-ABL kinase domain that mediate imatinib resistance in CML [134] as well as the emergence of mutations in MEK1 in BRAF-mutant melanomas resistant to MEK and B-RAF inhibitors [135]. In a similar approach, chemical mutagens, such as N-ethyl N-nitrosourea (ENU), have been used to identify resistant mutations. Following ENU mutagenesis of Ba/F3 cells expressing a sunitinib-sensitive KIT mutant, Guo and co-workers described a secondary mutation in the KIT activation loop that led to resistance to sunitinib [136]. Bradeen and co-workers employed ENU mutagenesis in Ba/F3-p210(BCR-ABL) cells to investigate the emergence of secondary mutations in the kinase domain following exposure to imatinib mesylate, dasatinib, and nilotinib as monotherapies and in dual combination [46].

A third *in vitro* approach to studying resistance to targeted therapy is through the use of systematic gain- and loss of function-screens through the use of open reading frame (ORF) and shRNA or RNAi libraries, respectively. Indeed, to elucidate the mechanism of resistance to the RAF inhibitor, PLX4720, in $BRAF^{V600E}$-mutant melanoma, ~600 kinase and kinase-related open reading frames (ORFs) were expressed in $BRAF^{V600E}$-mutant melanoma cells. As a result, MAP3K8 was identified as a novel kinase conferring resistance to RAF inhibition in these cell lines [137]. Conversely, the use of loss of function screens have shown promise in highlighting genes whose deletion might play a role in conferring drug resistance. For example, Berns and co-workers demonstrated through the use of an RNA interference screen that loss of *PTEN* is involved in resistance to trastuzumab in the treatment of breast cancer [45]. Likewise, similar studies using an RNAi screening library identified *CDK10* silencing as a fundamental component

to tamoxifen sensitivity in the treatment of breast cancer [138].

Rodent models of disease have proven to be invaluable comparative models. Their use in studying mechanisms of resistance to targeted therapies has provided insight to key regulators of resistance in a number to drug-tumor interactions. Similar to the *in vitro* studies outlined above, chronic treatment studies in genetically engineered mouse models have been equally informative of mechanisms of resistance. Politi and co-workers established erlotinib-resistant model of NSCLC in transgenic mice after chronic treatment with erlotinib. Following analysis of the tumor samples, T790M mutations or Met amplification were identified in a subset of the tumors in these mice. This an example of a mouse model that eloquently recapitulates the molecular changes previously established *in vitro* involved in erlotinib resistance in NSCLC [139].

Perhaps the most clinically relevant method by which to identify mechanisms of drug resistance is by direct genomic and molecular analysis of drug-resistant patient samples. That is, the collection of tumor samples at the time of relapse for downstream mutation and pathway analyses. In one study, sequencing of 138 cancer genes from a melanoma sample from a patient who became refractory to PLX4032, a BRAF and MEK inhibitor, after an initial response identified an activating mutation at codon 121 in the downstream kinase MEK1 that was not identified in the paired pretreatment tumor. This MEK1(C121S) mutation was subsequently shown to increase kinase activity and confer the observed resistance to both RAF and MEK inhibition *in vitro* [110]. Analysis of clinical material from imatinib-resistant CML patients revealed a single amino acid substitution in the Abl kinase domain that negatively affected drug binding. In addition, imatinib-resistance in a small subset of patients was conferred by *bcr-abl* gene amplification. Both mechanisms lead to reactivation of BCR-ABL signal transduction pathway and disease progression [100]. Bertucci and co-workers sequenced *c-kit* from a patient

with GIST before and after the development of imatinib resistance demonstrating acquisition of a secondary mutation in exon 13 of *c-kit* in the resistant sample, but absent in the treatment naïve sample [140]. In a similar, yet larger, study, imatinib-resistant GIST samples were sequenced of which 18.8% were characterized by acquisition of nonrandomly distributed secondary KIT mutations associated with decreased imatinib sensitivity [97].

## OVERCOMING RESISTANCE TO TYROSINE KINASE INHIBITORS

The inevitable development of resistance to targeted therapy underscores the limitations of their use as a monotherapy as well as the need to identify distinct molecular mechanisms of resistance in order to overcome or prevent this phenomenon. There are several proposed strategies to achieving more durable remission times. These largely include the development of novel, or second generation, therapies or the use to combination therapies to block or circumvent the resistant mechanism. As described previously, resistant mutations associated with the gatekeeper residues can produce steric hindrance to the drug-binding site in addition to alteration of drug contact points. Knowledge of this phenomenon has paved the way for the development of second-generation inhibitors. For example, AP24534 and HG-7-85-01 have been shown to be effective against imatinib-, nilotinib-, and dasatinib-resistant CML harboring T315I mutation [141,142]. Both are small, type II tyrosine kinase inhibitors that are not sterically hindered by this mutation, underscoring the importance of understanding the structural consequences of resistant mutations. In NSCLCs harboring T790M mutations, the advent of irreversible EGFR inhibitors that covalently bind Cyc 797 have shown promise in erlotinib- and gefitinib-resistant lung cancer [143,144]. Both irreversible compounds are characterized by increased affinity of the ATP-binding site compared to the ATP affinity produced by the T790M mutation.

Combinatorial approaches have shown encouraging results for resistance settings in which engagement of bypass pathways occurs. As discussed above, activation of MET signaling can bypass EGFR inhibition by gefitinib in NSCLC. Engelman and co-workers demonstrated a reversal of this resistant phenotype following simultaneous MET inhibition in NSCLC [98]. Likewise, melanoma patients with acquired resistance to BRAF inhibition have demonstrated restored sensitivity to treatment after the addition of combination treatment with IGF-1R/PI3K and MEK inhibitors [145]. This strategy of combined BRAF and MEK inhibition has shown clinical promise in BRAF-mutant melanoma [137]. As outlined above, a decrease in effective intracellular drug concentration by enhanced drug efflux or sequestration has been shown to be an important mechanism by which tumor develop resistance. As such, inhibition of these pathways is a reasonable approach to overcoming resistance by these mechanisms. Indeed, Bradshaw-Pierce and co-workers demonstrated increased gene and protein expression of the drug transporter, P-gp, in a subset of colorectal, hepatocellular, and renal cancer cell lines and patient-derived tumor xenografts, tumors that frequently express high levels of P-gp [104]. Furthermore, it was shown that tumors overexpressing P-gp were resistant to inhibition by the p21 activated kinase (PAK) inhibitor, PF-309, a substrate for P-gp. Tumor drug concentration was approximately fourfold lower in tumors that overexpress P-gp and this was directly correlated with tumor response. The addition of a P-gp inhibitor increased the sensitivity of cell lines and xenografts to the PAK inhibitor [104]. In another study, Mahon and co-workers generated nilotinib-resistant CML cells to investigate mechanisms of resistance [108]. Overexpression of the *MDR-1* gene was identified as a mechanism of drug resistance. The inhibitory effect of nilotinib, a P-gp substrate, was restored upon addition of P-gp inhibitors, verapamil or PSC833 [108]. These studies suggest that the addition of compounds that abrogate

the effect of drug transporters in a combinatorial approach is a reasonable approach to enhance the biological activity of compounds that are known substrates of drug transporters in tumors that demonstrate increased expression of MDR proteins. Regardless of rescue treatment strategy, identification and characterization of resistant mechanisms are paramount to developing new treatment paradigms to overcome clinical resistance even before it develops.

## CLINICAL TRANSLATION CHALLENGES

There are several challenges associated with advancing the data from preclinical studies of resistance into clinical strategies. Perhaps the most significant challenge arises from the clinical observation that multiple mechanisms of resistance can co-exist in a single patient. Differences have been reported between metastatic sites and between the primary tumor and sites of metastasis. Indeed, Liegl and co-workers analyzed 53 sites of metastasis in 14 GIST patients who had become refractory to either imatinib or sunitinib [146]. 83% of the patients developed secondary mutations in KIT. 67% percent of these patients had between two and five different secondary mutations in separate sites of metastasis. Furthermore, 34% of these cases demonstrated two different secondary KIT mutations within the same metastatic lesion. All the secondary KIT mutations identified consisted of point mutations clustered in and around the ATP-binding site [146]. In another example of resistance heterogeneity, both *MET* amplification and a T790M mutation in EGFR were identified in the same NSCLC tumor resistant to erlotinib and gefitinib [147], as well as in different metastatic sites [98]. A second challenge is the detection of drug resistant mutations initially defined in preclinical cell culture-based studies in clinical samples. The resistant mutations presumably exist in a small subpopulation of cells that are selected for upon administration of treatment. Detection by conventional sequencing

techniques may only be possible once significant expansion of the resistant subpopulation has occurred. In addition, for resistance caused by target gene amplification, it is poorly defined what constitutes a clinically significant amplification [89]. Finally, accurate and precise identification of which patients have drug resistant mutations and which specific mutation they have acquired is crucial in determining a rescue therapy [89]. This requires repeated biopsies at the time of development of resistance, innovative biomarker studies, followed by assaying for commonly encountered resistant mechanisms previously described in preclinical studies. These biopsies should be both patient matched and lesion matched in order to have an internal reference to compare subtle changes in gene and protein expression [90]. As tumors are the result of multiple genetic alterations so are the mechanisms of acquired resistance to targeted therapy. Development of novel, combinatorial, and individualized therapeutics must coincide with the discovery of new resistance mechanisms in order to overcome acquired resistance to targeted therapy in cancer.

## Project Rationale

The identification of central abnormalities in signaling pathways has advanced the development of targeted therapy. Aberrant signaling is commonly caused by protein kinases and small molecule inhibitors of these proteins have shown significant promise in the treatment of cancer. With this approach, small molecules bind with greater affinity to the ATP-binding site of protein kinase than ATP molecules. This competitive approach mitigates continued cell signaling and ultimately induces growth arrest and cell death. As additional aberrant signaling pathways are uncovered, additional targeted therapies will be developed. Despite the rapid expansion of targeted therapies in human medicine, these strategies are limited in veterinary medicine. This is

largely due to the lack of knowledge of key signaling pathways driving the pathogenesis of many tumors in veterinary species [29]. In addition, the use of targeted inhibitors developed for human medicine is largely cost-prohibitive. Two TKIs have been approved for use in veterinary medicine, specifically for the use of intermediate and high grade, non-resectable canine MCT. These include toceranib phosphate (Palladia®; Zoetis) and masitinib (Kinavet®; AB Science). Both are members of the multitargeted, split-kinase family of inhibitors with biological activity against KIT [80,81,85,148]. Since a significant subset of canine MCTs carry an activating mutation in the KIT receptor, it was hypothesized that measurable responses would be observed in these dogs. A series of proof-of-target and early phase clinical trials of toceranib (TOC) demonstrated a reduction in activated KIT and objective tumor responses, most notably in MCTs harboring internal tandem duplications in exon 11 of *c-kit* [5,7,88]. Despite encouraging objective response rates, the majority of responders' MCTs eventually progressed on treatment. This reported clinical picture of acquired resistance to toceranib phosphate formed the basis of the project presented herein. The aims of these studies were to development an *in vitro* model of TOC resistance in canine MCT, identify mechanisms that confer the observed resistance, and identify clinically relevant biomarkers of TOC resistance.

The first aim is addressed in **Chapter 2 (Development of an *in vitro* model of acquired resistance to toceranib phosphate (Palladia®) in canine mast cell tumor).** To begin to uncover the mechanisms of acquired resistance to TOC in canine MCT, we developed three TOC-resistant MCT cell lines by chronically exposing a TOC-sensitive, *c-kit*-mutant MCT cell line (C2) to increasing concentrations of TOC. We confirm the emergence of resistant clones by growth inhibition assays using both TOC and three other KIT inhibitors: imatinib, masitinib, and LY2457546. We further characterize the resistant phenotype by evaluating the differential

induction of apoptosis by TUNEL labeling in each subline. To evaluate drug effects on KIT activation, western analysis for phosphorylated KIT was performed. We found that while TOC inhibited KIT phosphorylation in the parental C2 line in a dose-dependent manner, phosphorylation of KIT was maintained in the presence of TOC in all three resistant sublines. From these data, we hypothesized that the acquisition of secondary mutations in *c-kit* confer the observed resistance to TOC. To test this, full-length canine *c-kit* from the TOC-sensitive and -resistant sublines was cloned and sequenced. This resulted in the identification of six novel point mutations in the juxtamembrane and kinase domains of the resistant clones.

In order to further characterize the secondary mutations identified in KIT in the TOC-resistant sublines, in **Chapter 3 (Acquisition of secondary mutations in *c-kit* confer resistance to toceranib phosphate (Palladia®) in canine mast cell tumor cells),** we pursued computational-based homology modeling of the TOC-resistant KIT proteins with respect to TOC-sensitive KIT. The TOC-sensitive and TOC-resistant KIT mutants were docked with the all four KIT inhibitors to explore the consequence of the point mutations on drug binding. We found by docking studies that all the secondary KIT mutations were predicted to bind less favorably than the TOC-sensitive KIT protein. Upon further analysis of the mutated structures, we identified a narrowing of the entrance to the drug binding sites in all three resistant proteins and well as loss of critical hydrogen binding necessary for the stability of the ATP- and allosteric binding sites. Finally, we used this structure-based prediction of mutation-induced drug resistance to predict response of TOC-resistant cells to the novel KIT inhibitor, ponatinib. We concluded that computer-based homology modeling of mutated target kinases demonstrate how defined mutations can confer resistance and underscores the model's predictive ability in testing sensitivity to new selective inhibitors.

Identification of mechansims of resistance to targeted therapy is critical to developing strategies for rational design of novel inhibitors to circumvent resistance once it develops. Early identification of patients that will not respond to a selected therapy underscores the importance for the development of sensitive and specific biomarkers. In **Chapter 4 (Expression of phosphorylated-KIT in canine mast cell tumor: significance as a marker of tumor aggressiveness and response to KIT inhibition)**, we developed a clinically relevant immunohistochemistry based assay to quickly assess KIT activation in response to TOC therapy. Dogs presenting to Colorado State University's Veterinary Teaching Hospital with MCT were enrolled in a clinical trial to investigate the utility of this assay. Six-millimeter punch biopsies were obtained prior to the first dose (2.75 mg/kg) of TOC ($t_0$) and 6 hours following TOC ($t_6$). Pre- and post-TOC biopsies were evaluated for differences in pKIT labeling with IHC and these responses were compared to tumor response using RECIST criteria. MCTs from 4/7 (57.1%) patients demonstrated a partial response to TOC therapy, 2/7 (28.6%) patients showed stable disease, and one patient demonstrated progressive disease. Of the four patients characterized by a PR, 3/4 (75%) demonstrated a reduction in pKIT 6 hours after the first dose of TOC. Of the two patients that were classified with SD, one dog showed no change in pre- and post-TOC pKIT activity while another dog demonstrated a 100% reduction in pKIT activity. Finally, one patient ultimately progressed on treatment despite showing an initial response to KIT inhibition, consistent with acquired resistance to TOC. While the cohort of dogs enrolled in this study was small, the trend suggests that assessment of KIT activation by pKIT with IHC provides a rapid pharmacodynamic biomarker that demonstrates successful or unsuccessful target modulation. Monitoring the pKIT status during the course of treatment could serve as a reasonable pharmacodynamic endpoint of response to TOC in order to identify non-responders that may

benefit from alternative therapy.

This dissertation has two main overarching goals: the first is to develop a model of acquired resistance to TOC in canine MCT and identify distinctive molecular features of resistance. The second goal is to characterize these molecular features by structural analysis of the target proteins that contain the resistance mutations. By developing a high quality template structure of the drug-protein complex, we established a structure-based method that shows promising capability for predicting response to novel KIT inhibitors.

## References


1. London CA, Seguin B (2003) Mast cell tumors in the dog. Veterinary Clinics of North America: Small Animal Practice 33: 473-489.
2. Thamm CALaDH (2013) Mast Cell Tumors; Stephen J. Withrow DMV, Rodney L. Page, editor.
3. Webster JD, Yuzbasiyan-Gurkan V, Kaneene JB, Miller R, Resau JH, et al. (2006) The role of c-KIT in tumorigenesis: evaluation in canine cutaneous mast cell tumors. Neoplasia 8: 104-111.
4. Roskoski R, Jr. (2005) Signaling by Kit protein-tyrosine kinase--the stem cell factor receptor. Biochem Biophys Res Commun 337: 1-13.
5. Letard S, Yang Y, Hanssens K, Palmerini F, Leventhal PS, et al. (2008) Gain-of-function mutations in the extracellular domain of KIT are common in canine mast cell tumors. Mol Cancer Res 6: 1137-1145.
6. Ma Y, Longley BJ, Wang X, Blount JL, Langley K, et al. (1999) Clustering of activating mutations in c-KIT's juxtamembrane coding region in canine mast cell neoplasms. J Invest Dermatol 112: 165-170.
7. London CA, Galli SJ, Yuuki T, Hu ZQ, Helfand SC, et al. (1999) Spontaneous canine mast cell tumors express tandem duplications in the proto-oncogene c-kit. Exp Hematol 27: 689-697.
8. Qiu FH, Ray P, Brown K, Barker PE, Jhanwar S, et al. (1988) Primary structure of c-kit: relationship with the CSF-1/PDGF receptor kinase family--oncogenic activation of v-kit involves deletion of extracellular domain and C terminus. EMBO J 7: 1003-1011.
9. Ronnstrand L (2004) Signal transduction via the stem cell factor receptor/c-Kit. Cell Mol Life Sci 61: 2535-2548.
10. Lyman SD, Jacobsen SE (1998) c-kit ligand and Flt3 ligand: stem/progenitor cell factors with overlapping yet distinct activities. Blood 91: 1101-1134.
11. Nocka K, Buck J, Levi E, Besmer P (1990) Candidate ligand for the c-kit transmembrane kinase receptor: KL, a fibroblast derived growth factor stimulates mast cells and erythroid progenitors. EMBO J 9: 3287-3294.
12. Griffith LKAaR (2013) Therapeutic targeting of c-KIT in cancer. Expert Opin Investig Drugs 22: 103-115.
13. Huang E, Nocka K, Beier DR, Chu TY, Buck J, et al. (1990) The hematopoietic growth factor KL is encoded by the Sl locus and is the ligand of the c-kit receptor, the gene product of the W locus. Cell 63: 225-233.
14. Meininger CJ, Yano H, Rottapel R, Bernstein A, Zsebo KM, et al. (1992) The c-kit receptor ligand functions as a mast cell chemoattractant. Blood 79: 958-963.
15. Dastych J, Metcalfe DD (1994) Stem cell factor induces mast cell adhesion to fibronectin. J Immunol 152: 213-219.
16. Tsai M, Takeishi T, Thompson H, Langley KE, Zsebo KM, et al. (1991) Induction of mast cell proliferation, maturation, and heparin synthesis by the rat c-kit ligand, stem cell factor. Proc Natl Acad Sci U S A 88: 6382-6386.
17. Kitamura Y, Go S, Hatanaka K (1978) Decrease of mast cells in W/Wv mice and their increase by bone marrow transplantation. Blood 52: 447-452.

18. Kitamura Y, Go S (1979) Decreased production of mast cells in S1/S1d anemic mice. Blood 53: 492-497.
19. Roskoski R, Jr. (2004) Src protein-tyrosine kinase structure and regulation. Biochem Biophys Res Commun 324: 1155-1164.
20. Linnekin D, DeBerry CS, Mou S (1997) Lyn associates with the juxtamembrane region of c-Kit and is activated by stem cell factor in hematopoietic cell lines and normal progenitor cells. J Biol Chem 272: 27450-27455.
21. Lennartsson J, Blume-Jensen P, Hermanson M, Ponten E, Carlberg M, et al. (1999) Phosphorylation of Shc by Src family kinases is necessary for stem cell factor receptor/c-kit mediated activation of the Ras/MAP kinase pathway and c-fos induction. Oncogene 18: 5546-5553.
22. Jensen BM, Akin C, Gilfillan AM (2008) Pharmacological targeting of the KIT growth factor receptor: a therapeutic consideration for mast cell disorders. Br J Pharmacol 154: 1572-1582.
23. Herbst R, Shearman MS, Jallal B, Schlessinger J, Ullrich A (1995) Formation of signal transfer complexes between stem cell and platelet-derived growth factor receptors and SH2 domain proteins in vitro. Biochemistry 34: 5971-5979.
24. Blume-Jensen P, Wernstedt C, Heldin CH, Ronnstrand L (1995) Identification of the major phosphorylation sites for protein kinase C in kit/stem cell factor receptor in vitro and in intact cells. J Biol Chem 270: 14192-14200.
25. Chen YT, Tan KA, Pang LY, Argyle DJ (2012) The class I PI3K/Akt pathway is critical for cancer cell survival in dogs and offers an opportunity for therapeutic intervention. BMC Vet Res 8: 73.
26. Pryer NK, Lee LB, Zadovaskaya R, Yu X, Sukbuntherng J, et al. (2003) Proof of target for SU11654: inhibition of KIT phosphorylation in canine mast cell tumors. Clin Cancer Res 9: 5729-5734.
27. Turner AM, Zsebo KM, Martin F, Jacobsen FW, Bennett LG, et al. (1992) Nonhematopoietic tumor cell lines express stem cell factor and display c-kit receptors. Blood 80: 374-381.
28. Heinrich MC, Blanke CD, Druker BJ, Corless CL (2002) Inhibition of KIT tyrosine kinase activity: a novel molecular approach to the treatment of KIT-positive malignancies. J Clin Oncol 20: 1692-1703.
29. London CA (2009) Tyrosine kinase inhibitors in veterinary medicine. Top Companion Anim Med 24: 106-112.
30. Deangelo DJ, Chen L, Guerin A, Styles A, Giguere-Duval P, et al. (2013) Impact of Timely Switching From Imatinib to a Second-Generation Tyrosine Kinase Inhibitor After 12-Month Complete Cytogenetic Response Failure: A Chart Review Analysis. Clin Lymphoma Myeloma Leuk.
31. Antonescu C (2012) Gastrointestinal stromal tumors. Curr Top Microbiol Immunol 355: 41-57.
32. Lerner NB, Nocka KH, Cole SR, Qiu FH, Strife A, et al. (1991) Monoclonal antibody YB5.B8 identifies the human c-kit protein product. Blood 77: 1876-1883.
33. Chan PM, Ilangumaran S, La Rose J, Chakrabartty A, Rottapel R (2003) Autoinhibition of the kit receptor tyrosine kinase by the cytosolic juxtamembrane region. Mol Cell Biol 23: 3067-3078.

34. Peter B, Hadzijusufovic E, Blatt K, Gleixner KV, Pickl WF, et al. (2010) KIT polymorphisms and mutations determine responses of neoplastic mast cells to bafetinib (INNO-406). Exp Hematol 38: 782-791.
35. Carlsten KS, London CA, Haney S, Burnett R, Avery AC, et al. (2012) Multicenter prospective trial of hypofractionated radiation treatment, toceranib, and prednisone for measurable canine mast cell tumors. J Vet Intern Med 26: 135-141.
36. Lin TY, Bear M, Du Z, Foley KP, Ying W, et al. (2008) The novel HSP90 inhibitor STA-9090 exhibits activity against Kit-dependent and -independent malignant mast cell tumors. Exp Hematol 36: 1266-1277.
37. Zemke D, Yamini B, Yuzbasiyan-Gurkan V (2002) Mutations in the Juxtamembrane Domain of c-KIT Are Associated with Higher Grade Mast Cell Tumors in Dogs. Veterinary Pathology 39: 529-535.
38. Takeuchi Y, Fujino Y, Fukushima K, Watanabe M, Nakagawa T, et al. (2012) Biological effect of tyrosine kinase inhibitors on three canine mast cell tumor cell lines with various KIT statuses. J Vet Pharmacol Ther 35: 97-104.
39. Byun JS, Kwak BK, Kim JK, Jung J, Ha BC, et al. (2013) Engraftment of human mesenchymal stem cells in a rat photothrombotic cerebral infarction model : comparison of intra-arterial and intravenous infusion using MRI and histological analysis. J Korean Neurosurg Soc 54: 467-476.
40. Jang HJ, Ha BK, Kim JW, Jung KH, Ahn J, et al. (2013) Comparison of extraction phases for a two-phase culture of a recombinant E. coli producing retinoids. Biotechnol Lett.
41. Wohl DA, Arnoczy G, Fichtenbaum CJ, Campbell T, Taiwo B, et al. (2013) Comparison of cardiovascular disease risk markers in HIV-infected patients receiving abacavir and tenofovir: the nucleoside inflammation, coagulation and endothelial function (NICE) study. Antivir Ther.
42. Lee KW, Kim Y, Perinpanayagam H, Lee JK, Yoo YJ, et al. (2014) Comparison of alternative image reformatting techniques in micro-computed tomography and tooth clearing for detailed canal morphology. J Endod 40: 417-422.
43. Yi JH, Shin JY, Ha BJ, Kim SW, Cho BJ, et al. (2009) The comparison of central and mean true-net power (Pentacam) in calculating IOL-power after refractive surgery. Korean J Ophthalmol 23: 1-5.
44. Won JB, Kim SW, Kim EK, Ha BJ, Kim TI (2008) Comparison of internal and total optical aberrations for 2 aberrometers: iTrace and OPD scan. Korean J Ophthalmol 22: 210-213.
45. Berns K, Horlings HM, Hennessy BT, Madiredjo M, Hijmans EM, et al. (2007) A functional genetic approach identifies the PI3K pathway as a major determinant of trastuzumab resistance in breast cancer. Cancer Cell 12: 395-402.
46. Bradeen HA, Eide CA, O'Hare T, Johnson KJ, Willis SG, et al. (2006) Comparison of imatinib mesylate, dasatinib (BMS-354825), and nilotinib (AMN107) in an N-ethyl-N-nitrosourea (ENU)-based mutagenesis screen: high efficacy of drug combinations. Blood 108: 2332-2338.
47. Downing S, Chien MB, Kass PH, Moore PE, London CA (2002) Prevalence and importance of internal tandem duplications in exons 11 and 12 of c-kit in mast cell tumors of dogs. Am J Vet Res 63: 1718-1723.
48. dos Santos LV, Lima JP, Abdalla KC, Bragagnoli AC, Santos FA, et al. (2013) Imatinib-induced bone edema: case report and review of literature. J Natl Compr Canc Netw 11: 1187-1191.

49. Chang NY, Wang J, Wen MC, Lee FY (2013) Langerhans Cell Sarcoma in a Chronic Myelogenous Leukemia Patient Undergoing Imatinib Mesylate Therapy: A Case Study and Review of the Literature. Int J Surg Pathol.
50. Akasbi Y, Arifi S, Brahmi SA, El Mrabet FZ, Mellas N, et al. (2013) Intolerance to Imatinib in Gastrointestinal Stromal Tumors: A Case Report and a Review of Literature. J Gastrointest Cancer.
51. Hoffmann VS, Baccarani M, Lindoerfer D, Castagnetti F, Turkina A, et al. (2013) The EUTOS prognostic score: review and validation in 1288 patients with CML treated frontline with imatinib. Leukemia 27: 2016-2022.
52. Brazzelli V, Grasso V, Borroni G (2013) Imatinib, dasatinib and nilotinib: a review of adverse cutaneous reactions with emphasis on our clinical experience. J Eur Acad Dermatol Venereol 27: 1471-1480.
53. Qu SQ, Wang Y, Sun XJ (2013) [FIP1L1-PDGFRA positive chronic eosinophilic leukemia with imatinib-resistant T674I mutant of PDGFRA gene: a case report and literature review]. Zhonghua Xue Ye Xue Za Zhi 34: 159-161.
54. Griffin JD, Guerin A, Chen L, Macalalad AR, Luo J, et al. (2013) Comparing nilotinib with dasatinib as second-line therapies in patients with chronic myelogenous leukemia resistant or intolerant to imatinib -- a retrospective chart review analysis. Curr Med Res Opin 29: 623-631.
55. Gotta V, Buclin T, Csajka C, Widmer N (2013) Systematic review of population pharmacokinetic analyses of imatinib and relationships with treatment outcomes. Ther Drug Monit 35: 150-167.
56. Mealing S, Barcena L, Hawkins N, Clark J, Eaton V, et al. (2013) The relative efficacy of imatinib, dasatinib and nilotinib for newly diagnosed chronic myeloid leukemia: a systematic review and network meta-analysis. Exp Hematol Oncol 2: 5.
57. Ichikawa K, Aritaka N, Sekiguchi Y, Sugimoto KJ, Imai H, et al. (2012) C-kit-positive acute myelogenous leukemia effectively treated with imatinib: a case report and review of the literature. Geriatr Gerontol Int 12: 762-764.
58. Chen L, Guerin A, Xie J, Wu EQ, Yu AP, et al. (2012) Monitoring and switching patterns of patients with chronic myeloid leukemia treated with imatinib in community settings: a chart review analysis. Curr Med Res Opin 28: 1831-1839.
59. Ran HH, Zhang R, Lu XC, Yang B, Fan H, et al. (2012) Imatinib-induced decompensated heart failure in an elderly patient with chronic myeloid leukemia: case report and literature review. J Geriatr Cardiol 9: 411-414.
60. Wang YD, Cui GH, You Y, Li M, Xia J, et al. (2012) [Reactivation of chronic hepatitis B infection related to imatinib mesylate therapy in patients with chronic myeloid leukemia: two cases report and literatures review]. Zhonghua Xue Ye Xue Za Zhi 33: 743-746.
61. Guo L, Chen XX, Gu YY, Zou HJ, Ye S (2012) Low-dose imatinib in the treatment of severe systemic sclerosis: a case series of six Chinese patients and literature review. Clin Rheumatol 31: 1395-1400.
62. Wu KN, Luo Y, Liu LZ, Zhao YM, Hu YX, et al. (2012) Twin pregnancy and childbirth after reduced-intensity conditioning allogeneic haematopoietic stem cell transplantation combined with imatinib mesylate for chronic myeloid leukaemia: case report and literature review. J Int Med Res 40: 2409-2415.
63. Michels GM, Knapp DW, DeNicola DB, Glickman N, Bonney P (2002) Prognosis following surgical excision of canine cutaneous mast cell tumors with histopathologically tumor-

free versus nontumor-free margins: a retrospective study of 31 cases. J Am Anim Hosp Assoc 38: 458-466.
64. Simpson AM, Ludwig LL, Newman SJ, Bergman PJ, Hottinger HA, et al. (2004) Evaluation of surgical margins required for complete excision of cutaneous mast cell tumors in dogs. J Am Vet Med Assoc 224: 236-240.
65. Fulcher RP, Ludwig LL, Bergman PJ, Newman SJ, Simpson AM, et al. (2006) Evaluation of a two-centimeter lateral surgical margin for excision of grade I and grade II cutaneous mast cell tumors in dogs. J Am Vet Med Assoc 228: 210-215.
66. Schultheiss PC, Gardiner DW, Rao S, Olea-Popelka F, Tuohy JL (2011) Association of histologic tumor characteristics and size of surgical margins with clinical outcome after surgical removal of cutaneous mast cell tumors in dogs. J Am Vet Med Assoc 238: 1464-1469.
67. Bournia VK, Evangelou K, Sfikakis PP (2013) Therapeutic inhibition of tyrosine kinases in systemic sclerosis: a review of published experience on the first 108 patients treated with imatinib. Semin Arthritis Rheum 42: 377-390.
68. Lejeune A, Skorupski K, Frazier S, Vanhaezebrouck I, Rebhun RB, et al. (2013) Aggressive local therapy combined with systemic chemotherapy provides long-term control in grade II stage 2 canine mast cell tumour: 21 cases (1999-2012). Vet Comp Oncol.
69. Webster JD, Yuzbasiyan-Gurkan V, Thamm DH, Hamilton E, Kiupel M (2008) Evaluation of prognostic markers for canine mast cell tumors treated with vinblastine and prednisone. BMC Vet Res 4: 32.
70. Treglia G, Mirk P, Stefanelli A, Rufini V, Giordano A, et al. (2012) 18F-Fluorodeoxyglucose positron emission tomography in evaluating treatment response to imatinib or other drugs in gastrointestinal stromal tumors: a systematic review. Clin Imaging 36: 167-175.
71. Rogers G, Hoyle M, Thompson Coon J, Moxham T, Liu Z, et al. (2012) Dasatinib and nilotinib for imatinib-resistant or -intolerant chronic myeloid leukaemia: a systematic review and economic evaluation. Health Technol Assess 16: 1-410.
72. Saad Aldin E, Mourad F, Tfayli A (2012) Gastric antral vascular ectasia in a patient with GIST after treatment with imatinib: case report and literature review. Jpn J Clin Oncol 42: 447-450.
73. Liao AT, Chien MB, Shenoy N, Mendel DB, McMahon G, et al. (2002) Inhibition of constitutively active forms of mutant kit by multitargeted indolinone tyrosine kinase inhibitors. Blood 100: 585-593.
74. Sleijfer S, Wiemer E, Seynaeve C, Verweij J (2007) Improved insight into resistance mechanisms to imatinib in gastrointestinal stromal tumors: a basis for novel approaches and individualization of treatment. Oncologist 12: 719-726.
75. Richters A, Ketzer J, Getlik M, Grutter C, Schneider R, et al. (2013) Targeting Gain of Function and Resistance Mutations in Abl and KIT by Hybrid Compound Design. J Med Chem.
76. Moen MD, McKeage K, Plosker GL, Siddiqui MA (2007) Imatinib: a review of its use in chronic myeloid leukaemia. Drugs 67: 299-320.
77. Isotani M, Ishida N, Tominaga M, Tamura K, Yagihara H, et al. (2008) Effect of tyrosine kinase inhibition by imatinib mesylate on mast cell tumors in dogs. J Vet Intern Med 22: 985-988.

78. Marconato L, Bettini G, Giacoboni C, Romanelli G, Cesari A, et al. (2008) Clinicopathological features and outcome for dogs with mast cell tumors and bone marrow involvement. J Vet Intern Med 22: 1001-1007.
79. Dubreuil P, Letard S, Ciufolini M, Gros L, Humbert M, et al. (2009) Masitinib (AB1010), a potent and selective tyrosine kinase inhibitor targeting KIT. PLoS One 4: e7258.
80. Hahn KA, Ogilvie G, Rusk T, Devauchelle P, Leblanc A, et al. (2008) Masitinib is safe and effective for the treatment of canine mast cell tumors. J Vet Intern Med 22: 1301-1309.
81. Marech I, Patruno R, Zizzo N, Gadaleta C, Introna M, et al. (2013) Masitinib (AB1010), from canine tumor model to human clinical development: Where we are? Crit Rev Oncol Hematol.
82. Hahn KA, Legendre AM, Shaw NG, Phillips B, Ogilvie GK, et al. (2010) Evaluation of 12- and 24-month survival rates after treatment with masitinib in dogs with nonresectable mast cell tumors. Am J Vet Res 71: 1354-1361.
83. He HS, Su GP, Chen BB (2011) [Initial therapy of imatinib mesylate for extramedullary T lymphoblastic crisis of chronic myeloid leukemia: a case report and review of the literature]. Zhonghua Xue Ye Xue Za Zhi 32: 477-478.
84. Mena AC, Pulido EG, Guillen-Ponce C (2010) Understanding the molecular-based mechanism of action of the tyrosine kinase inhibitor: sunitinib. Anticancer Drugs 21 Suppl 1: S3-11.
85. London CA, Malpas PB, Wood-Follis SL, Boucher JF, Rusk AW, et al. (2009) Multi-center, placebo-controlled, double-blind, randomized study of oral toceranib phosphate (SU11654), a receptor tyrosine kinase inhibitor, for the treatment of dogs with recurrent (either local or distant) mast cell tumor following surgical excision. Clin Cancer Res 15: 3856-3865.
86. Yancey MF, Merritt DA, Lesman SP, Boucher JF, Michels GM (2010) Pharmacokinetic properties of toceranib phosphate (Palladia, SU11654), a novel tyrosine kinase inhibitor, in laboratory dogs and dogs with mast cell tumors. J Vet Pharmacol Ther 33: 162-171.
87. Tanriverdi O, Unubol M, Taskin F, Meydan N, Sargin G, et al. (2012) Imatinib-associated bilateral gynecomastia and unilateral testicular hydrocele in male patient with metastatic gastrointestinal stromal tumor: a literature review. J Oncol Pharm Pract 18: 303-310.
88. London CA, Hannah AL, Zadovoskaya R, Chien MB, Kollias-Baker C, et al. (2003) Phase I dose-escalating study of SU11654, a small molecule receptor tyrosine kinase inhibitor, in dogs with spontaneous malignancies. Clin Cancer Res 9: 2755-2768.
89. Engelman JA, Janne PA (2008) Mechanisms of acquired resistance to epidermal growth factor receptor tyrosine kinase inhibitors in non-small cell lung cancer. Clin Cancer Res 14: 2895-2899.
90. Garraway LA, Janne PA (2012) Circumventing cancer drug resistance in the era of personalized medicine. Cancer Discov 2: 214-226.
91. Sierra JR, Cepero V, Giordano S (2010) Molecular mechanisms of acquired resistance to tyrosine kinase targeted therapy. Mol Cancer 9: 75.
92. Zhang J, Yang PL, Gray NS (2009) Targeting cancer with small molecule kinase inhibitors. Nat Rev Cancer 9: 28-39.
93. Sherbenou DW, Druker BJ (2007) Applying the discovery of the Philadelphia chromosome. J Clin Invest 117: 2067-2074.

94. Kuo T, Fisher GA (2005) Current status of small-molecule tyrosine kinase inhibitors targeting epidermal growth factor receptor in colorectal cancer. Clin Colorectal Cancer 5 Suppl 2: S62-70.
95. Ogino A, Kitao H, Hirano S, Uchida A, Ishiai M, et al. (2007) Emergence of epidermal growth factor receptor T790M mutation during chronic exposure to gefitinib in a non small cell lung cancer cell line. Cancer Res 67: 7807-7814.
96. Pao W, Miller VA, Politi KA, Riely GJ, Somwar R, et al. (2005) Acquired resistance of lung adenocarcinomas to gefitinib or erlotinib is associated with a second mutation in the EGFR kinase domain. PLoS Med 2: e73.
97. Heinrich MC, Corless CL, Blanke CD, Demetri GD, Joensuu H, et al. (2006) Molecular correlates of imatinib resistance in gastrointestinal stromal tumors. J Clin Oncol 24: 4764-4774.
98. Engelman JA, Zejnullahu K, Mitsudomi T, Song Y, Hyland C, et al. (2007) MET amplification leads to gefitinib resistance in lung cancer by activating ERBB3 signaling. Science 316: 1039-1043.
99. Yano S, Wang W, Li Q, Matsumoto K, Sakurama H, et al. (2008) Hepatocyte growth factor induces gefitinib resistance of lung adenocarcinoma with epidermal growth factor receptor-activating mutations. Cancer Res 68: 9479-9487.
100. Gorre ME, Mohammed M, Ellwood K, Hsu N, Paquette R, et al. (2001) Clinical resistance to STI-571 cancer therapy caused by BCR-ABL gene mutation or amplification. Science 293: 876-880.
101. Tipping AJ, Baluch S, Barnes DJ, Veach DR, Clarkson BM, et al. (2004) Efficacy of dual-specific Bcr-Abl and Src-family kinase inhibitors in cells sensitive and resistant to imatinib mesylate. Leukemia 18: 1352-1356.
102. King TR, Fang Y, Mahon ES, Anderson DH (2000) Using a phage display library to identify basic residues in A-Raf required to mediate binding to the Src homology 2 domains of the p85 subunit of phosphatidylinositol 3'-kinase. J Biol Chem 275: 36450-36456.
103. Gajiwala KS, Wu JC, Christensen J, Deshmukh GD, Diehl W, et al. (2009) KIT kinase mutants show unique mechanisms of drug resistance to imatinib and sunitinib in gastrointestinal stromal tumor patients. Proc Natl Acad Sci U S A 106: 1542-1547.
104. Bradshaw-Pierce EL, Pitts TM, Tan AC, McPhillips K, West M, et al. (2013) Tumor P-Glycoprotein Correlates with Efficacy of PF-3758309 in in vitro and in vivo Models of Colorectal Cancer. Front Pharmacol 4: 22.
105. Ercan D, Zejnullahu K, Yonesaka K, Xiao Y, Capelletti M, et al. (2010) Amplification of EGFR T790M causes resistance to an irreversible EGFR inhibitor. Oncogene 29: 2346-2356.
106. Mahadevan D, Cooke L, Riley C, Swart R, Simons B, et al. (2007) A novel tyrosine kinase switch is a mechanism of imatinib resistance in gastrointestinal stromal tumors. Oncogene 26: 3909-3919.
107. Sawabu T, Seno H, Kawashima T, Fukuda A, Uenoyama Y, et al. (2007) Growth arrest-specific gene 6 and Axl signaling enhances gastric cancer cell survival via Akt pathway. Mol Carcinog 46: 155-164.
108. Mahon FX, Hayette S, Lagarde V, Belloc F, Turcq B, et al. (2008) Evidence that resistance to nilotinib may be due to BCR-ABL, Pgp, or Src kinase overexpression. Cancer Res 68: 9809-9816.

109. Ito T, Tanaka H, Kimura A (2007) Establishment and characterization of a novel imatinib-sensitive chronic myeloid leukemia cell line MYL, and an imatinib-resistant subline MYL-R showing overexpression of Lyn. Eur J Haematol 78: 417-431.
110. Wagle N, Emery C, Berger MF, Davis MJ, Sawyer A, et al. (2011) Dissecting therapeutic resistance to RAF inhibition in melanoma by tumor genomic profiling. J Clin Oncol 29: 3085-3096.
111. Gustafson DL, Long ME (2001) Alterations in P-glycoprotein expression in mouse tissues by doxorubicin: implications for pharmacokinetics in multiple dosing regimens. Chem Biol Interact 138: 43-57.
112. Mahon FX, Belloc F, Lagarde V, Chollet C, Moreau-Gaudry F, et al. (2003) MDR1 gene overexpression confers resistance to imatinib mesylate in leukemia cell line models. Blood 101: 2368-2373.
113. Mistry P, Stewart AJ, Dangerfield W, Okiji S, Liddle C, et al. (2001) In vitro and in vivo reversal of P-glycoprotein-mediated multidrug resistance by a novel potent modulator, XR9576. Cancer Res 61: 749-758.
114. Zajchowski DA, Karlan BY, Shawver LK (2012) Treatment-related protein biomarker expression differs between primary and recurrent ovarian carcinomas. Mol Cancer Ther 11: 492-502.
115. Borst P, Schinkel AH, Smit JJ, Wagenaar E, Van Deemter L, et al. (1993) Classical and novel forms of multidrug resistance and the physiological functions of P-glycoproteins in mammals. Pharmacol Ther 60: 289-299.
116. Ling V (1997) Multidrug resistance: molecular mechanisms and clinical relevance. Cancer Chemother Pharmacol 40 Suppl: S3-8.
117. Che XF, Nakajima Y, Sumizawa T, Ikeda R, Ren XQ, et al. (2002) Reversal of P-glycoprotein mediated multidrug resistance by a newly synthesized 1,4-benzothiazipine derivative, JTV-519. Cancer Lett 187: 111-119.
118. Rumpold H, Wolf AM, Gruenewald K, Gastl G, Gunsilius E, et al. (2005) RNAi-mediated knockdown of P-glycoprotein using a transposon-based vector system durably restores imatinib sensitivity in imatinib-resistant CML cell lines. Exp Hematol 33: 767-775.
119. Widmer N, Rumpold H, Untergasser G, Fayet A, Buclin T, et al. (2007) Resistance reversal by RNAi silencing of MDR1 in CML cells associated with increase in imatinib intracellular levels. Leukemia 21: 1561-1562; author reply 1562-1564.
120. Diestra JE, Scheffer GL, Catala I, Maliepaard M, Schellens JH, et al. (2002) Frequent expression of the multi-drug resistance-associated protein BCRP/MXR/ABCP/ABCG2 in human tumours detected by the BXP-21 monoclonal antibody in paraffin-embedded material. J Pathol 198: 213-219.
121. Elkind NB, Szentpetery Z, Apati A, Ozvegy-Laczka C, Varady G, et al. (2005) Multidrug transporter ABCG2 prevents tumor cell death induced by the epidermal growth factor receptor inhibitor Iressa (ZD1839, Gefitinib). Cancer Res 65: 1770-1777.
122. Gambacorti-Passerini C, Zucchetti M, Russo D, Frapolli R, Verga M, et al. (2003) Alpha1 acid glycoprotein binds to imatinib (STI571) and substantially alters its pharmacokinetics in chronic myeloid leukemia patients. Clin Cancer Res 9: 625-632.
123. Gambacorti-Passerini C, Barni R, le Coutre P, Zucchetti M, Cabrita G, et al. (2000) Role of alpha1 acid glycoprotein in the in vivo resistance of human BCR-ABL(+) leukemic cells to the abl inhibitor STI571. J Natl Cancer Inst 92: 1641-1650.

124. le Coutre P, Kreuzer KA, Na IK, Lupberger J, Holdhoff M, et al. (2002) Determination of alpha-1 acid glycoprotein in patients with Ph+ chronic myeloid leukemia during the first 13 weeks of therapy with STI571. Blood Cells Mol Dis 28: 75-85.
125. Gotink KJ, Broxterman HJ, Labots M, de Haas RR, Dekker H, et al. (2011) Lysosomal sequestration of sunitinib: a novel mechanism of drug resistance. Clin Cancer Res 17: 7337-7346.
126. Hanahan D, Weinberg RA (2011) Hallmarks of cancer: the next generation. Cell 144: 646-674.
127. Kim H, Tu HC, Ren D, Takeuchi O, Jeffers JR, et al. (2009) Stepwise activation of BAX and BAK by tBID, BIM, and PUMA initiates mitochondrial apoptosis. Mol Cell 36: 487-499.
128. Faber AC, Corcoran RB, Ebi H, Sequist LV, Waltman BA, et al. (2011) BIM expression in treatment-naive cancers predicts responsiveness to kinase inhibitors. Cancer Discov 1: 352-365.
129. Nakagawa T, Takeuchi S, Yamada T, Ebi H, Sano T, et al. (2013) EGFR-TKI resistance due to BIM polymorphism can be circumvented in combination with HDAC inhibition. Cancer Res 73: 2428-2434.
130. Paraiso KH, Xiang Y, Rebecca VW, Abel EV, Chen YA, et al. (2011) PTEN loss confers BRAF inhibitor resistance to melanoma cells through the suppression of BIM expression. Cancer Res 71: 2750-2760.
131. LaCasse EC, Baird S, Korneluk RG, MacKenzie AE (1998) The inhibitors of apoptosis (IAPs) and their emerging role in cancer. Oncogene 17: 3247-3259.
132. Xia W, Bacus S, Hegde P, Husain I, Strum J, et al. (2006) A model of acquired autoresistance to a potent ErbB2 tyrosine kinase inhibitor and a therapeutic strategy to prevent its onset in breast cancer. Proc Natl Acad Sci U S A 103: 7795-7800.
133. Todd JR, Becker TM, Kefford RF, Rizos H (2013) Secondary c-Kit mutations confer acquired resistance to RTK inhibitors in c-Kit mutant melanoma cells. Pigment Cell Melanoma Res 26: 518-526.
134. Azam M, Latek RR, Daley GQ (2003) Mechanisms of autoinhibition and STI-571/imatinib resistance revealed by mutagenesis of BCR-ABL. Cell 112: 831-843.
135. Emery CM, Vijayendran KG, Zipser MC, Sawyer AM, Niu L, et al. (2009) MEK1 mutations confer resistance to MEK and B-RAF inhibition. Proc Natl Acad Sci U S A 106: 20411-20416.
136. Guo T, Hajdu M, Agaram NP, Shinoda H, Veach D, et al. (2009) Mechanisms of sunitinib resistance in gastrointestinal stromal tumors harboring KITAY502-3ins mutation: an in vitro mutagenesis screen for drug resistance. Clin Cancer Res 15: 6862-6870.
137. Johannessen CM, Boehm JS, Kim SY, Thomas SR, Wardwell L, et al. (2010) COT drives resistance to RAF inhibition through MAP kinase pathway reactivation. Nature 468: 968-972.
138. Iorns E, Turner NC, Elliott R, Syed N, Garrone O, et al. (2008) Identification of CDK10 as an important determinant of resistance to endocrine therapy for breast cancer. Cancer Cell 13: 91-104.
139. Politi K, Fan PD, Shen R, Zakowski M, Varmus H (2010) Erlotinib resistance in mouse models of epidermal growth factor receptor-induced lung adenocarcinoma. Dis Model Mech 3: 111-119.

140. Bertucci F, Goncalves A, Monges G, Madroszyk A, Guiramand J, et al. (2006) Acquired resistance to imatinib and secondary KIT exon 13 mutation in gastrointestinal stromal tumour. Oncol Rep 16: 97-101.
141. O'Hare T, Shakespeare WC, Zhu X, Eide CA, Rivera VM, et al. (2009) AP24534, a pan-BCR-ABL inhibitor for chronic myeloid leukemia, potently inhibits the T315I mutant and overcomes mutation-based resistance. Cancer Cell 16: 401-412.
142. Weisberg E, Choi HG, Ray A, Barrett R, Zhang J, et al. (2010) Discovery of a small-molecule type II inhibitor of wild-type and gatekeeper mutants of BCR-ABL, PDGFRalpha, Kit, and Src kinases: novel type II inhibitor of gatekeeper mutants. Blood 115: 4206-4216.
143. Li D, Ambrogio L, Shimamura T, Kubo S, Takahashi M, et al. (2008) BIBW2992, an irreversible EGFR/HER2 inhibitor highly effective in preclinical lung cancer models. Oncogene 27: 4702-4711.
144. Engelman JA, Zejnullahu K, Gale CM, Lifshits E, Gonzales AJ, et al. (2007) PF00299804, an irreversible pan-ERBB inhibitor, is effective in lung cancer models with EGFR and ERBB2 mutations that are resistant to gefitinib. Cancer Res 67: 11924-11932.
145. Villanueva J, Vultur A, Lee JT, Somasundaram R, Fukunaga-Kalabis M, et al. (2010) Acquired resistance to BRAF inhibitors mediated by a RAF kinase switch in melanoma can be overcome by cotargeting MEK and IGF-1R/PI3K. Cancer Cell 18: 683-695.
146. Liegl B, Kepten I, Le C, Zhu M, Demetri GD, et al. (2008) Heterogeneity of kinase inhibitor resistance mechanisms in GIST. J Pathol 216: 64-74.
147. Bean J, Brennan C, Shih JY, Riely G, Viale A, et al. (2007) MET amplification occurs with or without T790M mutations in EGFR mutant lung tumors with acquired resistance to gefitinib or erlotinib. Proc Natl Acad Sci U S A 104: 20932-20937.
148. Shukla S, Robey RW, Bates SE, Ambudkar SV (2009) Sunitinib (Sutent, SU11248), a small-molecule receptor tyrosine kinase inhibitor, blocks function of the ATP-binding cassette (ABC) transporters P-glycoprotein (ABCB1) and ABCG2. Drug Metab Dispos 37: 359-365.

## Chapter 2

# Development of an *in vitro* model of acquired resistance to toceranib phosphate (Palladia®) in canine mast cell tumor


## SUMMARY

Mast cell tumors (MCTs) are the most common skin tumors in dogs and exhibit variable biologic behavior. Mutations in the *c-kit* proto-oncogene are associated with the tumorigenesis of MCTs, resulting in growth factor-independent and constitutive phosphorylation of the KIT receptor tyrosine kinase (RTK). Toceranib (TOC) phosphate (Palladia®) is a KIT RTK inhibitor that has biological activity against MCTs. Despite these benefits, patients ultimately develop resistance to TOC. Therefore, there is a need to identify distinguishing clinical and molecular features of resistance in this population. The canine C2 mastocytoma cell line contains an activating mutation in *c-kit*. Three TOC-resistant C2 sublines (TR1, TR2, TR3) were established over seven months by growing cells in increasing concentrations of TOC. TOC inhibited KIT phosphorylation and cell proliferation in a dose-dependent manner in the treatment-naïve, parental C2 line ($IC_{50}$ <10 nM). In contrast, the three sublines were resistant to growth inhibition by TOC ($IC_{50}$ > 1,000 nM) and phosphorylation of the KIT receptor was less inhibited compared to the TOC-sensitive C2 cells. Interestingly, sensitivity to three structurally distinct KIT RTK inhibitors was variable among the sublines, and all 3 sublines retained sensitivity to the cytotoxic agents vinblastine and lomustine. Sequencing of *c-kit* revealed secondary mutations in the juxtamembrane and tyrosine kinase domains of the resistant sublines. These included point mutations in TR1 (Q574R, M835T), TR2 (K724R), and TR3 (K580R, R584G, A620S).

Additionally, chronic TOC exposure resulted in *c-kit* mRNA and KIT protein overexpression in the TOC-resistant sublines compared to the parental line. C2, TR1, TR2, and TR3 cells demonstrated minimal P-glycoprotein (P-gp) activity and no functional P-gp. This study demonstrates the development of an *in vitro* model of acquired resistance to targeted therapy in canine MCTs harboring a *c-kit*-activating mutation. This model may be used to investigate the molecular basis of and strategies to overcome TOC resistance.

## INTRODUCTION

The increased understanding of molecular mechanisms driving tumorigenesis in a wide array of neoplasms has led to the development of novel targeted therapies. While tyrosine kinase inhibitors (TKIs) are routinely employed in human oncology with success, their use in veterinary medicine is limited. Two small molecule TKIs, toceranib (TOC) phosphate (Palladia®; Zoetis, Madison, NJ) and masitinib (Masivet®, Kinavet®; AB Science, Paris, France) have been approved by the FDA for use in veterinary medicine for the treatment of recurrent, non-resectable intermediate and high grade canine cutaneous mast cell tumors (MCTs) [1]. The success of targeted therapies in both human and veterinary oncology, however, is largely tempered by the nearly inevitable development of drug resistance.

Cutaneous MCTs are the most common skin tumors in dogs, accounting for up to 21% of all canine cutaneous tumors, and exhibit variable biologic behavior [2-4]. Cutaneous MCTs commonly present as a solitary mass in older dogs with a mean age of onset of 9 years old. There is no sex predilection. While all breeds can be affected, Boxers, Boston terriers, Labrador retrievers, Weimaraners, Bulldogs, Beagles, and Schnauzers are over-represented [5].

Activating mutations in the juxtamembrane, kinase and ligand binding domains of the *c-kit* proto-oncogene have been associated with the tumorigenesis of canine MCTs, resulting in growth factor-independent and constitutive phosphorylation of the KIT receptor tyrosine kinase (RTK). Approximately one-third of canine MCTs carry a *c-kit* mutation and the majority of MCTs with *c-kit* mutations are histologically intermediate or high grade [2, 6, 7]. While the majority of gain-of-function mutations of *c-kit* have been identified in exon 11 of canine MCTs, exons 8 and 9, and less commonly exon 17, also acquire activating mutations [8, 9]. Our laboratory and others have shown that *c-kit* mutations, particularly internal tandem duplications (ITD) in the juxtamembrane domain, are significantly associated with an increased incidence of recurrent disease, metastasis, and death [2, 6-8, 10-12]. As such, small molecule inhibitors of KIT are an attractive therapeutic strategy for MCTs in dogs.

Toceranib phosphate is one such receptor tyrosine kinase inhibitor of KIT, approved for the treatment of recurrent, non-resectable grade 2 and 3 canine MCTs [13, 14]. While TOC has demonstrated significant biological activity, its usefulness is significantly limited by the eventual acquisition of drug resistance. In a multi-center, placebo-controlled, double-blind, randomized study of oral TOC, approximately 40% of dogs experienced an objective response while the remaining 60% demonstrated no response, likely due to *de novo* resistance. Two-thirds of the responders were positive for an activating mutation in *c-kit*. The average time to tumor progression in all responders was 18 weeks; therefore, virtually all dogs with MCTs have either intrinsic TOC resistance or eventually develop resistance [13]. Therefore, there exists a need to identify distinctive clinical and molecular features of resistance in this population.

The aim of the current study was to develop a model of acquired TOC resistance in canine MCT. Acquired resistance was modeled *in vitro* using the TOC-sensitive C2 canine MCT

cell line to subsequently allow us to investigate mechanisms of acquired resistance in order to ultimately develop second-line inhibitors as well as rational drug combination therapies for the treatment of TOC-resistant MCTs in dogs.

## METHODS

### Cell culture and generation of toceranib-resistant sublines from C2 cells

Toceranib phosphate was provided by Zoetis (Florham Park, NJ). Masitinib (AB1010, Kinavet®) and LY2457546 were provided by AB Science (Paris, France) and Elanco (Greenfield, IN), respectively. Imatinib was purchased from Selleck Chemical (Houston, TX). Vinblastine (VBL) and lomustine (CCNU) were purchased from Sigma (St. Louis, MO). Stock solutions of all drugs were prepared in DMSO and stored at -20°C. The *c-kit* mutant canine C2 mastocytoma cell line, derived from a spontaneously occurring cutaneous MCT, was used as the parental cell line [45]. Cells were propagated in RPMI 1640 supplemented with 2 mM L-glutamine, 10% FBS, 100 g/mL streptomycin, and 100 U/mL penicillin in a 37°C incubator under a humidified atmosphere of 5% $CO_2$. TOC-resistant C2 cells were selected by growing C2 cells in concentrations of TOC ranging from 0.02 uM to 0.3 uM and increasing in 0.025-0.05 uM increments. Three independent, TOC-resistant sublines were established over a period of 7 months.

### Drug Sensitivity Assays

The sensitivity and resistance of each cell line to TOC, three other TKIs, and the cytotoxic agents VBL or CCNU were determined by measuring relative viable cell number using

a bioreductive fluorometric assay (Alamar Blue, Promega; Madison, WI). All three C2 sublines as well as the treatment naïve, parental C2 cells were plated in triplicate in 96-well plates at densities of 2,000 cells per well. Cells were treated with increasing concentrations of TOC, three other KIT kinase inhibitors, VBL or CCNU for 72 hours. Alamar Blue reagent was added to all wells, plates were incubated for 1 hour at 37°C, and fluorescence was measured on a BioTek plate reader (BioTek, Winooski, VT). Dose-response curves were generated using Prism (GraphPad Software, La Jolla, CA).

**Terminal Deoxynucleotidyltransferase-Mediated dUTP Nick End Labeling (TUNEL) Apoptosis Assays**

To evaluate drug effects on the induction of apoptosis, the C2 parental and three TOC-resistant sublines were treated for 24 hr with increasing concentrations of TOC (0-100 nM) and the cytotoxic agents VBL and CCNU (0 ug/mL-100 ug/mL). Cells were harvested and resuspended in media. Approximately 250,000 cells were centrifuged at 40 x g for 4 minutes onto glass slides. Cytospins were dried and stored at 4°C overnight followed by fixation in 4% paraformaldehyde for 60 min at room temperature. Cells were permeabilized with 0.1% Triton X-100 in 0.1% sodium citrate solution for 2 min on ice. TUNEL staining was carried out following the manufacturer's instructions (Roche Applied Science, Indianapolis, IN). Slides were counterstained and mounted with DAPI (Vector, Burlingame, CA). Image analysis was performed using AxioVision 4.3 system software from Carl Zeiss using an Axioplan 2 imaging scope coupled with an AxioCam HRc Carl Zeiss camera.

**Western blot analysis**

To evaluate drug effects on KIT autophosphorylation, parental C2 cells and the resistant sublines were incubated for 24 hours with increasing concentrations of TOC (0-100 nM) and phosphorylated and total KIT were analyzed by western blot. Cells were resuspended in lysis buffer containing 1% Triton X-100, 100 nM sodium orthovanadate, 0.2 mM PMSF, 1 M Tris, 1 M NaCl, and 7X protease inhibitor cocktail (Roche Applied Science, Indianapolis, IN), incubated on ice for 15 min, and centrifuged for 5 min. Protein was separated by SDS-PAGE on a 6% acrylamide gel and transferred onto a polyvinylidene difluoride membrane. Membranes were blocked for 60 min at room temperature in 5% bovine serum albumin. Immunolabeling for KIT was performed using a rabbit polyclonal anti-human antibody (Dako, Carpinteria, CA) at 1:1000 while immunolabeling for pKIT was performed using a rabbit polyclonal anti-human antibody (Cell Signaling Technology, Beverly, MA) at 1:2000 for 16 hours at 4℃, followed by incubation with HRP-conjugated anti-rabbit antibody at 1:5000 for 30 min at room temperature. Immunoreactive bands were detected using enhanced chemiluminescent reagents (Thermo Scientific, Rockford, IL).

**Mutational Analysis: Cloning and Sequencing of *c-kit***

Full-length canine *c-kit* from the TOC-sensitive and -resistant sublines was cloned and sequenced. Total RNA was extracted from C2 cells using RNeasy Mini-kit after homogenization using QIA-shredder columns according to the manufacturer's instructions (Qiagen; Valencia, CA). First strand cDNA was synthesized using ThermoScript™ RT-PCR System (Invitrogen; Carlsbad, CA) according to the manufacturer's instructions. Full-length canine *c-kit* was amplified using Platinum® *Taq* DNA polymerase High Fidelity (Invitrogen) and the following

primers: *c-kit* Forward AGGCTATCGCAGCCACCGCGATGAG and *c-kit* Reverse GATCGCTCTTGTTGGGGAGAC. The conditions for PCR amplification were as follows: pre-denaturation at 94°C for 2 min, 40 cycles of denaturation at 94°C for 30 sec, annealing at 57°C for 30 sec, extension at 68°C for 3 min 30 sec and, following the final cycle, an additional extension at 68°C for 7 min was performed. The PCR products were purified according to the QIAquick PCR purification kit instructions. The concentration was determined using a Nanodrop 1000 spectrophotometer (Thermoscientific; Wilmington, DE). The cDNA fragment of interest was ligated into a pGEM®-T easy vector (Promega) by T4 ligase at 4°C overnight. The product was transfected to competent DH5α bacteria. Positive recombinants were selected on a Luria-Bertani (LB) plate with X-gal and 100 µg/mL ampicillin. The white bacterial colonies were selected, amplified and plasmids were extracted and purified using the QIAquick DNA reagent kit (Qiagen). Positive clones were selected by restriction endonuclease digestion with *Eco*RI and SpeI restriction enzymes and positive recombinants were sequenced. Sequencing was performed using the dideoxynucleotide chain termination method (Sanger Method) with an automated sequencer (ABI 3130xL Genetic Analyzer, Life Technologies, Grand Island, NY) using T7 and SP6 promoter primers and five internal sequencing primers (**Table 2.1, Figure 2.1**). Assembly, editing and comparison of all cDNA sequences was performed using Geneious Pro version 5.5.8 created by Biomatters (http://www.geneious.com/). Briefly, multiple clones from each cell line were compared to eliminate potential polymerase errors. For each clone, full-length *c-kit* sequence was assembled from a series of overlapping sequence reads. Contig assembly and multiple sequence alignments were performed using the "Assembly" and "Alignment" functions of Geneious, respectively.

**Table 2.1** Forward and Reverse Sequencing Primers for full-length *c-kit*.

| Primer | Sequence Range (bp) | Start Site | 5'-Sequence-3' |
|---|---|---|---|
| FOR1 | 501-1000 | 448 | GACGGACCCAGAAGTGACC |
| FOR2 | 1001-1500 | 948 | CCTTGGAAGTAGTAGATAAAGGATTC |
| FOR3 | 1501-2000 | 1453 | AGTGGTTCAGAGTTCCATCG |
| FOR4 | 2001-2500 | 1948 | CAAAGTCTTGAGTTACCTCGG |
| FOR5 | 2501-3000 | 2950 | TGTGTGAAGCAGGAGGAGTG |
| REV1 | 500-1 | 552 | CTGATCGTGATGCCAGCTT |
| REV2 | 1000-501 | 1040 | CAATCAGATCCACATTCTGTCC |
| REV3 | 1500--1001 | 1542 | GCAGAACTCCTGCCTACATTG |
| REV4 | 2000--1501 | 2040 | TATTCTGTAATGACCAAGGTGGG |
| REV5 | 2500--2001 | 2552 | TGAAAATGCTCTCAGGGGC |

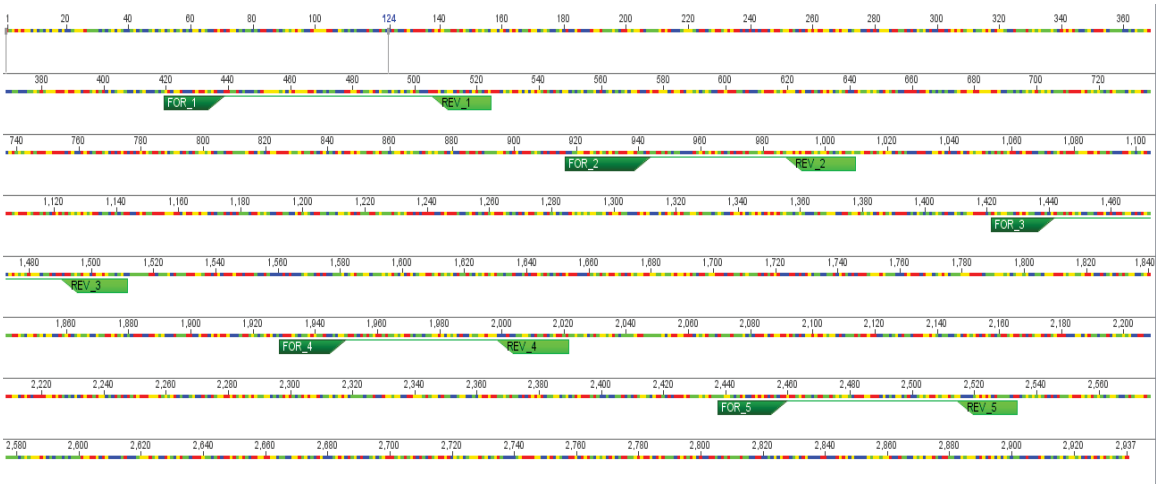


**Figure 2.1** Sequencing strategy of full-length canine *c-kit* with forward and reverse internal sequencing primers

## *c-kit* and KIT Expression

***Real Time-quantitative PCR (RT-qPCR)*:** To evaluate the effects of chronic TOC exposure on mRNA expression of *c-kit*, RT-qPCR was performed on both TOC-sensitive and –resistant C2 cells. RNA was extracted, purified, and cDNA synthesis performed as described above. RT-qPCR was performed on five biological replicates in triplicate with denaturation at 94°C for 2 minutes and 40 cycles of 30 seconds at 94°C (melting) and 60 seconds at 57°C and 3 minutes and 30 seconds at 68°C (annealing and elongation) followed by 7 minutes at 68°C using the iQ SYBR Green Supermix (Bio-Rad, Hercules, CA, USA) and 25 ng equivalent RNA input

in 25 μL reactions on a Stratagene Mx3000P thermal cycler (Stratagene; La Jolla, CA). Primers were designed to be intron-spanning using Geneious. The standard curves, dissociation curves, and amplification data were collected using Mx3000P software and analyzed with the $2^{(-_{\Delta\Delta}Ct)}$ method [46]. In all cases, the amplification efficiencies were greater than 90% and both amplicon size and sequence were confirmed. Expression levels were normalized to hypoxanthine phosphoribosyltransferase 1 (HPRT1) expression. HPRT was selected as a reference gene since it did not exhibit significant variation among our experimental samples. The *c-kit* forward primer sequence was 5'- TTGGTCTAGCCAGAGACATCAA -3', the *c-kit* reverse primer sequence was 5' TGAAAATGCTCTCAGGGGC -3', the HPRT1 forward primer sequence was 5'-TGC TCG AGA TGT GAT CAA GG-3' and the HPRT1 reverse primer sequence was 5'-TCC CCT GTT GAC TGG TCA TT-3'.

***Flow Cytometry*:** To evaluate the effects of chronic TOC exposure on KIT expression, flow cytometric analysis was performed on three biological replicates of TOC-sensitive and –resistant lines in triplicate. 250,000 parental C2 and TR1, TR2, and TR3 cells were incubated with 0.4 ug PE-conjugated rat anti-mouse monoclonal CD117 (BD Pharmingen; San Jose, CA) for 30 minutes in the dark at room temperature, washed with 1X PBS, centrifuged at 200 x g for 5 minutes, and resuspended in 1X PBS. Data was acquired using a Gallios flow cytometer and Gallios software (Beckman Coulter; Brea, CA). Results were analyzed using Kaluza Analysis Software (Beckman Coulter). Cells were gated based on forward scatter and side scatter properties.

**P-gp Expression/Function**

To evaluate the expression and function of P-gp in the TOC-sensitive and -resistant sublines, western blotting and rhodamine uptake/efflux was performed, respectively. C2, TR1, TR2, and TR3 cells were lysed as described above. As a positive control, MDR1-over-expressing canine Madin Darby Canine Kidney (MDCK) cells were used (kindly received from Dr. Michael Gottesmann, Laboratory of Cell Biology, National Cancer Institute, NIH, Bethesda, MD). Protein was separated by SDS-PAGE on a 6% acrylamide gel and transferred onto a polyvinylidene difluoride membrane. Membranes were blocked for 60 min at room temperature in 4% milk. Immunolabeling for MDR-1/Pg-p/ABCB1 was performed using a rabbit polyclonal anti-human antibody (Novus Biologicals, Littleton, CO) at 1:1000 followed by incubation with HRP-conjugated anti-rabbit antibody at 1:5000 for 30 min at room temperature. Immunoreactive bands were detected using enhanced chemiluminescent reagents (Thermo Scientific; Rockford, IL). Rhodamine uptake/efflux assays were performed as previously described [47, 48]. Briefly, 200,000 cells were seeded in 6-well plates 24 hr prior to assay. Cells were incubated in rhodamine (3 μM) or rhodamine and verapamil (50 μg/mL) for 1 hr at 37°C. Rhodamine-containing media was removed, replaced with fresh media or media and verapamil, and placed at 37°C for 1 hr. Cells were harvested, washed, and flow cytometry was performed to measure fluorescence intensity.

## RESULTS

### Toceranib-resistant C2 cells emerged during chronic, stepwise TOC treatment.

To explore mechanisms of acquired TOC resistance in canine MCT, we generated three resistant sublines from the TOC-sensitive exon 11 ITD *c-kit* mutant C2 cell line designated TR1, TR2, and TR3. Growth of the parental C2 cells was inhibited by TOC in a dose-dependent manner with an $IC_{50}$ of <10 nM. In contrast, TR1, TR2, and TR3 sublines were resistant to inhibition by TOC ($IC_{50}$ > 1,000 nM). (**Figure 2.2**). Sensitivity to three other KIT RTK inhibitors was similar to the observed resistance to TOC. The parental line as well as all three sublines retained sensitivity to the cytotoxic agents vinblastine (VBL) and CCNU (**Figure 2.3**). Following 72 hr culture in the presence of increasing concentrations of TOC, treatment naïve, parental C2 cells detached from the culture flask and became rounded, shrunken, and clumped with increased exposure to TOC. In contrast, TOC-induced morphologic differences were not identified in the resistant sublines.

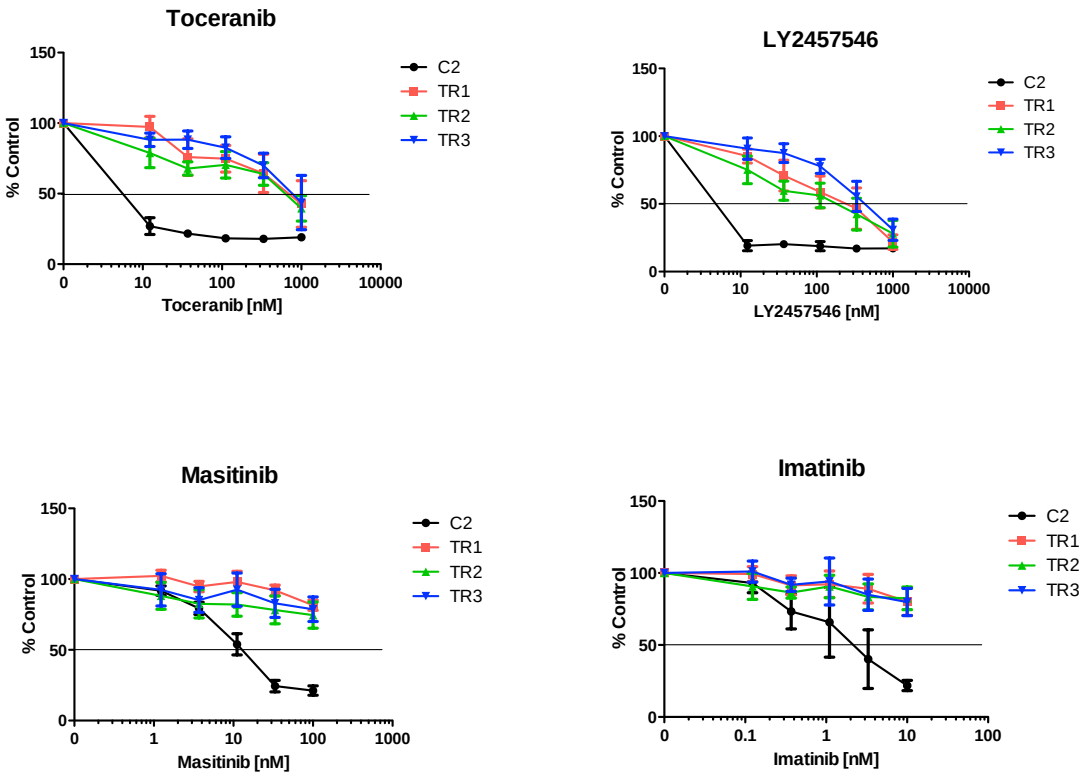


**Figure 2.2:** Dose-dependent growth inhibition of parental line (C2) and three resistant sublines (TR1, TR2, TR3) after incubation with increasing concentrations of toceranib phosphate and three other KIT receptor tyrosine kinase inhibitors (LY2457546, masitinib, imatinib) for 72 hours

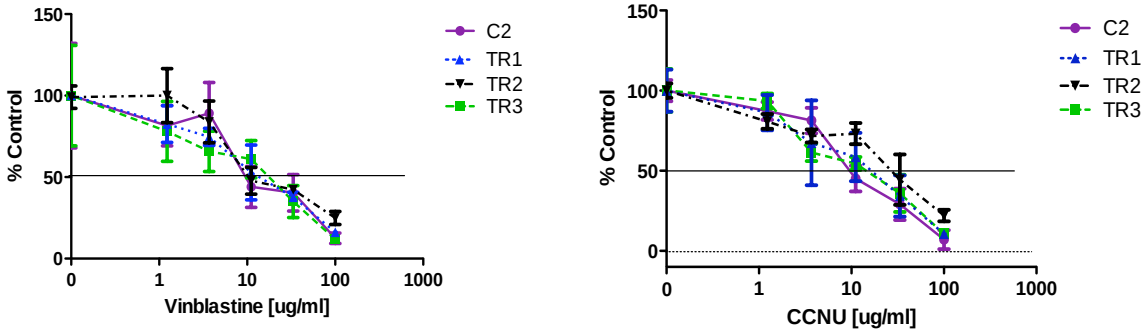


**Figure 2.3** Dose-dependent growth inhibition of parental line (C2) and three resistant sublines (TR1, TR2, TR3) after incubation with increasing concentrations of vinblastine or CCNU (lomustine) for 72 hours.

**Toceranib induces apoptosis in parental C2 cells, but not the TOC-resistant sublines.**

Tyrosine kinase inhibitors have been shown to promote growth inhibition in C2 cells by induction of apoptosis and cell-cycle arrest [15]. To explore this, Terminal Deoxynucleotidyltransferase-Mediated dUTP Nick End Labeling (TUNEL) assays and morphological evaluations were performed on all four cell lines to determine the effects of TOC and the cytotoxic agents, VBL and CCNU, on apoptosis. Following 72 hr of increasing exposure to TOC, a qualitative increase in the number of cells displaying increased TUNEL reactivity and morphologic evidence of apoptosis (chromatin condensation and nuclear fragmentation) was observed in the parental line. In contrast, no increase in either positive TUNEL staining or morphologic evidence of apoptosis was observed in the three TOC-resistant sublines (**Figure 2.4**). The parental line and all three resistant sublines demonstrated an equivalent increase in both TUNEL staining and apoptotic morphology after 72 hr of VBL (**Figure 2.5**) or CCNU exposure.

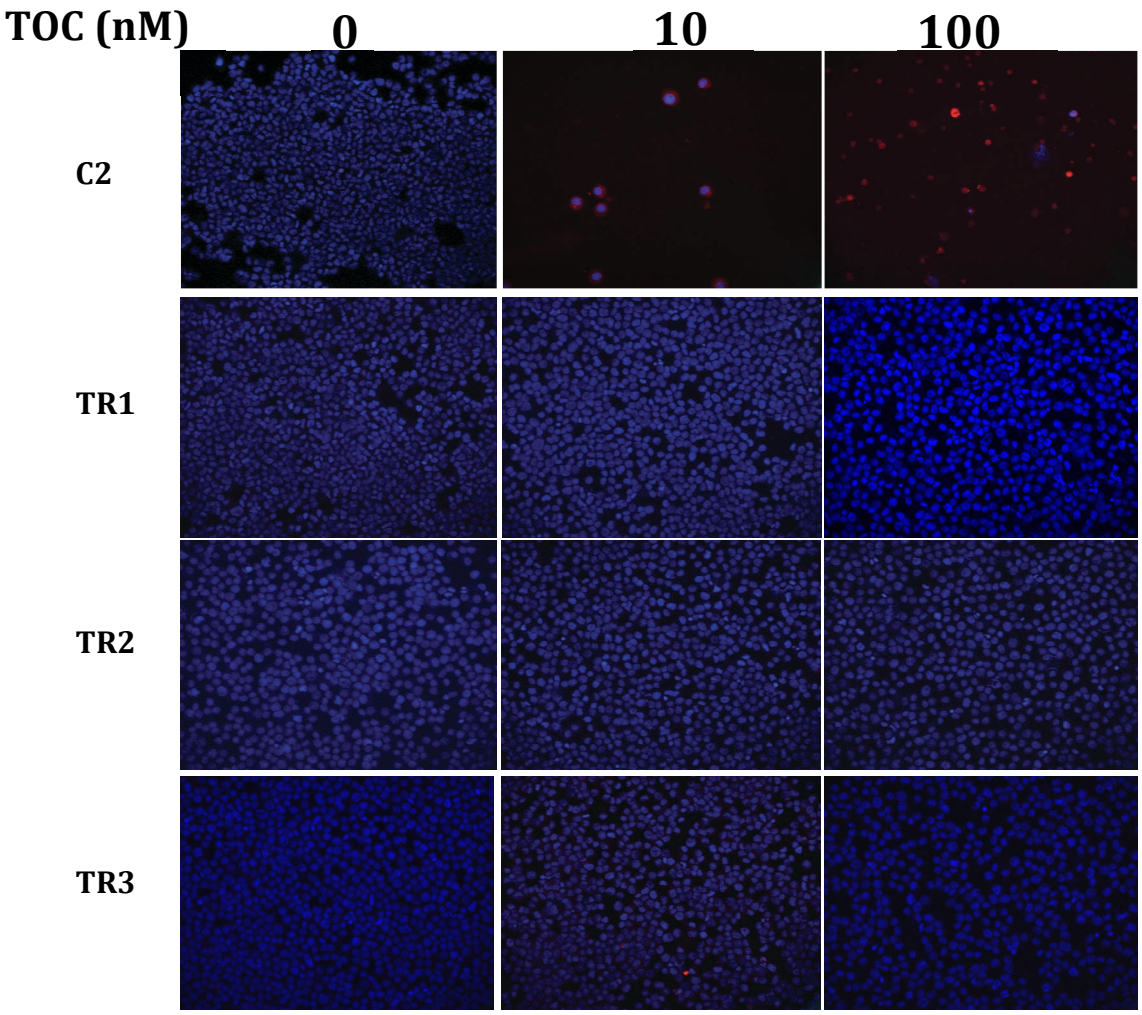


**Figure 2.4** Effect of toceranib and vinblastine (B) on the induction of apoptosis in C2, TR1, TR2, and TR3 cells; Red- TUNEL; DAPI counterstain

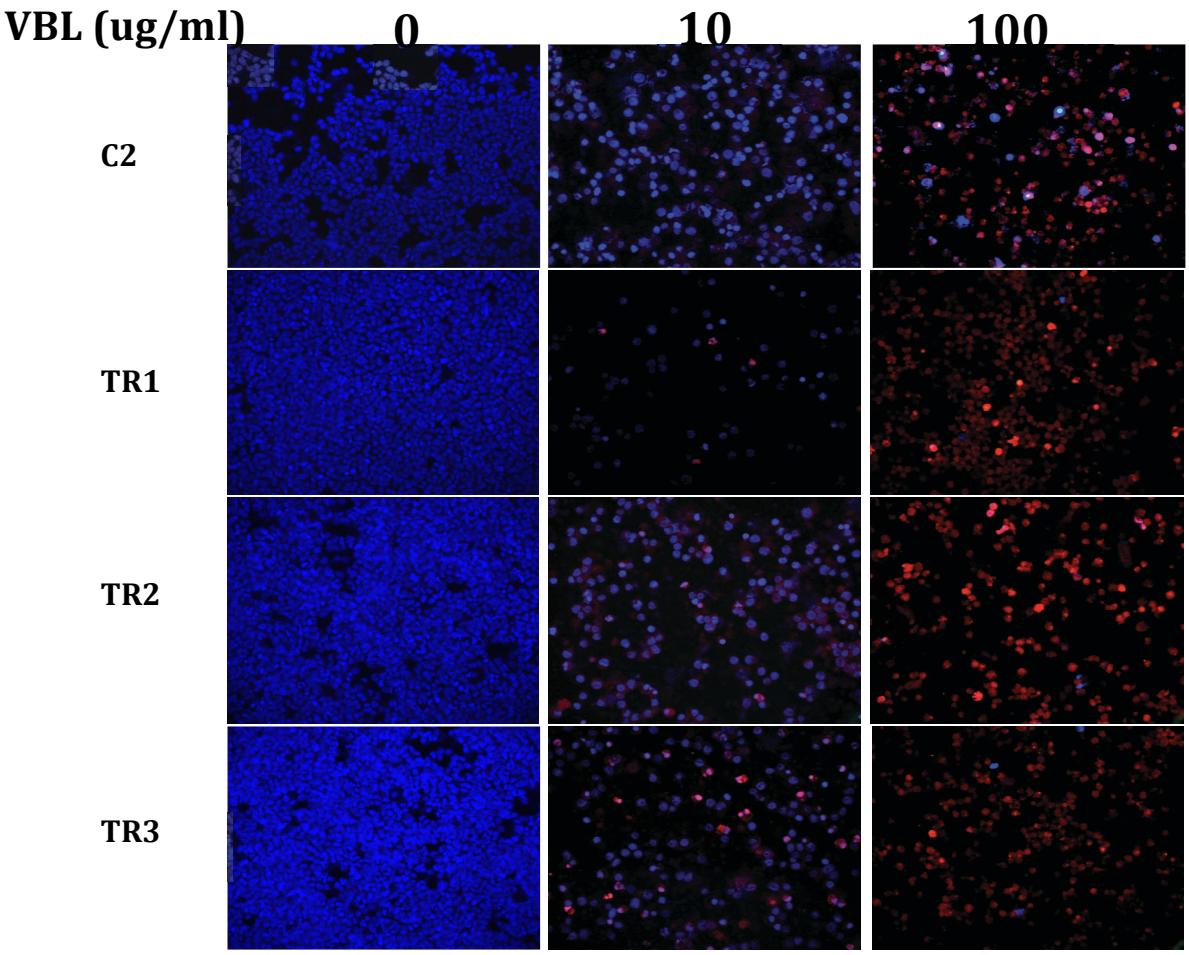


**Figure 2.5** Effect of vinblastine on the induction of apoptosis in C2, TR1, TR2, and TR3 cells; Red- TUNEL; DAPI counterstain

**KIT phosphorylation in resistant cells does not decrease after toceranib treatment.**

To determine whether the lack of growth inhibition observed in the resistant sublines in Figure 1A was due to a lack of inhibition of autophosphorylation by TOC, the cells were incubated with increasing concentrations of TOC for 24 hours and western analysis for phosphorylated and total KIT was performed. TOC inhibited KIT phosphorylation in the parental C2 line in a dose-dependent manner while phosphorylation of the KIT receptor was maintained in the presence of TOC in all three resistant sublines (**Figure 2.6**). Densitometric analysis of pKIT expression is shown in **Figure 2.7**.

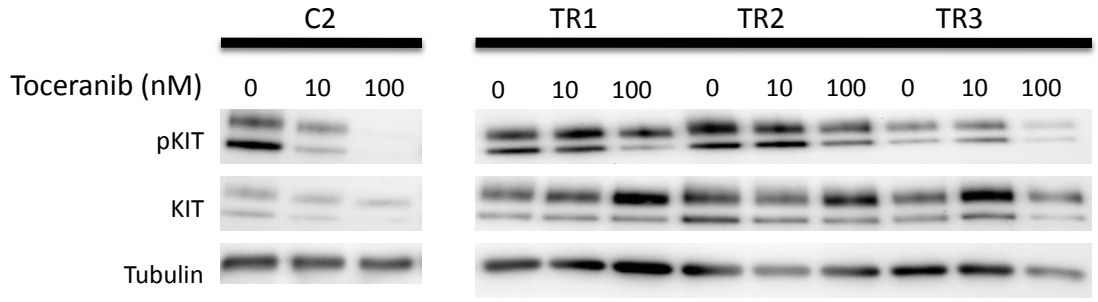


**Figure 2.6** Western blot analysis of KIT activation (phosphorylated KIT) in parental line (C2) and three resistant sublines (TR1, TR2, TR3) after incubation with increasing concentrations of toceranib phosphate for 24 hours

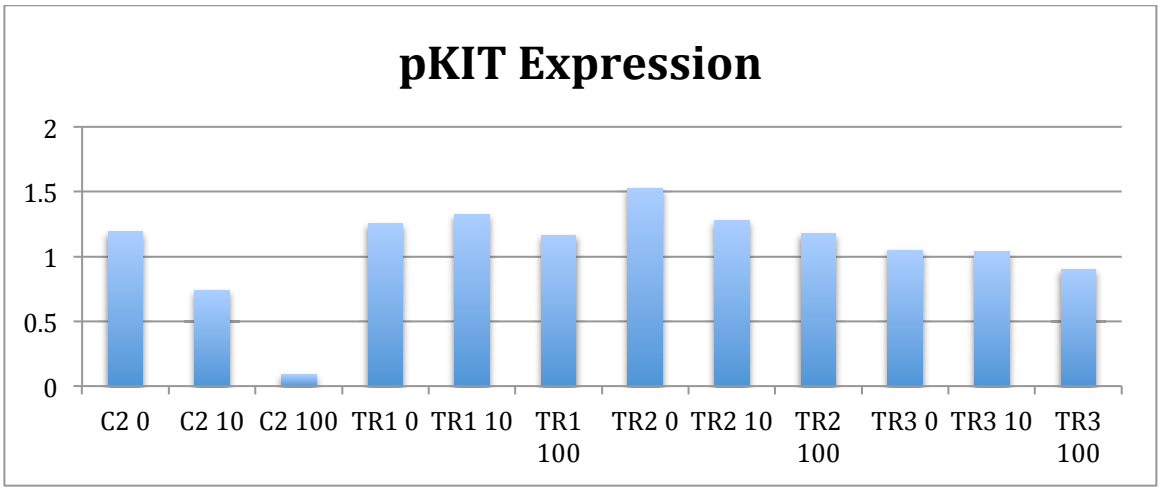


**Figure 2.7** Densitometric analysis of pKIT expression of western blot shown in Figure 2.6.

**Chronic TOC exposure resulted in significant overexpression of *c-kit* mRNA and KIT protein in the TOC-resistant sublines.**

To investigate whether overexpression of the target kinase contributes to the observed TOC resistance, *c-kit* mRNA and KIT protein expression was measured by real-time quantitative PCR and flow cytometry, respectively. Indeed, TOC-resistant sublines demonstrated up to a four-fold increase in KIT receptor expression compared to the parental, treatment naïve C2 cells (**Figure 2.7 A and B**). Additionally, densitometric analysis of chemiluminescent signals of total

KIT from Figure 5 was performed using Image J software (National Institutes of Health, Bethesda, MD), which demonstrated significant overexpression of KIT in all three resistant sublines compared to the parental line (**Figure 2.8**).

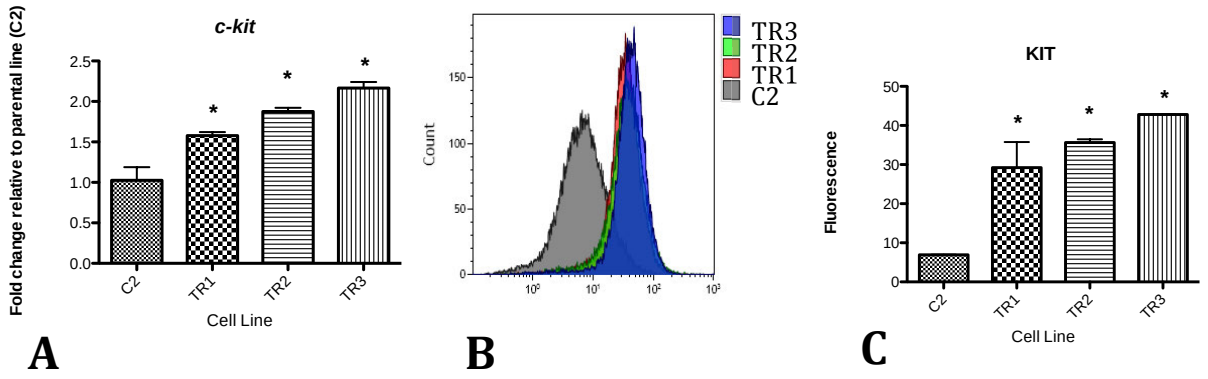


**Figure 2.8** Analysis of *c-kit* and KIT expression in C2, TR1, TR2, and TR3 cells by RT-qPCR (A) and flow cytometry (B, C). Asterisks denote significant differences (*p<0.05).

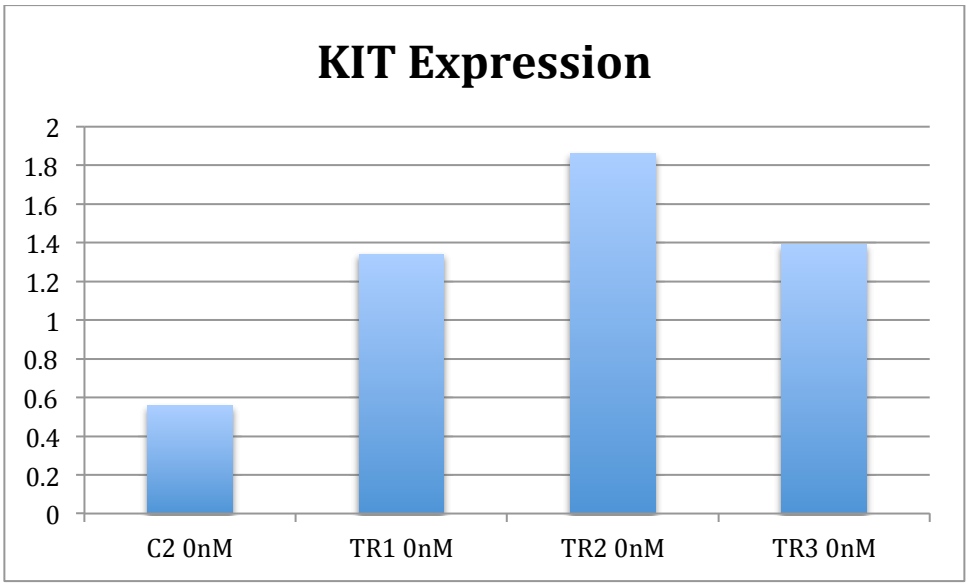


**Figure 2.9** Densitometric analysis of western blot of KIT expression in C2, TR1, TR2, and TR3 cells.

**C2, TR1, TR2, and TR3 sublines demonstrate minimal P-gp activity and no functional P-gp.**

To determine if TOC resistance is caused by overexpression and increased functional activity of the drug transporter P-glycoprotein (P-gp), western analysis and rhodamine uptake/efflux assays were performed, respectively, in all four sublines. While MDR1-overexpressing MDCK cells showed significant overexpression of P-gp, all four sublines demonstrated little to no P-gp expression, even when blots were overexposed (**Figure 2.8A**). The activity of P-gp in the same cells was determined by rhodamine uptake/efflux. As expected, MDR1-MDCK cells demonstrated a lower fluorescence signal compared to C2, TR1, TR2, and TR3 cells. Administration of the P-gp inhibitor, verapamil, increased the fluorescence signal in the MDR1-MDCK cells, however, no shift in the fluorescence signal was detected in the C2, TR1, TR2, and TR3 cells (**Figure 2.8B**).

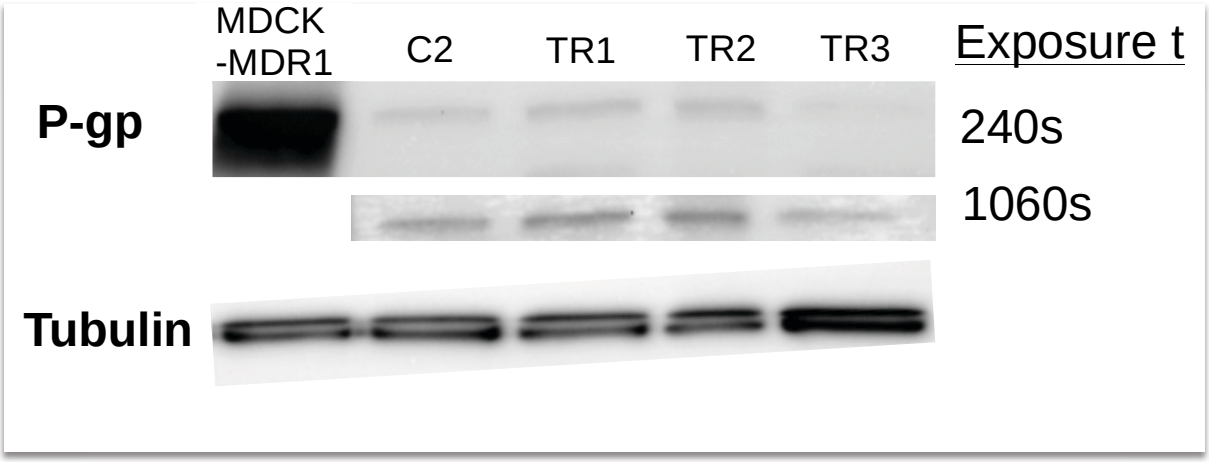


A

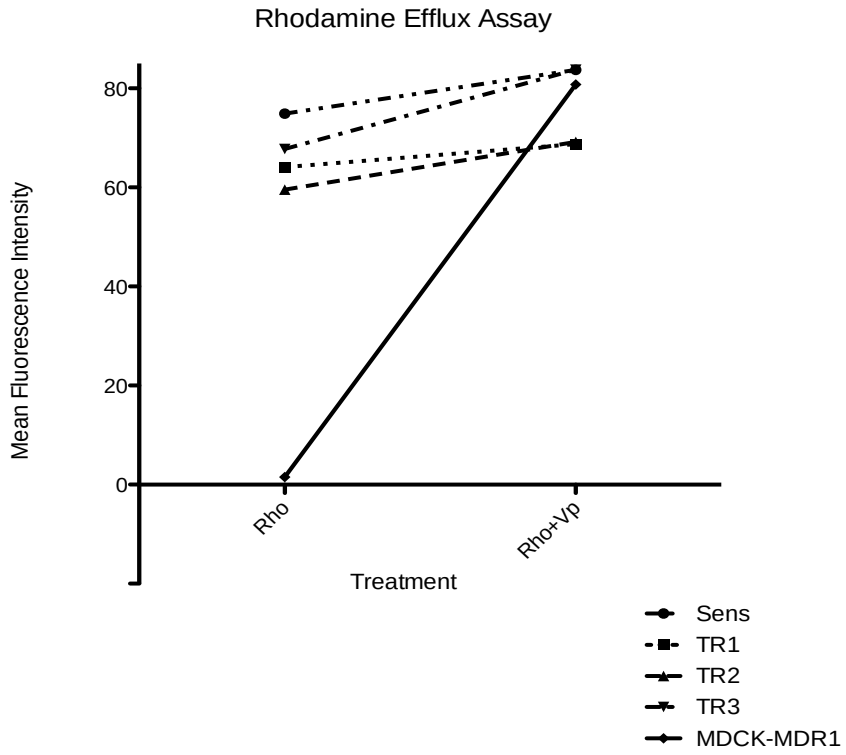


B

**Figure 2.10** (A) Western blot analysis of P-gp expression in C2, TR1, TR2, and TR3 cells at 240 and 1060 second exposures. MDR1-overexpressing Madin-Darby canine kidney cell (MDCK) lysate was used as a positive control. (B) Rhodamine efflux/uptake assay in the same cells as A. Administration of the P-gp inhibitor, verapamil, increases fluorescence signal in lines with functional P-gp (MDCK-MDR1) with relatively no change in signal in lines without functional P-gp (C2, TR1, TR2, TR3).

**Secondary *c-kit* mutations are present in the juxtamembrane and kinase domains of *c-kit* in resistant sublines.**

To assess whether the development of secondary mutations in the *c-kit* gene conferred the observed resistance to TOC, full-length canine *c-kit* from the TOC-sensitive and -resistant sublines was cloned and sequenced. cDNA sequence analyses of full length *c-kit* from each clone after assembly and comparison of 7-10 clones from each subline was performed. A total of six novel point mutations were identified in the juxtamembrane and kinase domains of 30-50% of the resistant clones. These included Q574R in exon 11 and M835T in exon 18 of TR1; K724R in

exon 15 of TR2; and K58R in exon 11, R584G in exon 11, and A620S in exon 12 of TR3 (**Figure 2.9**). These novel mutations were not identified in any of the parental C2 clones. Additionally, alternative splice sites between exons 9 and 10 and exons 17 and 18 were identified in all sublines. These transcripts utilize alternate splice donors (GT) 3' to exons 9 and 17. Furthermore, retention of the original 48-bp internal tandem duplication in exon 11 of the parental line was observed in all three resistant sublines.

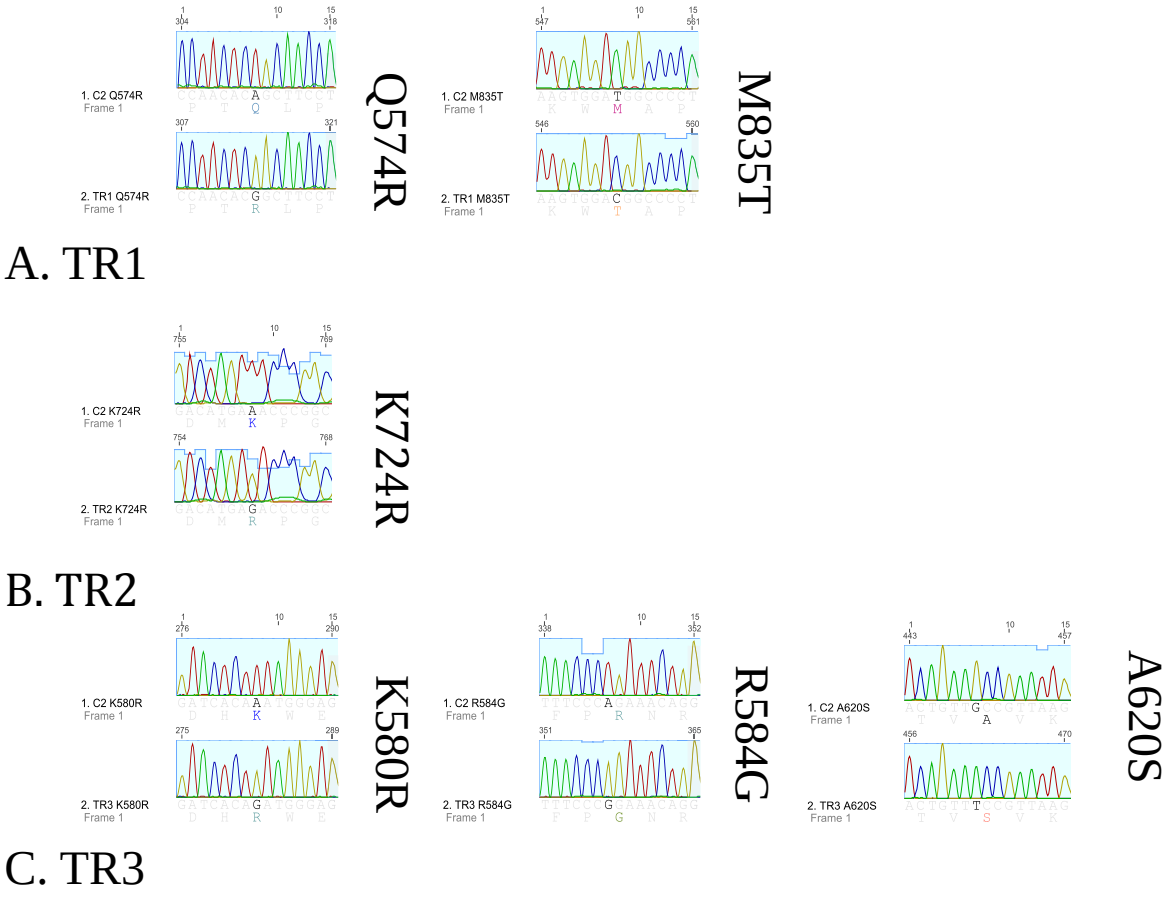


**Figure 2.11** Point mutations identified in 7-10 clones of full-length *c-kit* from TR1, TR2, and TR3 sublines. Mutations were commonly identified in functional domains of the KIT receptor.

## DISCUSSION

The identification of protein kinases as instrumental regulators in the tumorigenesis of many forms of neoplasia has led to the development of numerous small molecule kinase inhibitors for the treatment of cancer. The understanding of the molecular pathway driving the development of at least some canine cutaneous MCT, its addiction to a dominant oncogene, coupled with the identification of a "druggable" target has resulted in significant progress toward its treatment. Activating mutations in the *c-kit* proto-oncogene confer growth-factor independent activation of the KIT receptor tyrosine kinase, subsequent downstream signaling, and enhanced proliferation and survival of malignant mast cells [4, 16]. Ligand-independent activation of the KIT pathway most commonly occurs due to a mutation in the juxtamembrane domain in exon 11 [6]. This domain has a negative regulatory function by maintaining the KIT receptor in its inactive conformation in the absence of ligand binding. Mutations in this domain result in an active conformation due to disruption of the inhibitory motif resulting in autophosphorylation of the KIT receptor and downstream signaling [17]. Upon binding the ATP-binding pocket within the TK domain, the small molecule KIT receptor tyrosine kinase inhibitors abrogate KIT signaling and induce growth inhibition and apoptosis [14, 18]. Dogs with MCTs harboring an activating mutation in the *c-kit* proto-oncogene have demonstrated significantly increased response rates to TOC [13]. Despite these benefits, the responses are often transitory as tumors commonly develop resistance to TOC.

To begin to identify mechanisms of acquired resistance to TOC, we have successfully developed a model of acquired resistance using a canine MCT cell line by continuously exposing cells to increasing concentrations of TOC, resulting in three independent sublines that are resistant to TOC. The C2 MCT cell line harbors the KIT-activating ITD mutation in exon 11,

which represents the most common mutation in canine MCT [8, 10]. In one study, 64% of KIT mutations identified in canine MCT were ITDs in exon 11 [8]. As such, the C2 cell line is a clinically relevant canine MCT line for these investigations. While the parental C2 line demonstrated dose-dependent growth inhibition following treatment with TOC, the three sublines, TR1, TR2, and TR3, remained resistant to TOC exposure. Similarly, TOC exposure caused an induction of apoptosis in the parental line while no evidence of apoptosis was observed in the three sublines following similar TOC exposure. Importantly, the TOC-resistant sublines retained sensitivity to the cytotoxic agents VBL and CCNU, and demonstrated variable sensitivity to other KIT kinase inhibitors. This lack of apparent cross-resistance to the conventional cytotoxic agents VBL and CCNU suggests that these drugs may remain active in patients with TOC-refractory disease.

There are several reported pathway-dependent mechanisms of acquired resistance to TKIs. One of the most common mechanisms is acquisition of secondary mutations within the target oncogene leading to either reactivation of the target protein or induction of a conformational change in the drug binding pocket resulting in reduced binding affinity [19-23]. As KIT TKIs bind to the ATP-binding pocket of a kinase in a competitive fashion, mutations located in the in the drug/ATP-binding pocket of the receptor are associated with acquired drug resistance. Heinrich and co-workers showed that secondary point mutations located in the ATP-binding pocket of the KIT receptor (encoded by exons 13 and 14) are associated with resistance to imatinib, a KIT receptor TKI, in gastrointestinal stromal tumors (GISTs) [24]. In the current study, the observed variable resistance to the three other KIT inhibitors, both between the three inhibitors (imatinib, masitinib and LY2457546) and among the three resistant sublines, suggests that there may be differences in drug binding kinetics among the four compounds and perhaps

differences in mechanisms of acquired resistance between the three sublines, respectively.

Engagement of alternative or bypass signaling pathways is another common mechanism of acquired resistance to receptor tyrosine kinase inhibitors [25-28]. This can occur independent of the target oncogene to which a tumor is addicted. Indeed, the activation of a bypass pathway has been shown to overcome KIT inhibition in human GISTs. GIST cells resistant to imatinib demonstrated increased activation of the AKT pathway leading to continued cell growth and survival [29, 30]. Nazarian and co-workers showed that melanomas harboring a BRAF (V600E) mutation eventually become resistant to the RAF-selective inhibitor, PLX4032, by activation of an alternative survival pathway mediated by PDGFRβ [31].

In addition to secondary mutations in the target oncogene and activation of bypass signaling pathways, resistance to targeted therapies can also occur through activation of effector proteins upstream and/or downstream of the intended target. Nazarian and co-workers also demonstrated reactivation of NRAS signaling in PLX4032-refractory melanomas leading to MAPK pathway reactivation and disease progression [31]. Similarly, Wagle and co-workers demonstrated activating mutations in MEK1 and subsequent reactivation of the MAPK pathway following treatment of melanoma with PLX40 [32].

To begin to explore these possibilities in our TOC-resistant canine MCT model, we examined KIT activation status in the parental and TOC-resistant C2 sublines by western blot analysis using an antibody against KIT phosphorylated at Tyr719. While phosphorylated KIT was reduced in a dose-dependent manner in the parental line, KIT activation was maintained in the presence of increasing concentrations of TOC in all three resistant sublines. These data led to the hypothesis that acquisition of a secondary mutation in the *c-kit* proto-oncogene would be, in part, responsible for the observed TOC resistance. To that end, full-length canine *c-kit* was

cloned and sequenced. The original ITD mutation in exon 11 was maintained in all three resistant sublines. Indeed, we detected several different point mutations in the resistant sublines leading to amino acid substitutions. Interestingly, all of these mutations were located in the functional domains of the KIT receptor. Computational modeling of these mutations is in process to ascertain whether they impede contact between the KIT inhibitors, including TOC, and their binding sites or alter spatial conformation of the target protein. The frequency with which these mutations were identified in the resistant clones was between 30-50%. This likely represents the heterogeneity associated with resistance mechanisms. It has been shown that multiple drug-resistant mutations and disparate mechanisms of resistance can frequently occur in a single population of tumor cells [27, 33-35]. These include from multiple secondary mutations in the target kinase as well as independent mechanisms such as activation of a bypass pathway. Other single nucleotide polymorphisms (SNPs) were identified in single clones. These are likely a result of polymerase error when observed in a single clone, but when duplicated represent transcript heterogeneity resulting from genomic instability perhaps as a result of deficiencies in the DNA repair machinery. Alternative signaling pathways that bypass inhibition of the target protein, KIT, were not pursued in the current study. Constitutive activation of KIT in the presence of TOC in the resistant sublines strongly suggests that the mechanism of resistance occurs at the level of the KIT receptor.

A final pathway-dependent mechanism of acquired resistance is through genomic amplification of the target gene. Amplification of the target gene and subsequent overexpression of the target kinase, can alter the drug-target stoichiometry such that inhibition is diminished and cell survival and proliferation persists [36-40]. Genomic amplification of *c-kit* has been reported in imatinib-resistant GISTs as a mechanism of acquired resistance [41]. Ercan and co-workers

demonstrated that although non-small lung cancers harboring a *EGFR* T790M mutation transiently respond to EGFR inhibitors, clones over-expressing *EGFR* T790M eventually emerge leading to clinical resistance [38]. Increased expression of the target protein BCR/ABL, resulting from genomic oncogene amplification, was observed in chronic myelogenous leukemia (CML) cell lines that became refractory to the selective ABL tyrosine kinase inhibitor imatinib [37]. In the current study, analysis of *c-kit* mRNA expression by real-time quantitative PCR demonstrated a significant increase in *c-kit* expression in the TOC-resistant C2 sublines compared to the treatment-naïve parental C2 cells. To determine if this increase in *c-kit* transcript led to a subsequent increase in KIT receptor expression, flow cytometry was performed. Indeed, a significant increase in KIT receptor expression was demonstrated in the three TOC-resistant C2 sublines compared to the TOC-sensitive parental C2 cells. This could confer the observed resistance as binding of TOC to the overexpressed target could deplete the amount of intracellular drug available. As such, increasing the dose of TOC would be a reasonable therapeutic approach to overcome KIT-overpexpressing TOC-resistant canine MCTs. However, in the current model, growth inhibition assays were carried out to doses of TOC 100-fold the $IC_{50}$ of the treatment naïve parental C2 cells and an $IC_{50}$ was not reached in all three resistant lines. Therefore, these data suggest that a four-fold increase in expression of the target protein by itself is likely not adequate to confer the observed resistance. Amplification of the target oncogene, and subsequent overexpression of the encoded target protein, may have been driven in response to continued pressure by the KIT inhibitor. Alternatively, because the TOC-resistant sublines initially responded to TOC and maintained the original ITD activating *c-kit* mutation in exon 11, it is possible that the resistant sublines were derived from a distinct *c-kit*-amplified subpopulation of *c-kit*-mutant cells that were subsequently selected for during TOC

administration.

While the current study focuses on pathway-dependent mechanisms of KIT RTK resistance, there are several reported pathway-independent mechanisms of resistance that were investigated. These include pharmacological factors that ultimately diminish drug exposure. Drug-efflux pumps, such as P-glycoprotein (P-gp) encoded by *MDR1*, have been shown to be overexpressed in several TKI-resistant tumors and cell lines. Mahone and co-workers reported a significant overexpression of P-gp in imatinib-resistant leukemia cell lines [42]. Furthermore, sensitivity was restored following administration of several P-gp inhibitors. Nakaichi and co-workers reported the expression of P-gp and *MDR-1* by western blot analysis and RT-PCR, respectively, in several canine MCT cell lines, excluding C2 [43]. Sunitinib, a structural analog of toceranib, has been shown to be a substrate of P-gp. As such, we investigated the role of drug efflux in TOC-resistant canine C2 cells as a mechanism of resistance by measuring P-gp expression and function [44]. The expression of P-gp was determined in all four C2 sublines and MDR1-overexpressing MDCK cells by western analysis. While the presence of P-gp was confirmed in all four sublines, there were no significant differences in expression between the TOC-sensitive cells and TOC-resistant cells. Furthermore, all four C2 sublines showed minimal functional P-gp as measured by rhodamine efflux with or without administration of the P-gp inhibitor, verapamil.

Sustained KIT signaling appears required for *c-kit* mutant MCT survival. Regardless of the specific mechanism of acquired TOC resistance outlined above, all may lead to reactivation of the KIT signaling pathway and ultimately tumor progression. Our results demonstrate that continuous, chronic exposure of C2 cells to TOC causes eventual drug resistance. We demonstrate that overexpression of the KIT receptor is, in part, responsible for the observed TOC

resistance, and have identified several candidate mutations that may play a role in resistance acquisition. The identification of these and other potential mechanisms of TOC resistance is necessary for the identification of second line KIT inhibitors or alternate therapeutic strategies for the treatment of high grade, non-resectable canine MCT that are refractory to TOC. Furthermore, we have created *in vitro* tools that can be utilized for future study of re-sensitization strategies for TOC-resistant canine MCT.

## References


1. Bavcar S, Argyle DJ: Receptor tyrosine kinase inhibitors: molecularly targeted drugs for veterinary cancer therapy. Vet Comp Oncol 2012, 10(3):163-173.
2. Zemke D, Yamini B, Yuzbasiyan-Gurkan V: Mutations in the Juxtamembrane Domain of c-KIT Are Associated with Higher Grade Mast Cell Tumors in Dogs. Veterinary Pathology 2002, 39(5):529-535.
3. Webster JD, Kiupel M, Kaneene JB, Miller R, Yuzbasiyan-Gurkan V: The use of KIT and tryptase expression patterns as prognostic tools for canine cutaneous mast cell tumors. Vet Pathol 2004, 41(4):371-377.
4. London CA, Galli SJ, Yuuki T, Hu ZQ, Helfand SC, Geissler EN: Spontaneous canine mast cell tumors express tandem duplications in the proto-oncogene c-kit. Exp Hematol 1999, 27(4):689-697.
5. London CA, Thamm DH: Mast cell tumors. In: Small Animal Clinical Oncology. 5th edn. Edited by Withrow SJ, Vail DM, Page RL. St. Louis: Elsevier Saunders; 2013: 335-355.
6. Downing S, Chien MB, Kass PH, Moore PE, London CA: Prevalence and importance of internal tandem duplications in exons 11 and 12 of c-kit in mast cell tumors of dogs. Am J Vet Res 2002, 63(12):1718-1723.
7. Webster JD, Yuzbasiyan-Gurkan V, Kaneene JB, Miller R, Resau JH, Kiupel M: The role of c-KIT in tumorigenesis: evaluation in canine cutaneous mast cell tumors. Neoplasia 2006, 8(2):104-111.
8. Letard S, Yang Y, Hanssens K, Palmerini F, Leventhal PS, Guery S, Moussy A, Kinet JP, Hermine O, Dubreuil P: Gain-of-function mutations in the extracellular domain of KIT are common in canine mast cell tumors. Mol Cancer Res 2008, 6(7):1137-1145.
9. Pryer NK, Lee LB, Zadovaskaya R, Yu X, Sukbuntherng J, Cherrington JM, London CA: Proof of target for SU11654: inhibition of KIT phosphorylation in canine mast cell tumors. Clin Cancer Res 2003, 9(15):5729-5734.
10. Webster JD, Yuzbasiyan-Gurkan V, Thamm DH, Hamilton E, Kiupel M: Evaluation of prognostic markers for canine mast cell tumors treated with vinblastine and prednisone. BMC Vet Res 2008, 4:32.
11. Carlsten KS, London CA, Haney S, Burnett R, Avery AC, Thamm DH: Multicenter prospective trial of hypofractionated radiation treatment, toceranib, and prednisone for measurable canine mast cell tumors. J Vet Intern Med 2012, 26(1):135-141.
12. Avery AC: Molecular diagnostics of hematologic malignancies in small animals. Vet Clin North Am Small Anim Pract 2012, 42(1):97-110.
13. London CA, Malpas PB, Wood-Follis SL, Boucher JF, Rusk AW, Rosenberg MP, Henry CJ, Mitchener KL, Klein MK, Hintermeister JG et al: Multi-center, placebo-controlled, double-blind, randomized study of oral toceranib phosphate (SU11654), a receptor tyrosine kinase inhibitor, for the treatment of dogs with recurrent (either local or distant) mast cell tumor following surgical excision. Clin Cancer Res 2009, 15(11):3856-3865.
14. Robat C, London C, Bunting L, McCartan L, Stingle N, Selting K, Kurzman I, Vail DM: Safety evaluation of combination vinblastine and toceranib phosphate (Palladia(R)) in dogs: a phase I dose-finding study. Vet Comp Oncol 2012, 10(3):174-183.

15. Gleixner KV, Rebuzzi L, Mayerhofer M, Gruze A, Hadzijusufovic E, Sonneck K, Vales A, Kneidinger M, Samorapoompichit P, Thaiwong T et al: Synergistic antiproliferative effects of KIT tyrosine kinase inhibitors on neoplastic canine mast cells. Exp Hematol 2007, 35(10):1510-1521.
16. London CA, Seguin B: Mast cell tumors in the dog. Veterinary Clinics of North America: Small Animal Practice 2003, 33(3):473-489.
17. Roskoski R, Jr.: Signaling by Kit protein-tyrosine kinase--the stem cell factor receptor. Biochem Biophys Res Commun 2005, 337(1):1-13.
18. Faivre S, Demetri G, Sargent W, Raymond E: Molecular basis for sunitinib efficacy and future clinical development. Nat Rev Drug Discov 2007, 6(9):734-745.
19. Garraway LA, Janne PA: Circumventing cancer drug resistance in the era of personalized medicine. Cancer Discov 2012, 2(3):214-226.
20. Nguyen KS, Kobayashi S, Costa DB: Acquired resistance to epidermal growth factor receptor tyrosine kinase inhibitors in non-small-cell lung cancers dependent on the epidermal growth factor receptor pathway. Clin Lung Cancer 2009, 10(4):281-289.
21. Pao W, Miller VA, Politi KA, Riely GJ, Somwar R, Zakowski MF, Kris MG, Varmus H: Acquired resistance of lung adenocarcinomas to gefitinib or erlotinib is associated with a second mutation in the EGFR kinase domain. PLoS Med 2005, 2(3):e73.
22. Heinrich MC, Corless CL, Blanke CD, Demetri GD, Joensuu H, Roberts PJ, Eisenberg BL, von Mehren M, Fletcher CD, Sandau K et al: Molecular correlates of imatinib resistance in gastrointestinal stromal tumors. J Clin Oncol 2006, 24(29):4764-4774.
23. Nishida T, Kanda T, Nishitani A, Takahashi T, Nakajima K, Ishikawa T, Hirota S: Secondary mutations in the kinase domain of the KIT gene are predominant in imatinib-resistant gastrointestinal stromal tumor. Cancer Sci 2008, 99(4):799-804.
24. Heinrich MC, Maki RG, Corless CL, Antonescu CR, Harlow A, Griffith D, Town A, McKinley A, Ou WB, Fletcher JA et al: Primary and secondary kinase genotypes correlate with the biological and clinical activity of sunitinib in imatinib-resistant gastrointestinal stromal tumor. J Clin Oncol 2008, 26(33):5352-5359.
25. Engelman JA, Janne PA: Mechanisms of acquired resistance to epidermal growth factor receptor tyrosine kinase inhibitors in non-small cell lung cancer. Clin Cancer Res 2008, 14(10):2895-2899.
26. Johannessen CM, Boehm JS, Kim SY, Thomas SR, Wardwell L, Johnson LA, Emery CM, Stransky N, Cogdill AP, Barretina J et al: COT drives resistance to RAF inhibition through MAP kinase pathway reactivation. Nature 2010, 468(7326):968-972.
27. Qi J, McTigue MA, Rogers A, Lifshits E, Christensen JG, Janne PA, Engelman JA: Multiple mutations and bypass mechanisms can contribute to development of acquired resistance to MET inhibitors. Cancer research 2011, 71(3):1081-1091.
28. Ercan D, Xu C, Yanagita M, Monast CS, Pratilas CA, Montero J, Butaney M, Shimamura T, Sholl L, Ivanova EV et al: Reactivation of ERK signaling causes resistance to EGFR kinase inhibitors. Cancer Discov 2012, 2(10):934-947.
29. Sawabu T, Seno H, Kawashima T, Fukuda A, Uenoyama Y, Kawada M, Kanda N, Sekikawa A, Fukui H, Yanagita M et al: Growth arrest-specific gene 6 and Axl signaling enhances gastric cancer cell survival via Akt pathway. Mol Carcinog 2007, 46(2):155-164.

30. Mahadevan D, Cooke L, Riley C, Swart R, Simons B, Della Croce K, Wisner L, Iorio M, Shakalya K, Garewal H et al: A novel tyrosine kinase switch is a mechanism of imatinib resistance in gastrointestinal stromal tumors. Oncogene 2007, 26(27):3909-3919.
31. Nazarian R, Shi H, Wang Q, Kong X, Koya RC, Lee H, Chen Z, Lee MK, Attar N, Sazegar H et al: Melanomas acquire resistance to B-RAF(V600E) inhibition by RTK or N-RAS upregulation. Nature 2010, 468(7326):973-977.
32. Wagle N, Emery C, Berger MF, Davis MJ, Sawyer A, Pochanard P, Kehoe SM, Johannessen CM, Macconaill LE, Hahn WC et al: Dissecting therapeutic resistance to RAF inhibition in melanoma by tumor genomic profiling. J Clin Oncol 2011, 29(22):3085-3096.
33. Liegl B, Kepten I, Le C, Zhu M, Demetri GD, Heinrich MC, Fletcher CD, Corless CL, Fletcher JA: Heterogeneity of kinase inhibitor resistance mechanisms in GIST. J Pathol 2008, 216(1):64-74.
34. Gramza AW, Corless CL, Heinrich MC: Resistance to Tyrosine Kinase Inhibitors in Gastrointestinal Stromal Tumors. Clin Cancer Res 2009, 15(24):7510-7518.
35. Engelman JA, Settleman J: Acquired resistance to tyrosine kinase inhibitors during cancer therapy. Curr Opin Genet Dev 2008, 18(1):73-79.
36. Smolen GA, Sordella R, Muir B, Mohapatra G, Barmettler A, Archibald H, Kim WJ, Okimoto RA, Bell DW, Sgroi DC et al: Amplification of MET may identify a subset of cancers with extreme sensitivity to the selective tyrosine kinase inhibitor PHA-665752. Proc Natl Acad Sci U S A 2006, 103(7):2316-2321.
37. Gorre ME, Mohammed M, Ellwood K, Hsu N, Paquette R, Rao PN, Sawyers CL: Clinical resistance to STI-571 cancer therapy caused by BCR-ABL gene mutation or amplification. Science 2001, 293(5531):876-880.
38. Ercan D, Zejnullahu K, Yonesaka K, Xiao Y, Capelletti M, Rogers A, Lifshits E, Brown A, Lee C, Christensen JG et al: Amplification of EGFR T790M causes resistance to an irreversible EGFR inhibitor. Oncogene 2010, 29(16):2346-2356.
39. Bean J, Brennan C, Shih JY, Riely G, Viale A, Wang L, Chitale D, Motoi N, Szoke J, Broderick S et al: MET amplification occurs with or without T790M mutations in EGFR mutant lung tumors with acquired resistance to gefitinib or erlotinib. Proc Natl Acad Sci U S A 2007, 104(52):20932-20937.
40. Engelman JA, Zejnullahu K, Mitsudomi T, Song Y, Hyland C, Park JO, Lindeman N, Gale CM, Zhao X, Christensen J et al: MET amplification leads to gefitinib resistance in lung cancer by activating ERBB3 signaling. Science 2007, 316(5827):1039-1043.
41. Debiec-Rychter M, Cools J, Dumez H, Sciot R, Stul M, Mentens N, Vranckx H, Wasag B, Prenen H, Roesel J et al: Mechanisms of resistance to imatinib mesylate in gastrointestinal stromal tumors and activity of the PKC412 inhibitor against imatinib-resistant mutants. Gastroenterology 2005, 128(2):270-279.
42. Mahon FX, Belloc F, Lagarde V, Chollet C, Moreau-Gaudry F, Reiffers J, Goldman JM, Melo JV: MDR1 gene overexpression confers resistance to imatinib mesylate in leukemia cell line models. Blood 2003, 101(6):2368-2373.
43. Nakaichi M, Takeshita Y, Okuda M, Nakamoto Y, Itamoto K, Une S, Sasaki N, Kadosawa T, Takahashi T, Taura Y: Expression of the MDR1 gene and P-glycoprotein in canine mast cell tumor cell lines. J Vet Med Sci 2007, 69(2):111-115.
44. Shukla S, Robey RW, Bates SE, Ambudkar SV: Sunitinib (Sutent, SU11248), a small-molecule receptor tyrosine kinase inhibitor, blocks function of the ATP-binding cassette

(ABC) transporters P-glycoprotein (ABCB1) and ABCG2. Drug Metab Dispos 2009, 37(2):359-365.
45. DeVinney R, Gold WM: Establishment of two dog mastocytoma cell lines in continuous culture. Am J Respir Cell Mol Biol 1990, 3(5):413-420.
46. Livak KJ, Schmittgen TD: Analysis of relative gene expression data using real-time quantitative PCR and the 2(-Delta Delta C(T)) Method. Methods 2001, 25(4):402-408.
47. Lee JS, Paull K, Alvarez M, Hose C, Monks A, Grever M, Fojo AT, Bates SE: Rhodamine efflux patterns predict P-glycoprotein substrates in the National Cancer Institute drug screen. Mol Pharmacol 1994, 46(4):627-638.
48. Bradshaw-Pierce EL, Pitts TM, Tan AC, McPhillips K, West M, Gustafson DL, Halsey C, Nguyen L, Lee NV, Kan JL et al: Tumor P-Glycoprotein Correlates with Efficacy of PF-3758309 in in vitro and in vivo Models of Colorectal Cancer. Front Pharmacol 2013, 4:22.

# Chapter 3

## Acquisition of secondary mutations in *c-kit* confer resistance to toceranib phosphate (Palladia®) in canine mast cell tumor cells


### SUMMARY

Toceranib (TOC) phosphate (Palladia®**)** is KIT inhibitor that has been approved in for the treatment of canine cutaneous mast cell tumor. Despite its clinical benefit, its use is largely limited by the nearly inevitable development of resistance. We have generated three TOC-resistant sublines, TR1, TR2, and TR3, after chronic exposure of the TOC-sensitive, *c-kit* mutant canine C2 MCT cell line to TOC. Acquisition of secondary mutations in the juxtamembrane and kinase domains were previously identified after sequencing of canine *c-kit*. We constructed four *in silico* homology models of the cytoplasmic region of TOC-sensitive and -resistant canine KIT to predict the consequent structures of the drug binding site. Utilizing computational-based small molecule docking techniques, we calculated the predicted binding energies and orientations of TOC and the three other KIT inhibitors within the KIT mutant homology models to determine the structural basis of TOC resistance *in vitro*. This resulted in decreased favorability of the predicted binding of TOC and the three other KIT inhibitors to each of the three drug resistant mutants. To evaluate the utility of *in silico* homology modeling and small molecule docking methodologies in predicting response to a novel KIT inhibitor, we docked the novel KIT inhibitor, ponatinib, into the intracellular domain of the TOC-sensitive and each of the three TOC-resistant KIT mutant protein structures, followed by binding energy calculations. Ponatinib

was predicted to bind favorably to TOC-sensitive KIT, but showed a decrease in the favorability of the predicted binding to each of the three TOC-resistant mutants. Growth inhibition assays supported these findings. These results demonstrate the proposed structural mechanism by which secondary KIT mutations confer resistance to TOC in canine MCT cell lines and introduce a novel computer-based model for predicting response to KIT inhibitors.

## INTRODUCTION

Aberrantly regulated receptor tyrosine kinases (RTK) have been implicated in the pathogenesis of human and canine cancer. Mechanisms of dysregulation include activating mutations, overexpression, and autocrine loops of activation [1,2]. Some canine mast cell tumors (MCT) appear to be driven by activating mutations in the juxtamembrane, kinase, and ligand-binding domains of the *c-kit* proto-oncogene [3]. *c-kit* encodes the RTK KIT, a 145-kDa type III receptor protein-tyrosine kinase, that is comprised of an extracellular ligand binding domain composed of five immunoglobulin-like loops and encoded by exons 1-9, a transmembrane domain, encoded by exon 10, a split cytoplasmic kinase domain encoded by exons 11-21, including a negative regulatory juxtamembrane (exon 11), an ATP-binding domain (exon 13), and a phosphotransferase domain (exon 17) [3-6]. The *c-kit* proto-oncogene was first identified as the normal cellular homolog of the feline sarcoma viral oncogene *v-kit*, which induces feline retroviral sarcomas [7]. The KIT receptor shares structural similarity with other Type III RTK such as fms-related tyrosine kinase 3 (Flt-3), platelet derived growth factor receptor (PDGFR), and colony-stimulating factor-1 receptor (CSF-1R) [8].

Three common mechanisms of KIT activation in tumors have been described. These include paracrine and/or autocrine stimulation of the receptor by the ligand stem cell factor (SCF),

activation by other kinases and/or loss of inhibitory mechanisms, and most commonly, activating mutations in the *c-kit* gene [9,10]. Mutated forms of *c-kit* have been implicated in the tumorigenesis of gastrointestinal stromal tumor (GIST) and acute myelogenous leukemia as well as mast cell disease in humans [11,12]. Similarly, activating mutations in *c-kit* have been identified in canine MCT. Most commonly, an internal tandem duplication (ITD) has been identified in exon 11 of canine *c-kit* [3,4,7]. Exon 11 encodes the juxtamembrane domain of the KIT receptor, which has an inhibitory function in regulating KIT kinase activity. This inhibitory function is lost in oncogenic forms of KIT harboring ITD in exon 11 [13]. Less frequently, mutations in the *c-kit* gene occur in exons 8 and 9, which encode the extracellular domain of KIT, and exon 17, which encodes the kinase domain. Mutations are characterized by ITD (exon 8) and amino acids substitutions and insertions (exons 8 and 9) [3,14,15]. These mutations are associated with ligand-independent autophosphorylation of the KIT receptor and self-sufficient growth of neoplastic mast cells. Up to 40% of histologically intermediate or high-grade MCTs harbor ITDs in the juxtamembrane domain of KIT. Mutated KIT is significantly associated with increased incidence of recurrent disease, metastasis, and death in dogs with MCT [3,4,16-19]. As such, targeting of KIT by tyrosine kinase inhibitors (TKIs) has recently emerged as a therapeutic strategy in veterinary medicine with the approval of toceranib (TOC) phosphate (Palladia®) and masitinib (Kinavet®, Masivet®), the only TKIs approved in veterinary medicine for use in non-resectable, recurrent canine MCT. Despite the clinical benefit of TOC, the eventual development of resistance remains a therapeutic impediment.

We have recently described the development of an *in vitro* model of resistance to TOC in canine MCT cell lines and identified secondary mutations in the functional domains of KIT. We generated three TOC-resistant sublines, TR1, TR2, and TR3, after chronic exposure of the TOC-

sensitive canine C2 MCT cell line to TOC. Analysis of KIT activation revealed that TOC failed to inhibit autophosphorylation of the KIT receptor in the resistant lines; therefore, we hypothesized that acquisition of secondary mutations in the *c-kit* gene could potentially be responsible for the observed TOC resistance. By sequencing full-length *c-kit*, we identified six newly acquired missense mutations within the juxtamembrane and kinase domains of the KIT receptor.

We present here the analysis of these mutations by computational-based modeling to determine if these mutations are likely to confer the observed resistance to TOC. In addition, we examine these mutations in relation to three other KIT inhibitors that show variable sensitivity to the resistant sublines. To accomplish this, we constructed four *in silico* homology models of the cytoplasmic region of TOC-sensitive and -resistant canine KIT to predict the consequent structures of the drug binding site. Utilizing computational-based small molecule docking techniques, we calculated the predicted binding energies and orientations of TOC and the three other KIT inhibitors within the KIT mutant homology models to determine the structural basis of TOC resistance *in vitro* in the context of canine MCT. Finally, we tested whether this computational approach can serve as a predictor of *in vitro* drug sensitivity for novel kinase inhibitors.

## METHODS

### Cell culture

Toceranib phosphate (Palladia®) was provided by Zoetis (Madison, NJ). Masitinib (AB1010, Kinavet®) and LY2457546 were provided by AB Science (Paris, France) and Elanco (Greenfield, IN), respectively. Imatinib was purchased from Selleck Chemical (Houston, TX).

Ponatinib (Inclusig®) was purchased from Selleck. Stock solutions of all drugs were prepared in DMSO and stored at -20°C. The canine C2 mastocytoma cell line, derived from a spontaneously occurring cutaneous MCT and harboring an ITD in exon 11, was used as the parental cell line [20]. Cells were propagated in RPMI 1640 supplemented with 2 mM L-glutamine, 10% FBS (source?), 100 g/mL streptomycin, and 100 U/mL penicillin at 37°C with a humidified atmosphere of 5% $CO_2$.

**Generation of toceranib-resistant C2 sublines**

TOC-resistant C2 cells were established as previously described (Halsey, et al). Briefly, C2 cells were grown continuously in up to 100 nM, 200 nM, or 250 nM TOC in increasing increments of 25-50 nM. Culture media and drug were changed every 72 hours. Over a period of 7 months, three sub-lines were established and designated TOC-resistant (TR)1, TR2, and TR3.

**Drug sensitivity tests.** The sensitivity and resistance of each cell line to the KIT inhibitors were determined by measuring relative viable cell number using a bioreductive fluorometric assay (Alamar Blue, Promega, WI). All three TR sublines as well as the treatment naïve, parental C2 cells were seeded in triplicate in 96-well plates at 2,000 cells per well. Serial dilutions of the KIT inhibitors were prepared in media and cells treated for 72 hours. Alamar Blue reagent was added to all wells, plates were incubated for 1 hour at 37°C, and fluorescence was measured on a Synergy multiparameter microplate reader (BioTek, Winooski, VT) to determine cell viability. Dose-response curves were generated using Prism (GraphPad Software, La Jolla, CA).

**Computational-based molecular modeling**

All molecular modeling studies were conducted using Accelrys Discovery Studio 3.5 (Accelrys Software, Inc., San Diego, CA; http://accelrys.com) and all crystal structure coordinates were downloaded from the protein data bank (www.pdb.org). The homology model of the intracellular domain of canine KIT was constructed with the MODELLER protocol [21] using the crystal structures of human KIT as a template (PDB IDs: 1T46 and 3G0E; 88.3% identity, 93.5% similarity) for the bulk of the model [22,23]. The region from Gln693 to Arg742 of the canine KIT sequence was modeled using human 1-phosphatidylinositol-4,5-bisphosphate phosphodiesterase beta-3 (PDB ID: 3OHM; 24% identity, 43% similarity) [24] and the loop containing residues Ile742 to Thr752 was refined using the LOOPER algorithm [25]. Mutant structures were generated by altering the identity of the relevant residues to the mutant form. The resulting final structures were subjected to energy minimization utilizing the conjugate gradient minimization protocol with a CHARMm forcefield and the Generalized Born implicit solvent model with molecular volume [26]. All minimization calculations converged to an RMS gradient of < 0.001 kcal/mol. The flexible docking algorithm was used to predict the binding orientations of TOC and the three other compounds in each of the four KIT protein models [27]. A total of 16 KIT-ligand complexes (example shown in **Figure 3.1)** underwent energy minimization *in situ* using the conjugate gradient method (10,000 iterations) followed by binding energy calculations using the Generalized Born implicit solvent model with molecular volume [26].

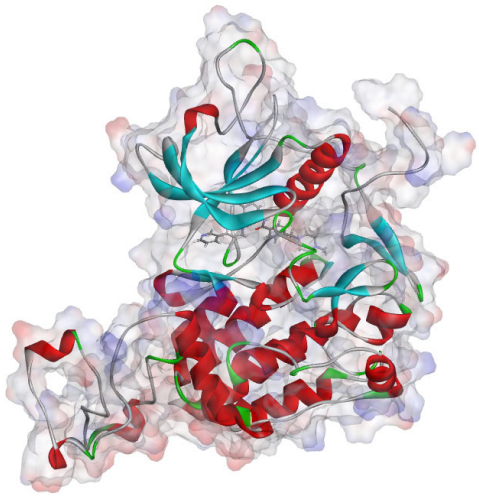

**Figure 3.1:** Homology model of the intracellular domain of canine KIT with TOC bound.

## RESULTS

### Toceranib-resistant C2 cells emerged during chronic, stepwise TOC treatment.

To explore mechanisms of acquired TOC resistance in canine MCT, we generated three resistant sublines from the TOC-sensitive exon 11 ITD *c-kit* mutant C2 cell line designated TR1, TR2, and TR3. Growth of the parental C2 cells was inhibited by TOC in a dose-dependent manner with an $IC_{50}$ of <10 nM. In contrast, TOC failed to inhibit growth of TR1, TR2, and TR3 sublines ($IC_{50}$ > 1,000 nM). Sensitivity to the other three KIT RTK inhibitors was similar with some variability between the sublines suggesting different mechanisms of resistance. (**Figure 2.2**).

### Predicted effects of the mutations on KIT protein structure.

We previously identified the following point mutations in the three TOC-resistant sublines: TR1 (Q574R, M835T), TR2 (K724R), and TR3 (K580R, R584G, A620S). To determine whether the previously identified secondary mutations in KIT participated in the

observed TOC resistance, mutant structures of the homology models of the intracellular domain of canine KIT were constructed. **Figure 3.2** illustrates the locations of each mutated residue identified in each subline, with the mutations summarized in **Table 1**. The various point mutations identified in the TOC resistant KIT sequences were almost exclusively located outside of the ATP binding site. The one exception was Ala620, which lies within the ATP site at the entrance to the allosteric site. Thus, it does not appear that the mutations would necessarily alter the drug-protein interaction directly (i.e. the mutant residues do not appear to be involved in direct interactions with the drug itself). In order to assess potential conformational changes to the KIT protein induced by the various mutations, the TOC-sensitive and three TOC-resistant protein structures were subjected to implicit solvent-based energy minimization. Interestingly, each of the three drug resistant mutants was predicted to induce a conformational change in the region of the binding site to a greater or lesser degree (**Figure 3.3**). Compared to the parental C2 drug binding site (Figure 4A), the binding site of the TR1 subline appeared to be the least altered (**Figure 3.3B**), while TR2 and TR3 binding sites appeared to be similarly but more profoundly altered in this region of the protein. TR2 was predicted to induce a further narrowing of the entrance to the allosteric site, while TR3 shifted the position of the opening in relation to the allosteric site itself (**Figure 3.3C and D**).

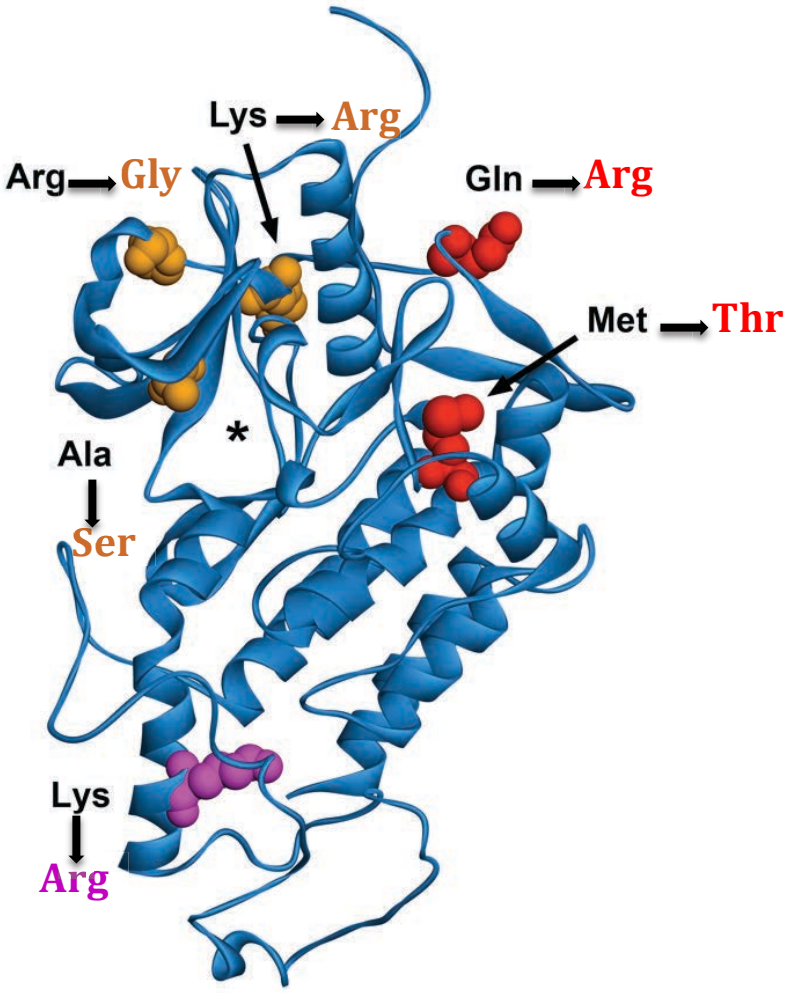


**Figure 3.2** Protein homology model of canine KIT. Ribbon structure of the cytoplasmic region of canine KIT showing the locations of each mutated residue identified in each subline in a different color. (Mutant TR1 residues- red, TR2- magenta, and TR3- orange). The asterisk denotes the location of the ATP-binding site.

**Table 3.1:** Acquired secondary KIT mutations in the three resistant sublines

| Subline | Nucleotide Position | Nucleotide Change | Amino Acid Position | Amino Acid Change |
|---|---|---|---|---|
| TR1 | 1781 | A->G | 574 | Gln->Arg |
| | 2567 | T->C | 835 | Met->Thr |
| TR2 | 2231 | A->G | 724 | Lys->Arg |
| TR3 | 1799 | A->G | 580 | Lys->Arg |
| | 1813 | A->G | 584 | Arg->Gly |
| | 1918 | G->T | 620 | Ala->Ser |

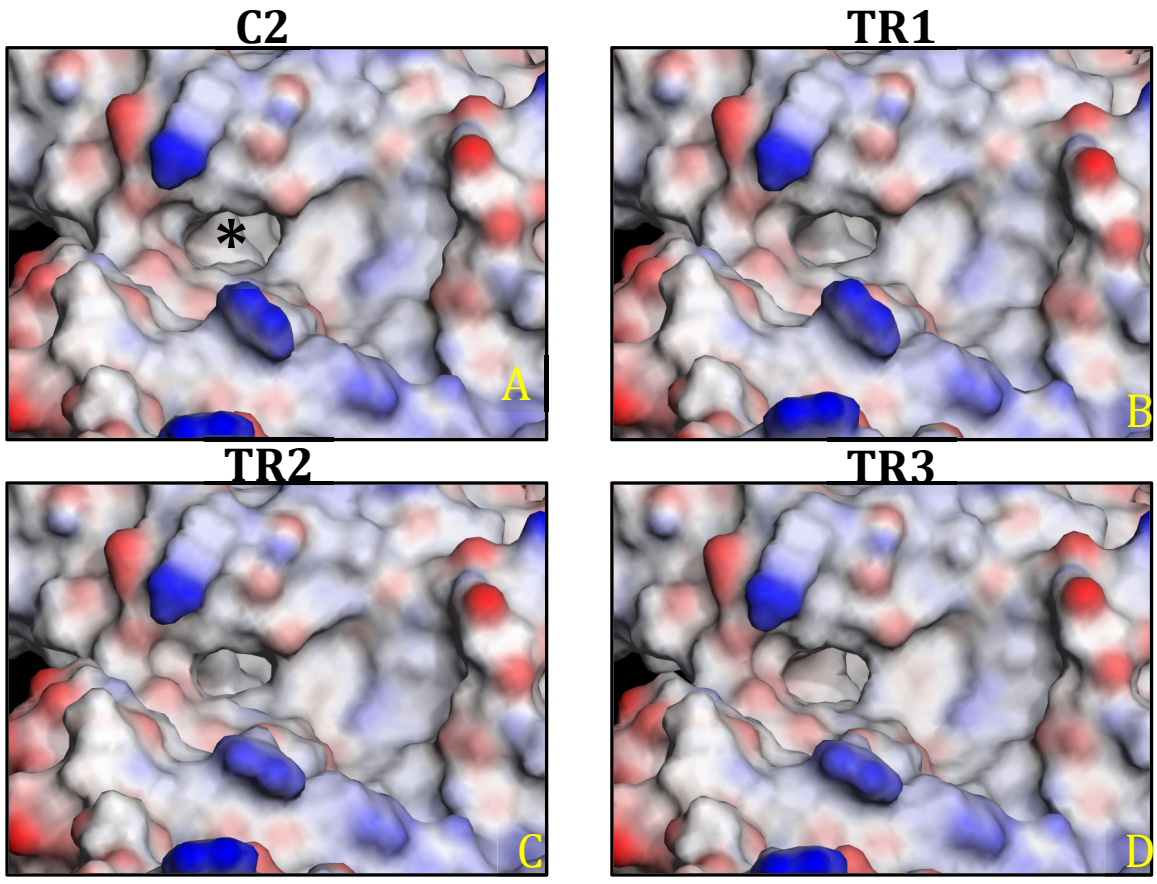


**Figure 3.3:** Predicted structural alterations induced by the various drug resistant mutations. Surface representation of the drug-binding sites of parental and TOC-resistant KIT. The asterisk denotes the location of the ATP-binding site.

**Effects of the drug-resistant mutations on predicted drug binding.**

Given that the mutations were predicted to induce conformational changes in the drug binding site of the KIT protein, we performed small molecule docking and binding energy calculations for each of the four drugs in each of the four KIT protein models to evaluate whether these changes translated to a decrease in affinity of the proteins for each of the drugs. This resulted in decreased favorability of the predicted binding of TOC to each of the three drug resistant mutants (**Table 3.2**). Similar results were also obtained for each of the three drug resistant mutations on LY2457546 binding. The TR1 mutation, however, was predicted to have only minor effects on the binding of masitinib and imatinib, while both TR2 and TR3 mutations induced a substantial decrease in predicted binding affinity for these compounds. To determine the relationship between these predicted binding energies determined *in silico* and growth inhibition determined *in vitro*, the coefficient of determination was calculated by linear regression analysis (**Figure 3.4**). While there was a positive correlation between predicted binding energies and % control at 10 nM for all four compounds, statistical significance was not reached. In order to make a more direct comparison of drug binding and inhibition of drug target, the coefficient of determination was calculated for the predicted binding energies of TOC in a all four KIT proteins and phosphorylated KIT, as determined by densitometry of western blot shown in **Figure 2.7**. As shown in **Figure 3.5**, there was a significant positive correlation between pKIT expression at 10 nM TOC and predicted binding energy ($r^2$=0.90; $p<0.05$) and a similar, but not significant, trend for pKIT expression at 100 nM TOC and predicted binding energy ($r^2$=0.88; p=0.057).

**Table 3.2:** Solvent corrected predicted binding energies (kcal/mol) of four compounds to four KIT homology models (C2, TR1, TR2, TR3). (Generalized Born with Molecular Volume implicit solvent model).

| | C2 | TR1 | TR2 | TR3 |
|---|---|---|---|---|
| Toceranib | -52.6 | -36.5 | -27.0 | -31.1 |
| LY2457546 | -58.7 | -30.7 | -31.1 | -37.6 |
| Masitinib | -82.2 | -74.6 | -37.4 | -34.2 |
| Imatinib | -86.3 | -72.9 | -30.1 | -30.2 |

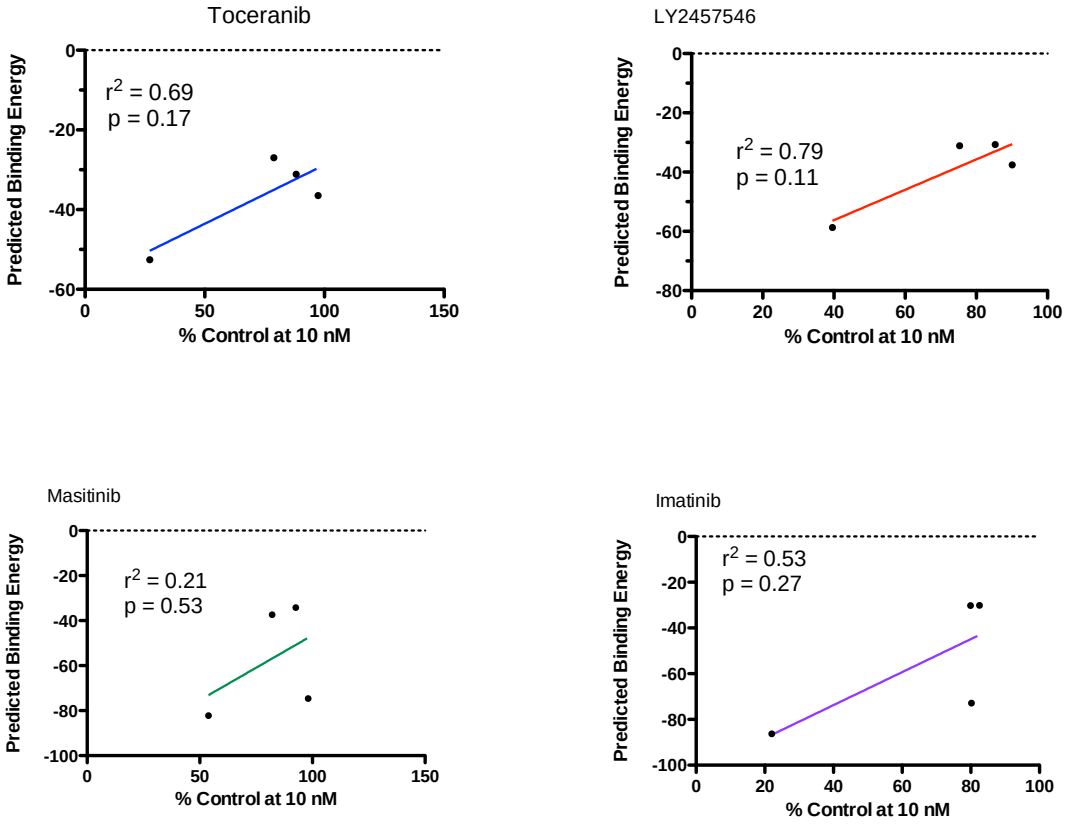


**Figure 3.4:** Correlation of predicted binding energy to growth inhibition (% control at 10nM drug) by linear regression.

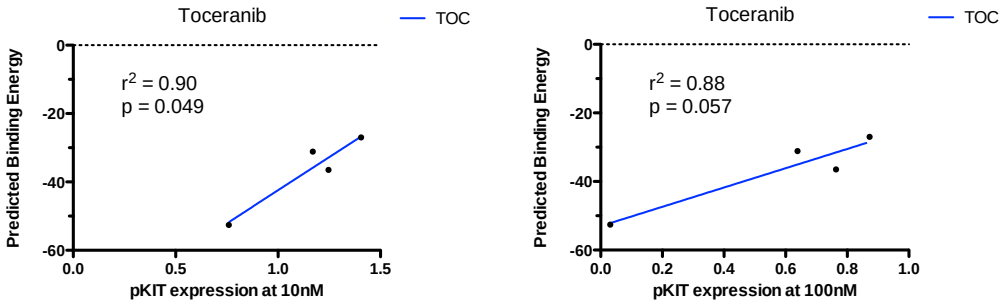


**Figure 3.5:** Correlation of predicted binding energy to phosphorylated KIT expression at 10 nM and 100 nM drug) by linear regression.

**Homology modeling as an *a priori* predictor of response to second line KIT inhibitors in TOC-resistant MCT cells.**

To evaluate the usefulness of *in silico* homology modeling and small molecule docking methodologies in predicting response to a novel KIT inhibitor, we docked ponatinib into the intracellular domain of the TOC-sensitive and each of the three TOC-resistant KIT mutant protein structures, followed by binding energy calculations as described above. As shown in **Table 3.3**, ponatinib was predicted to bind favorably to TOC-sensitive KIT, but exhibited a substantial decrease in the favorability of the predicted binding to each of the three TOC-resistant mutants. To determine if these predicted binding energies for ponatinib correlated to growth inhibition, or lack thereof, *in vitro*, MTS assays were performed on the C2, TR1, TR2, and TR3 cells treated with ponatinib. In concordance with the predicted binding energies, ponatinib inhibited the growth of the TOC-sensitive C2 cells in a dose-dependent manner and failed to inhibit growth of the TOC-resistant cells (**Figure 3.6**). Furthermore, there was a significant correlation between predicted binding energy and growth inhibition by ponatinib (**Figure 3.7**).

**Table 3.3:** Solvent corrected predicted binding energies (kcal/mol) of ponatinib to four KIT homology models (C2, TR1, TR2, TR3). (Generalized Born with Molecular Volume implicit solvent model. Kcal/mol).

| | C2 | TR1 | TR2 | TR3 |
|---|---|---|---|---|
| Ponatinib | -78.9 | -36.8 | -31.4 | -40.1 |

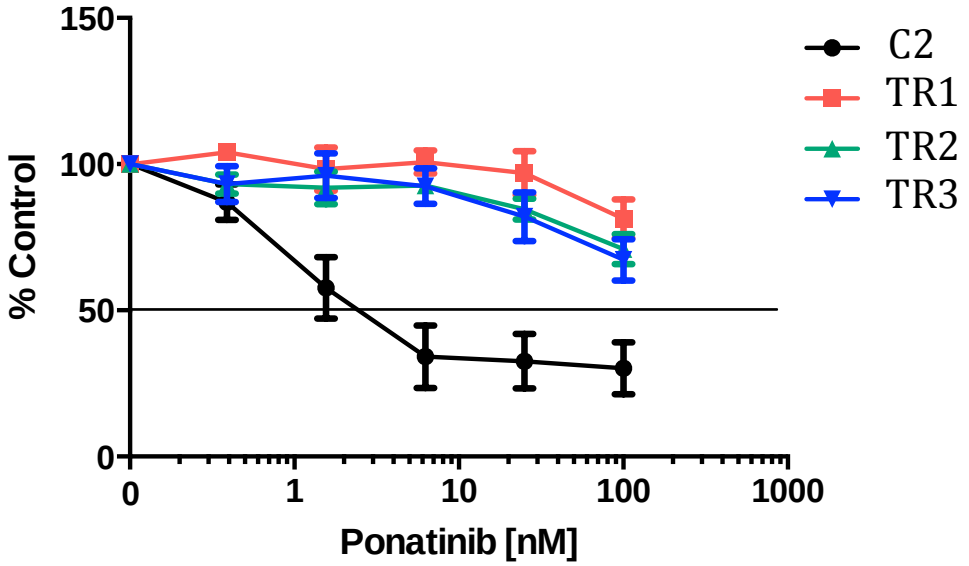


**Figure 3.6:** Dose-dependent growth inhibition of parental line (C2) and three resistant sublines (TR1, TR2, TR3) after incubation with increasing concentrations of ponatinib for 72 hours.

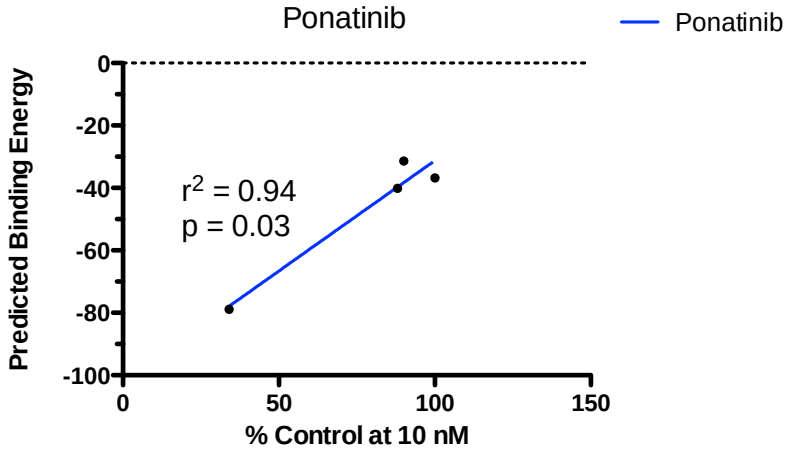


**Figure 3.7:** Correlation of predicted binding energy to growth inhibition (% control at 10 nM drug) by linear regression.

## DISCUSSION

Malignancies harboring specific gain-of-function mutations in protein kinases are often exquisitely sensitive to small molecule TKIs and partial disease remission is often achieved. Despite these successes, remission is often transitory as the majority of these tumors with once drug-sensitizing mutations eventually progress on treatment as they acquire resistance. One of the most commonly reported mechanisms of resistance to TKIs is the acquisition of secondary mutations in the target kinase [28-34]. In this study, we have described this phenomenon in the context of TOC and its use in the treatment of canine MCT.

Similar to other tyrosine kinase inhibitors, TOC exerts its inhibitory effect on the KIT RTK by binding to the ATP-binding site in a competitive approach, thereby blocking cross-phosphorylation of tyrosine residues and subsequent downstream signaling [35-38]. Acquisition of secondary genetic mutations conferring TKI resistance is commonly reported in and around the ATP-binding site [28,33,39,40]. These nucleotides encode amino acids that control access or contribute to the hydrophobic pocket near the ATP-binding site [40,41]. Mutations in this region lead to abrogation of drug binding by loss of the hydrophobic interactions necessary for drug binding and/or creation of steric hindrance that precludes the inhibitor from entering the binding pocket [40]. In the current study, all four of the KIT inhibitors examined are predicted to bind in both the ATP site and the allosteric site of the KIT kinase receptor. All of the missense mutations identified in TR1, TR2, or TR3 were predicted to induce a conformational change in this region of the protein, resulting in alterations in the size and shape of the entrance to the allosteric site. The structural changes in this area were sufficient to alter the predicted binding energies of the various compounds to a greater or lesser degree. The structures of the four compounds examined are shown in **Figure 3.8**, which highlight the ATP-binding and allosteric

portions. The ATP-binding portions of TOC and LY2457546 consist of fused ring structures. Masitinib and imatinib are structurally distinct from TOC and LY2457546 in that their ATP-binding portions consist of a single ring and a secondary amine, thus they are less bulky and more flexible in this region. The observed changes to the binding site occurs around the ATP-binding site portion of the pocket. As such, the change in conformation of this area is sufficient to impair the binding of TOC and LY2457546 in all three of the mutants, but masitinib and imatinib are flexible and small enough to be less affected by the TR1 mutation. The TR2 and TR3 changes, which were greater in magnitude, appeared sufficient to impair the binding of masitinib and imatinib.

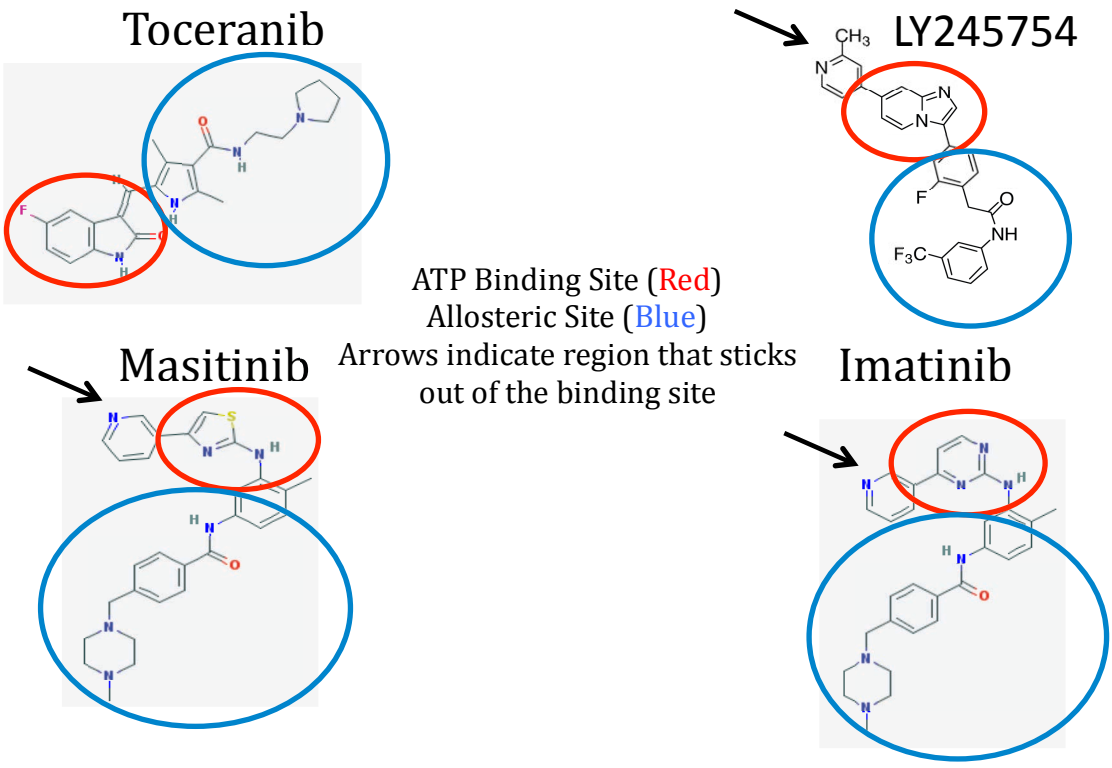


**Figure 3.8:** Chemical structures of TOC, LY2457546, masitinib, and imatinib.

The TR1 mutation induced a predicted narrowing of the allosteric site opening, likely due in part to the substitution of Met835 with a Thr residue, which altered the pattern of hydrogen bond interactions in this area, replacing a relatively weak hydrogen bond interaction between Tyr845 and Met835 (**Figure 3.9A**), with two stronger hydrogen bonds, one between the side chains of Ser839 and Tyr845 and the other between Thr835 and the backbone carbonyl of Val832 (**Figure 3.9B**). As a result, this mutation likely plays a more substantial role in the observed conformational changes induced by the TR1 mutation as opposed to the substitution of Gln574, which has a more peripheral location on the protein. The TR2 mutation induced a greater constriction of the entrance to the allosteric site compared to TR1, further suggesting that the introduction of steric clashes with the bulkier heterocycles may likely be the mechanism responsible for the predicted decrease in binding affinity. In contrast, the TR3 mutation was predicted to shift the position of the allosteric site entrance, rather than substantially altering the size of the opening. This may be due to the fact that Arg585 is involved in hydrogen bond interactions with the backbone carbonyls of both Val661 and Pro664 (**Figure 3.9C**) and these interactions appear to be involved in maintaining the proper position of the allosteric site entrance. Mutation of this residue to a Gly eliminates these interactions (**Figure 3.9D**) and likely plays a substantial role in the observed positional change to the entrance. In both instances (TR2 and TR3), compounds with smaller and/or more flexible moieties that bind this region, such as masitinib and imatinib, would be more likely to tolerate conformational changes such as these. Overall, these results are generally consistent with the relative drug resistance observed *in vitro* and would suggest that the predicted changes to the entrance of the allosteric site play a role in the observed decrease in the predicted binding energies and may provide a mechanistic basis for the drug resistance induced by these mutations.

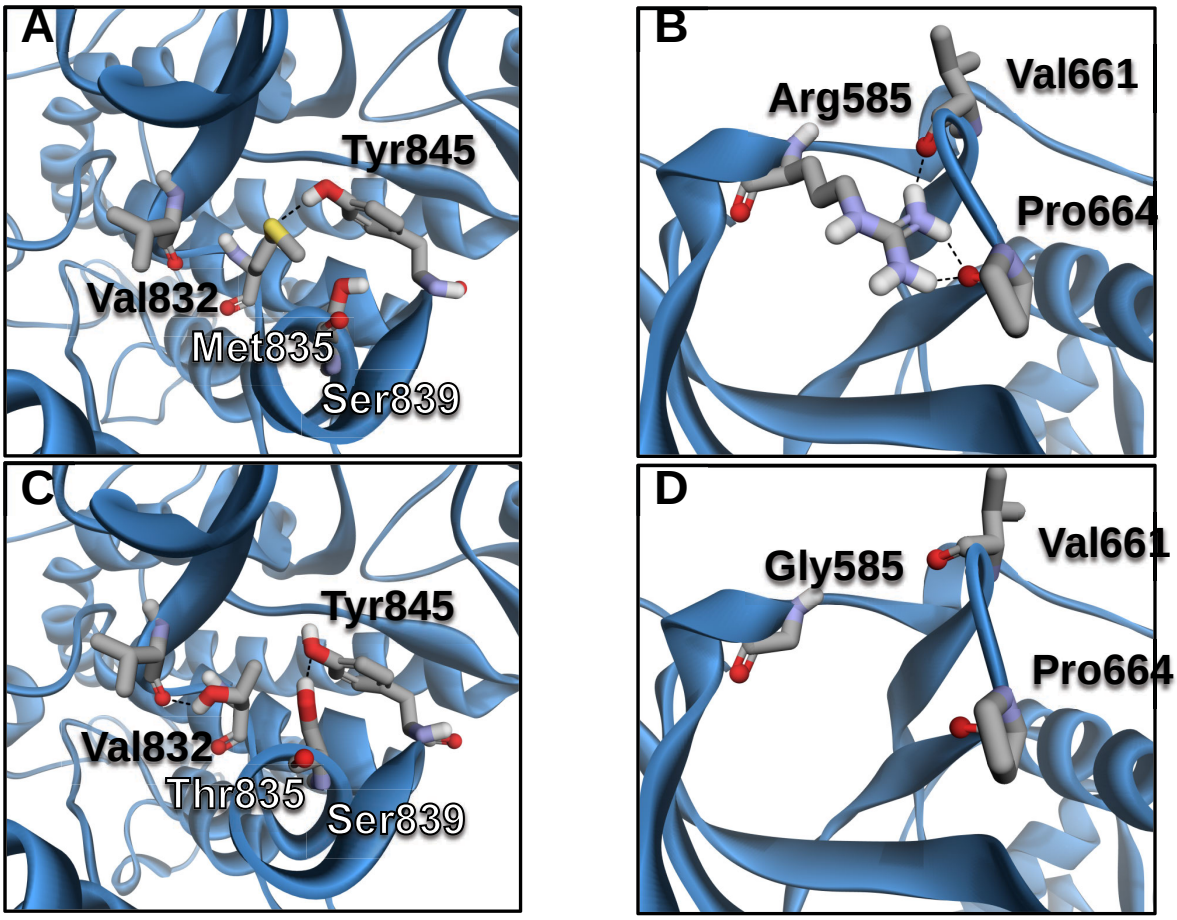


**Figure 3.9:** Predicted structural effects of selected point mutations occurring in TR1 and TR3. Close up views of the regions of the TOC-sensitive canine KIT containing (A) Met835 and (B) Arg585 and their corresponding mutations in (C) TR1 (M835T) and (D) TR3 (R585G). Both mutations were predicted to alter the hydrogen bonding patterns in these areas and may play a role in the predicted structural alterations to the protein as well as the differences in drug sensitivity observed *in vitro*.

The observed decrease in binding affinity may be playing a role in the upregulation of KIT expression observed in each of the drug resistant cell lines in response to TOC treatment shown in **Figure 2.8**. While there was a predicted decrease in binding affinity, the binding energies did not indicate a complete lack of drug binding. Therefore, some inhibition of KIT by TOC is predicted to occurr in all of the resistant sublines. While the drug concentrations used may not be sufficient to result in cell death or growth inhibition, exertion of some inhibition of

KIT signaling by TOC is likely resulting in the enhanced expression of KIT in these cells as an adaptive response. Indeed, modifications in protein expression in tumor cells that allows them to continue to survive in adverse conditions has been reported as a mechanism of resistance [32,42-44].

The nearly inevitable development of resistance to targeted therapies highlights the need to develop second line therapies. We have shown that computational approaches are valuable tools to investigate the molecular mechanisms of mutation-induced drug resistance. In addition, we investigated the utility of these computational strategies to predict the response of TOC-resistant KIT mutants to a novel RTK inhibitor. Ponatinib is a third-generation kinase inhibitor with activity primarily against wild-type BCR-ABL1 as well as PDGFRA, KIT and FGFR1 [45,46]. Quantitative *a priori* prediction of the binding affinity of ponatinib to the homology models of drug resistant canine KIT showed a decreased favorability of the predicted binding of ponatinib to each of the three TOC-resistant mutants. This correlated significantly with the growth inhibition curves generated *in vitro*. Since the vast majority of tyrosine kinase inhibitors exert their inhibitory effect by competitively binding the ATP-binding site, and the majority of the resistant mutations thus far identified were either located in or around the ATP-binding site or were predicted to alter the conformation of this region of the protein, the proposed model is likely a good predictor of response to other inhibitors that bind in a similar fashion. Indeed, when the correlation of the predicted binding energies to growth inhibition *in vitro* for the four original compounds are combined, there is a significant correlation between these two variables, suggesting that this model is applicable in a drug-independent manner (**Figure 3.10)**. That is, the utility of this model is best demonstrated in predicting the relative binding affinities of drugs that compete for the ATP-binding site.

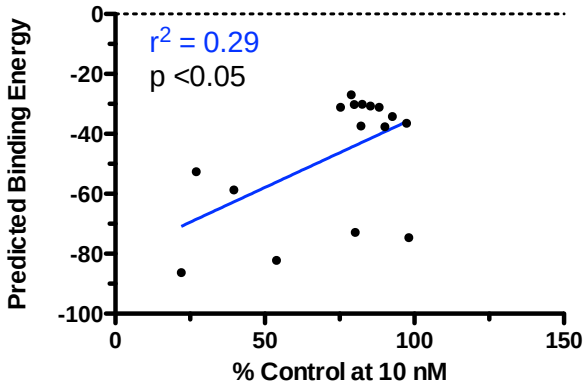


**Figure 3.10:** Correlation of predicted binding energy to growth inhibition (% control at 10 nM drug) by linear regression for all four compounds collectively.

In summary, we have generated three TOC-resistant canine MCT cell lines following chronic exposure of C2 cells to TOC. Resistance likely occurred as a result of the acquisition of secondary missense mutations in the KIT receptor. These mutations occurred in the area of the drug binding pocket, inducing a conformational change to the entrance of the binding pocket which consequently interfered with the interactions between TOC and KIT. The observed overexpression of the target kinase likely functions as an adaptive reaction to KIT inhibition. To the authors' knowledge, this is the first effort in veterinary oncology to describe mechanisms of acquired resistance to targeted therapy by computational modeling. Future studies should include large-scale screening of relapsed patient-derived tumor samples for *c-kit* mutations to determine whether the secondary alterations identified in KIT are clinically relevant and to determine the relative frequency with which these mutations occur. Despite the necessity of future *in vivo* studies, there is considerable evidence that mechanisms of resistance described *in vitro* are validated in RTK inhibitor- refractory patient-derived tumor samples [47-50].

The development and use of alternative KIT inhibitors may be useful to overcome TOC resistance mediated by acquisition of secondary KIT mutations. Furthermore, the use of

combinatorial approaches to targeted inhibition may circumvent acquisition of disparate secondary mutations as demonstrated here. Finally, we have shown that homology modeling of mutated target kinases can demonstrate how defined mutations can confer resistance and underscores the model's predictive ability in testing new selective inhibitors.

## References


1. Fabbro D, Ruetz S, Buchdunger E, Cowan-Jacob SW, Fendrich G, et al. (2002) Protein kinases as targets for anticancer agents: from inhibitors to useful drugs. Pharmacol Ther 93: 79-98.
2. Traxler P (2003) Tyrosine kinases as targets in cancer therapy - successes and failures. Expert Opin Ther Targets 7: 215-234.
3. Letard S, Yang Y, Hanssens K, Palmerini F, Leventhal PS, et al. (2008) Gain-of-function mutations in the extracellular domain of KIT are common in canine mast cell tumors. Mol Cancer Res 6: 1137-1145.
4. Webster JD, Yuzbasiyan-Gurkan V, Kaneene JB, Miller R, Resau JH, et al. (2006) The role of c-KIT in tumorigenesis: evaluation in canine cutaneous mast cell tumors. Neoplasia 8: 104-111.
5. Roskoski R, Jr. (2005) Signaling by Kit protein-tyrosine kinase--the stem cell factor receptor. Biochem Biophys Res Commun 337: 1-13.
6. Ma Y, Longley BJ, Wang X, Blount JL, Langley K, et al. (1999) Clustering of activating mutations in c-KIT's juxtamembrane coding region in canine mast cell neoplasms. J Invest Dermatol 112: 165-170.
7. London CA, Galli SJ, Yuuki T, Hu ZQ, Helfand SC, et al. (1999) Spontaneous canine mast cell tumors express tandem duplications in the proto-oncogene c-kit. Exp Hematol 27: 689-697.
8. Qiu FH, Ray P, Brown K, Barker PE, Jhanwar S, et al. (1988) Primary structure of c-kit: relationship with the CSF-1/PDGF receptor kinase family--oncogenic activation of v-kit involves deletion of extracellular domain and C terminus. EMBO J 7: 1003-1011.
9. Turner AM, Zsebo KM, Martin F, Jacobsen FW, Bennett LG, et al. (1992) Nonhematopoietic tumor cell lines express stem cell factor and display c-kit receptors. Blood 80: 374-381.
10. Heinrich MC, Blanke CD, Druker BJ, Corless CL (2002) Inhibition of KIT tyrosine kinase activity: a novel molecular approach to the treatment of KIT-positive malignancies. J Clin Oncol 20: 1692-1703.
11. Antonescu C (2012) Gastrointestinal stromal tumors. Curr Top Microbiol Immunol 355: 41-57.
12. Lerner NB, Nocka KH, Cole SR, Qiu FH, Strife A, et al. (1991) Monoclonal antibody YB5.B8 identifies the human c-kit protein product. Blood 77: 1876-1883.
13. Chan PM, Ilangumaran S, La Rose J, Chakrabartty A, Rottapel R (2003) Autoinhibition of the kit receptor tyrosine kinase by the cytosolic juxtamembrane region. Mol Cell Biol 23: 3067-3078.
14. Peter B, Hadzijusufovic E, Blatt K, Gleixner KV, Pickl WF, et al. (2010) KIT polymorphisms and mutations determine responses of neoplastic mast cells to bafetinib (INNO-406). Exp Hematol 38: 782-791.
15. Carlsten KS, London CA, Haney S, Burnett R, Avery AC, et al. (2012) Multicenter prospective trial of hypofractionated radiation treatment, toceranib, and prednisone for measurable canine mast cell tumors. J Vet Intern Med 26: 135-141.

16. Lin TY, Bear M, Du Z, Foley KP, Ying W, et al. (2008) The novel HSP90 inhibitor STA-9090 exhibits activity against Kit-dependent and -independent malignant mast cell tumors. Exp Hematol 36: 1266-1277.
17. Zemke D, Yamini B, Yuzbasiyan-Gurkan V (2002) Mutations in the Juxtamembrane Domain of c-KIT Are Associated with Higher Grade Mast Cell Tumors in Dogs. Veterinary Pathology 39: 529-535.
18. Thamm CALaDH (2013) Mast Cell Tumors; Stephen J. Withrow DMV, Rodney L. Page, editor.
19. Takeuchi Y, Fujino Y, Fukushima K, Watanabe M, Nakagawa T, et al. (2012) Biological effect of tyrosine kinase inhibitors on three canine mast cell tumor cell lines with various KIT statuses. J Vet Pharmacol Ther 35: 97-104.
20. DeVinney R, Gold WM (1990) Establishment of two dog mastocytoma cell lines in continuous culture. Am J Respir Cell Mol Biol 3: 413-420.
21. Eswar N, Eramian D, Webb B, Shen MY, Sali A (2008) Protein structure modeling with MODELLER. Methods Mol Biol 426: 145-159.
22. Mol CD, Dougan DR, Schneider TR, Skene RJ, Kraus ML, et al. (2004) Structural basis for the autoinhibition and STI-571 inhibition of c-Kit tyrosine kinase. J Biol Chem 279: 31655-31663.
23. Gajiwala KS, Wu JC, Christensen J, Deshmukh GD, Diehl W, et al. (2009) KIT kinase mutants show unique mechanisms of drug resistance to imatinib and sunitinib in gastrointestinal stromal tumor patients. Proc Natl Acad Sci U S A 106: 1542-1547.
24. Waldo GL, Ricks TK, Hicks SN, Cheever ML, Kawano T, et al. (2010) Kinetic scaffolding mediated by a phospholipase C-beta and Gq signaling complex. Science 330: 974-980.
25. Spassov VZ, Flook PK, Yan L (2008) LOOPER: a molecular mechanics-based algorithm for protein loop prediction. Protein Eng Des Sel 21: 91-100.
26. Feig M, Im W, Brooks CL, 3rd (2004) Implicit solvation based on generalized Born theory in different dielectric environments. J Chem Phys 120: 903-911.
27. Koska J, Spassov VZ, Maynard AJ, Yan L, Austin N, et al. (2008) Fully automated molecular mechanics based induced fit protein-ligand docking method. J Chem Inf Model 48: 1965-1973.
28. Engelman JA, Janne PA (2008) Mechanisms of acquired resistance to epidermal growth factor receptor tyrosine kinase inhibitors in non-small cell lung cancer. Clin Cancer Res 14: 2895-2899.
29. Engelman JA, Settleman J (2008) Acquired resistance to tyrosine kinase inhibitors during cancer therapy. Curr Opin Genet Dev 18: 73-79.
30. Janne PA, Gray N, Settleman J (2009) Factors underlying sensitivity of cancers to small-molecule kinase inhibitors. Nat Rev Drug Discov 8: 709-723.
31. Gounder MM, Maki RG (2011) Molecular basis for primary and secondary tyrosine kinase inhibitor resistance in gastrointestinal stromal tumor. Cancer Chemother Pharmacol 67 Suppl 1: S25-43.
32. Sierra JR, Cepero V, Giordano S (2010) Molecular mechanisms of acquired resistance to tyrosine kinase targeted therapy. Mol Cancer 9: 75.
33. Antonescu CR, Besmer P, Guo T, Arkun K, Hom G, et al. (2005) Acquired resistance to imatinib in gastrointestinal stromal tumor occurs through secondary gene mutation. Clin Cancer Res 11: 4182-4190.

34. Ellis LM, Hicklin DJ (2009) Resistance to Targeted Therapies: Refining Anticancer Therapy in the Era of Molecular Oncology. Clin Cancer Res 15: 7471-7478.
35. Pryer NK, Lee LB, Zadovaskaya R, Yu X, Sukbuntherng J, et al. (2003) Proof of target for SU11654: inhibition of KIT phosphorylation in canine mast cell tumors. Clin Cancer Res 9: 5729-5734.
36. London CA (2009) Tyrosine kinase inhibitors in veterinary medicine. Top Companion Anim Med 24: 106-112.
37. London CA, Malpas PB, Wood-Follis SL, Boucher JF, Rusk AW, et al. (2009) Multi-center, placebo-controlled, double-blind, randomized study of oral toceranib phosphate (SU11654), a receptor tyrosine kinase inhibitor, for the treatment of dogs with recurrent (either local or distant) mast cell tumor following surgical excision. Clin Cancer Res 15: 3856-3865.
38. London CA, Hannah AL, Zadovoskaya R, Chien MB, Kollias-Baker C, et al. (2003) Phase I dose-escalating study of SU11654, a small molecule receptor tyrosine kinase inhibitor, in dogs with spontaneous malignancies. Clin Cancer Res 9: 2755-2768.
39. Pao W, Miller VA, Politi KA, Riely GJ, Somwar R, et al. (2005) Acquired resistance of lung adenocarcinomas to gefitinib or erlotinib is associated with a second mutation in the EGFR kinase domain. PLoS Med 2: e73.
40. Stehle F, Schulz K, Seliger B (2013) Towards defining biomarkers indicating resistances to targeted therapies. Biochim Biophys Acta.
41. Zhang J, Yang PL, Gray NS (2009) Targeting cancer with small molecule kinase inhibitors. Nat Rev Cancer 9: 28-39.
42. Mahon FX, Hayette S, Lagarde V, Belloc F, Turcq B, et al. (2008) Evidence that resistance to nilotinib may be due to BCR-ABL, Pgp, or Src kinase overexpression. Cancer Res 68: 9809-9816.
43. Morinaga K, Yamauchi T, Kimura S, Maekawa T, Ueda T (2008) Overcoming imatinib resistance using Src inhibitor CGP76030, Abl inhibitor nilotinib and Abl/Lyn inhibitor INNO-406 in newly established K562 variants with BCR-ABL gene amplification. Int J Cancer 122: 2621-2627.
44. Donato NJ, Wu JY, Stapley J, Gallick G, Lin H, et al. (2003) BCR-ABL independence and LYN kinase overexpression in chronic myelogenous leukemia cells selected for resistance to STI571. Blood 101: 690-698.
45. Lierman E, Smits S, Cools J, Dewaele B, Debiec-Rychter M, et al. (2012) Ponatinib is active against imatinib-resistant mutants of FIP1L1-PDGFRA and KIT, and against FGFR1-derived fusion kinases. Leukemia 26: 1693-1695.
46. O'Hare T, Shakespeare WC, Zhu X, Eide CA, Rivera VM, et al. (2009) AP24534, a pan-BCR-ABL inhibitor for chronic myeloid leukemia, potently inhibits the T315I mutant and overcomes mutation-based resistance. Cancer Cell 16: 401-412.
47. Todd JR, Becker TM, Kefford RF, Rizos H (2013) Secondary c-Kit mutations confer acquired resistance to RTK inhibitors in c-Kit mutant melanoma cells. Pigment Cell Melanoma Res 26: 518-526.
48. Nazarian R, Shi H, Wang Q, Kong X, Koya RC, et al. (2010) Melanomas acquire resistance to B-RAF(V600E) inhibition by RTK or N-RAS upregulation. Nature 468: 973-977.
49. Villanueva J, Vultur A, Lee JT, Somasundaram R, Fukunaga-Kalabis M, et al. (2010) Acquired resistance to BRAF inhibitors mediated by a RAF kinase switch in melanoma can be overcome by cotargeting MEK and IGF-1R/PI3K. Cancer Cell 18: 683-695.

50. Azam M, Latek RR, Daley GQ (2003) Mechanisms of autoinhibition and STI-571/imatinib resistance revealed by mutagenesis of BCR-ABL. Cell 112: 831-843.

# Chapter 4

## Expression of phosphorylated KIT in canine mast cell tumor: significance as a marker of tumor aggressiveness and response to KIT inhibition


### SUMMARY

Canine cutaneous mast cell tumor (MCT) represents the most common skin tumor in dogs and often exhibits variable biologic behavior. Signaling through the KIT receptor tyrosine kinase promotes proliferation and increased cell survival and has been shown to play an important role in MCT progression. Despite investigations into numerous biomarkers and the proposal of several grading schemas, no single marker or grading system can accurately predict outcome in canine MCT. The first aim of the current study was to develop an immunohistochemical-based assay to directly measure phosphorylated KIT (pKIT) in order to investigate its association with two commonly used grading systems as well as other established prognostic markers (KIT localization, Ki67 expression, mitotic index, and *c-kit* mutation status) for canine MCT. Thirty-four archived MCTs were evaluated for expression of phosphorylated KIT and Ki67, KIT localization, mitotic index, and mutations in exons 8 and 11 in *c-kit* as well as grading by the Patnaik and 2-tier systems. Expression of phosphorylated KIT was significantly ($p<0.05$) correlated with MI, Ki67, *c-kit* mutation, and grade by 2-tier. Because KIT signaling has been shown to drive the tumorigenesis of MCT, inhibitors of KIT are an attractive therapeutic strategy. Toceranib phosphate (TOC) is an inhibitor of KIT that has biological activity against canine MCT. An additional aim of this study was to determine whether pKIT labeling provides a pharmacodynamic marker for monitoring response to TOC in canine MCTs

in order to identify patients that respond to TOC and those that are refractory and might benefit from an alternative treatment. MCTs from 4/7 (57.1%) patients (Dogs 1, 2, 5, and 7) demonstrated a partial response to TOC therapy, 2/7 (28.6%) patients (Dogs 3 and 6) showed stable disease, and one patient (Dog 4) demonstrated progressive disease. Of the four patients characterized by a PR, 3/4 (75%) demonstrated a reduction in pKIT 6 hours after the first dose of TOC.

## INTRODUCTION

Mast cell tumors (MCTs) are the most common cutaneous tumors in dogs, accounting for up to 21% of all canine cutaneous tumors, and exhibit extremely variable biologic behavior [1-3]. MCT behavior is partially dependent on aberrant signaling of certain proteins, which cannot be detected by routine histopathological evaluation. Activating mutations in the juxtamembrane, kinase and ligand binding domains of the *c-kit* proto-oncogene have been associated with the pathogenesis and aggressiveness of canine MCTs, resulting in growth factor-independent constitutive phosphorylation of the KIT receptor tyrosine kinase (RTK) [1,4-6]. Approximately 30-50% of canine MCTs carry a *c-kit* mutation and the majority of MCTs harboring *c-kit* mutations are histologically intermediate or high grade [1,3]. Our lab and others have shown that *c-kit* mutations, particularly internal tandem duplications in the juxtamembrane domain of exon 11, are associated with an increased incidence of recurrent disease, metastasis, and death [1,3,7,8]. Such mutations in *c-kit* have been associated with aberrant KIT protein localization. While the majority of gain-of-function mutations of *c-kit* have been identified in exon 11 of canine MCTs, exons 8 and 9, and less commonly exon 17, also acquire activating mutations [6]. Others have shown that differential staining patterns of KIT by

immunohistochemistry (IHC) in MCTs, associated with mutations in the *c*-kit proto-oncogene, are indicators of biologic behavior [2,5]. Kiupel and co-workers have shown that MCTs exhibiting benign biologic behavior demonstrated membrane-associated KIT expression while MCTs associated with malignant transformation and aggressive biologic behavior were more likely to demonstrate a redistribution of KIT expression to the cytoplasm [2]. Additionally, markers of cellular proliferation such as Ki67 and AgNOR have been significantly associated with progression of canine MCT [9,10]. These studies demonstrate that markers of proliferation, *c-kit* mutation status, and KIT protein localization are useful markers of tumor aggressiveness in canine MCT.

Despite this progress in prognostic indicators for canine MCT, additional molecular markers need to be evaluated to further identify the subset of MCT that are histologically low or intermediate grade but biologically high grade. To date, there are no reports that have examined the relationship between KIT activation status and clinicopathologic features in MCT. The aim of the current study is to retrospectively investigate the relationship between activated KIT expression (phosphorylated KIT) and proliferation indices, KIT localization, *c-kit* mutation status, and grade in canine MCT by developing a immunohistochemistry-based assay for phosphorylated KIT (pKIT) for use in formalin-fixed paraffin embedded tumor samples.

In addition to its prognostic impact, the aberrant expression of proteins intimately involved in the tumorigenesis of various neoplasms also serves as a therapeutic target. As the above studies suggest, KIT plays a significant role in MCT progression and survival. Therefore, small molecule inhibitors of KIT are an attractive therapeutic strategy for MCTs in dogs. Toceranib (TOC) phosphate (Palladia®) is one such inhibitor of KIT that has biological activity against canine MCTs. Indeed, Pryer and co-workers demonstrated a reduction in pKIT by

western blot analysis in MCT eight hours after treatment with TOC compared to pre-treatment biopsies [11]. In a subsequent clinical trial, London and co-workers further demonstrated the clinical response to TOC. Approximately 40% of dogs experience an objective response to TOC. The remaining 60% were refractory suggesting intrinsic resistance to this targeted therapy [12]. Therefore, there exists a subpopulation of dogs that will not benefit from TOC treatment. As such, there is a need to identify distinctive *a priori* molecular markers of resistance in this population. An additional aim of this study is to apply the IHC-based assay for pKIT as a clinically-relevant, analytical method for monitoring response to TOC in canine MCTs in order to discriminate patients that respond to TOC from those that are refractory and might benefit from an alternative treatment.

## METHODS

### Tissue collection

For the retrospective analysis of KIT activation by pKIT labeling compared to established prognostic parameters for MCT, a total of 34 formalin-fixed, paraffin embedded (FFPE) primary cutaneous MCTs submitted for MCT profiles were selected from the Colorado State University Molecular Pathology Laboratory archives. For monitoring response or resistance of MCT to TOC, seven client-owned dogs presenting to the CSU Animal Cancer Center for MCT were enrolled in a clinical trial. Six-millimeter punch biopsies were obtained prior to the first dose (2.75 mg/kg) of TOC ($t_0$) and 6 hours following TOC ($t_6$). Tissue was collected in 10% neutral buffered formalin and processed routinely.

**Phospho-KIT antibody validation**

Immunohistochemical detection of activated KIT with a phospho-KIT antibody was validated by western blot analysis and FFPE HistoGel-embedded cell pellets of *c-kit*-mutant C2 mastocytoma cells treated with or without TOC. C2 cells were incubated for 6 or 24 hours with increasing concentrations of TOC (0-100 nM). For western blot analysis, cells were resuspended in lysis buffer containing 1% Triton X-100, 100 nM sodium orthovanadate, 0.2 mM PMSF, 1 M Tris, 1 M NaCl, and 7X protease inhibitor cocktail (Roche Applied Science, Indianapolis, IN), incubated on ice for 15 min, and centrifuged for 5 min. Protein was separated by SDS-PAGE on a 6% acrylamide gel and transferred onto a polyvinylidene difluoride membrane. Membranes were blocked for 60 min at room temperature in 5% bovine serum albumin. Immunolabeling for KIT was performed using a rabbit polyclonal anti-human antibody (Dako, Carpinteria, CA) at 1:1000 and immunolabeling for pKIT was performed using a rabbit polyclonal anti-human antibody targeting the Tyr721 residue (Bioss, Woburn, MA) at 1:1000 for 16 hours at 4℃, followed by incubation with HRP-conjugated anti-rabbit antibody at 1:5000 for 30 min at room temperature. Immunoreactive bands were detected using enhanced chemiluminescent reagent (Thermo Scientific, Rockford, IL).

For histogel embedding, HistoGel (Thermo Scientific, Pittsburg, PA) was heated in a microwave on low for 5-15 seconds. HistoGel was allowed to cool to 50°C before approximately 250,000 cells were resuspended in 40 uL of HistoGel. Cells pellets and HistoGel were placed in 10% neutral buffered formalin at 4°C overnight. The HistoGel/cell pellet was removed and placed inside a tissue cassette with a sponge. HistoGel “plugs” containing the cell pellet were processed, embedded, and sectioned as a standard histology specimen. Immunohistochemical staining for phosphorylated KIT was performed as described below.

**Immunohistochemistry**

Immunohistochemical staining of FFPE sections was performed by the following procedures. Slides were deparaffinized and rehydrated in descending concentrations of alcohol and water. Heat-induced epitope retrieval with EDTA buffer (pH 9.0) for 30 minutes was followed by endogenous peroxidase blocking with 3% hydrogen peroxide, non-specific signal blocking with Sniper Blocking Reagent (Biocare, Concord, CA), and incubation with the primary antibody at 4°C overnight. The primary antibody used for KIT was a polyclonal rabbit anti-human KIT (CD117) antibody at a dilution of 1:500 (Dako, Carpinteria, CA). The primary antibody used for pKIT was a polyclonal rabbit anti-human pKIT antibody at a dilution of 1:50 (Bioss, Woburn, MA). The primary antibody used for Ki67 was a rabbit polyclonal (MIB-1 clone) at a dilution of 1:50. Slides were incubated in a prediluted, HRP-conjugated secondary antibody, Envision, (Dako, Carpinteria, CA) and immunoreactive complexes were detected using a DAB MAP detection kit (Ventana Medical Systems, Tucson, AZ). Slides were counterstained with Mayer's hematoxylin (Sigma Aldrich, St. Louis, MO).

**Analysis of canine MCT biopsies**

Slides were evaluated using light microscopy by two Board-certified veterinary pathologists (CHH and EJE). MCTs from the archived samples were graded by both the Patnaik and 2-tiered grading schema [13,14]. The MI was determined on H&E-stained slides by counting the number of mitotic figures in 10 consecutive, non-overlapping 400X fields and expressed as the number of mitoses/10 hpf. The growth fraction was determined by counting the number of neoplastic cells immunolabeling for Ki67 in areas demonstrating the greatest immunoreactivity (“hot spots”). This fraction was categorized as “high” or “low” based on 0-30% or >30%

immunopositive neoplastic cells [10]. In the retrospective cases, phospho-KIT (pKIT) was categorized as “positive” (>30% of neoplastic cells) or “negative” (minimal to no staining). In addition, varying staining and intensity patterns were defined as 1- no staining; 2- diffusely cytoplasmic; 3- faint stippled cytoplasmic to perinuclear; and 4- intense cytoplasmic stippling to perinuclear. For the clinical trial cases, pre- and post-TOC biopsies were evaluated for differences in pKIT staining in addition to the pattern/intensity pattern as described above, pKIT staining was scored as a percentage of positive tumor cells (the number of positive tumor cells over the total number of tumor cells). Percent reduction was determined using the calculation: (post-TOC pKIT score - pre-TOC pKIT score)/pre-TOC pKIT score x 100. RECIST criteria were used to assess clinical response to TOC therapy [15]. Response criteria was defined as follows: complete response (CR): resolution of all lesions; partial response (PR): greater than or equal to 30% decrease in sum of diameters of all lesions; progressive disease (PD): greater than or equal to 20% increase in sum of diameters of all lesions or appearance of new lesion; stable disease (SD): less than 30% decrease or less than 20% increase [15]. Similarly, percent tumor reduction was determined using the calculation: (best response - baseline)/baseline x 100. KIT localization and scoring were determined as previously described [2]. Briefly, the KIT-staining patterns were identified as Pattern I) membrane-associated staining; Pattern II) focal to stippled cytoplasmic staining with decreased or loss of membrane-associated staining, and Pattern III) diffuse cytoplasmic staining. A percentage of each staining pattern was determined for each MCT. A final pattern, I, II, or III, was assigned based on the predominant staining present. Finally, mutational analysis for internal tandem duplications in exons 8 and 11 of *c-kit* was determined using an automated capillary gel electrophoresis and primers designed to amplify the areas of reported mutation (**Table 4.1**). Together, these two primer pairs detect 80% of the

activating mutations reported in the canine *c-kit* gene [6,7].

**Table 4.1:** Forward and reverse primers for detection of exon 8 and 11 *c-kit* mutations.

| Exon | Primer Name | Location | Sequence |
|---|---|---|---|
| 8 | Ci7fa | Forward | GGT GAG GTG TTC CAG CAG TC |
| 8 | Ci8r | Reverse | CCT TCC CTC GTG CAC ATT A |
| 11 | Ce11f | Forward | CAG TGG AAG GTT GTT GAG GAG |
| 11 | Ci11r | Reverse | CAT GGA AAG CCC CTA TTT CA |

**Statistics**

Pearson's correlation coefficients were used to determine the correlation of pKIT to other MCT profile parameters (mitotic index, Ki67, KIT localization, and *c-kit* mutation status). Linear regression was used to analyze the relationship between response and target modulation (pKIT). A $p$ value of $<0.05$ was considered significant.

## RESULTS

**Phospho-KIT antibody validation.**

To determine if the anti-human phospho-KIT antibody could detect activated (phosphorylated) canine KIT, TOC-sensitive exon 11-mutant C2 cells were treated for 24 hours with increasing concentrations of TOC. As shown in **Figure 4.1**, the anti-phospho-KIT antibody was able to detect a dose-dependent decrease in activated KIT relative to tubulin. (Densitometric analysis **Figure 4.2.**)

Similarly, to investigate the use of the anti-phospho-KIT antibody in FFPE sections, treated (100 nM TOC) and untreated C2 cells were embedded in HistoGel, processed as standard histologic specimens, and immunostained for pKIT. As shown in **Figure 4.2A**, untreated cells demonstrated diffuse and intense cytoplasmic immunoreactivity, suggesting widespread

activation of the KIT receptor. This activation, however, was inhibited after treatment of the cells with 100 nM TOC for 6 and 24 hours (**Figure 4.2B and 4.2C, respectively**) demonstrated by a decrease in the staining intensity and percentage of cells immunopositive for pKIT. The density of viable cells decreased dramatically after 24 hours of TOC exposure.

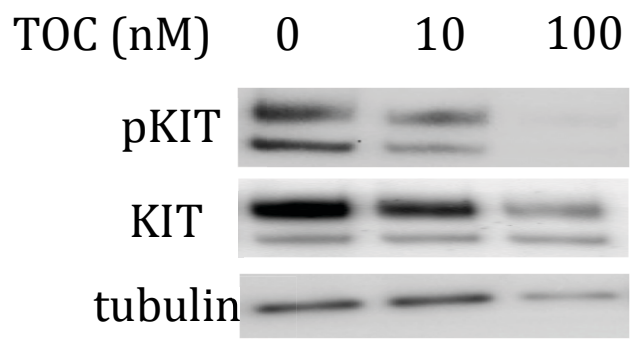


**Figure 4.1:** Figure 4.1: Expression of activated KIT (pKIT) by western blot in response to 24 hr TOC exposure.

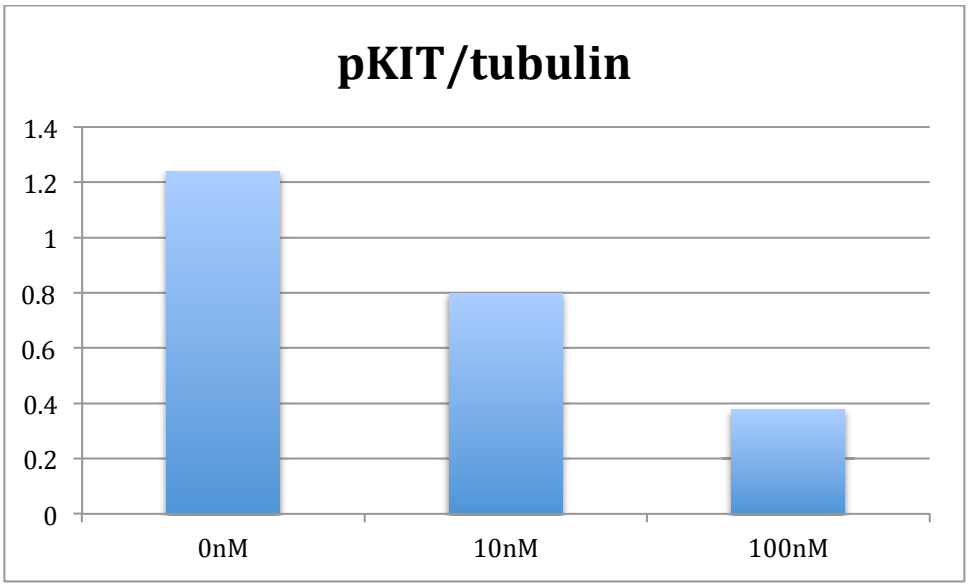


**Figure 4.2** Densitometric analysis of western blot shown in Figure 4.1.

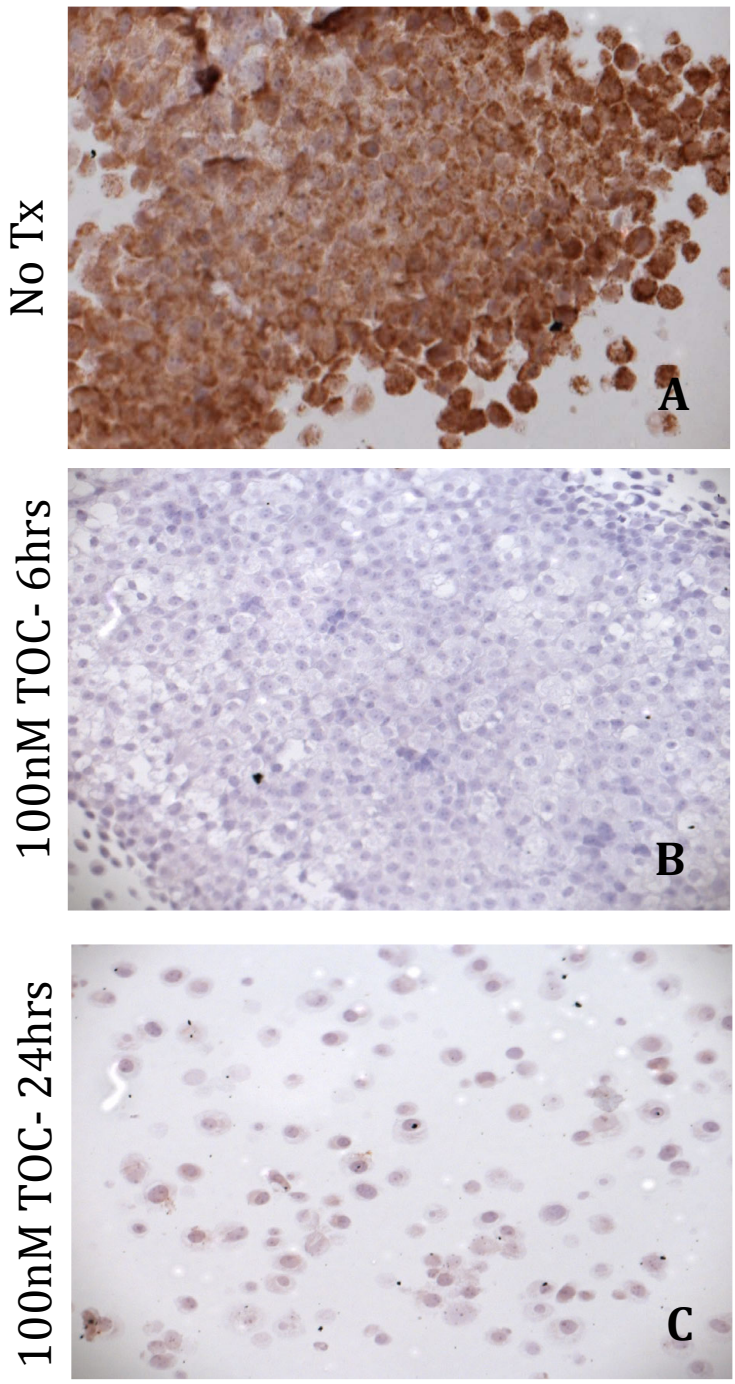


**Figure 4.3:** Phosphorylated KIT labeling of 6 hr and 24 hr TOC-treated and –untreated formalin-fixed, paraffin embedded C2 cell pellets following resuspension in HistoGel.

**Phospho-KIT staining of tumor sections.**

One representative slide from each case (archived and clinical trial cases) was reviewed by two Board-certified veterinary pathologists (CHH and EJE). pKIT staining was localized to the cytoplasm in three patterns as demonstrated in **Figure 4.3**. These included diffuse cytoplasmic staining (**Figure 4.3B**) or stippled to globular cytoplasmic staining of low to moderate intensity (**Figure 4.3C**) or high intensity (**Figure 4.3D**), often characterized by intimate association with the nuclear membrane (**Figure 4.3D inset)**. **Figure 3A** demonstrates a MCT section negative for pKIT labeling.

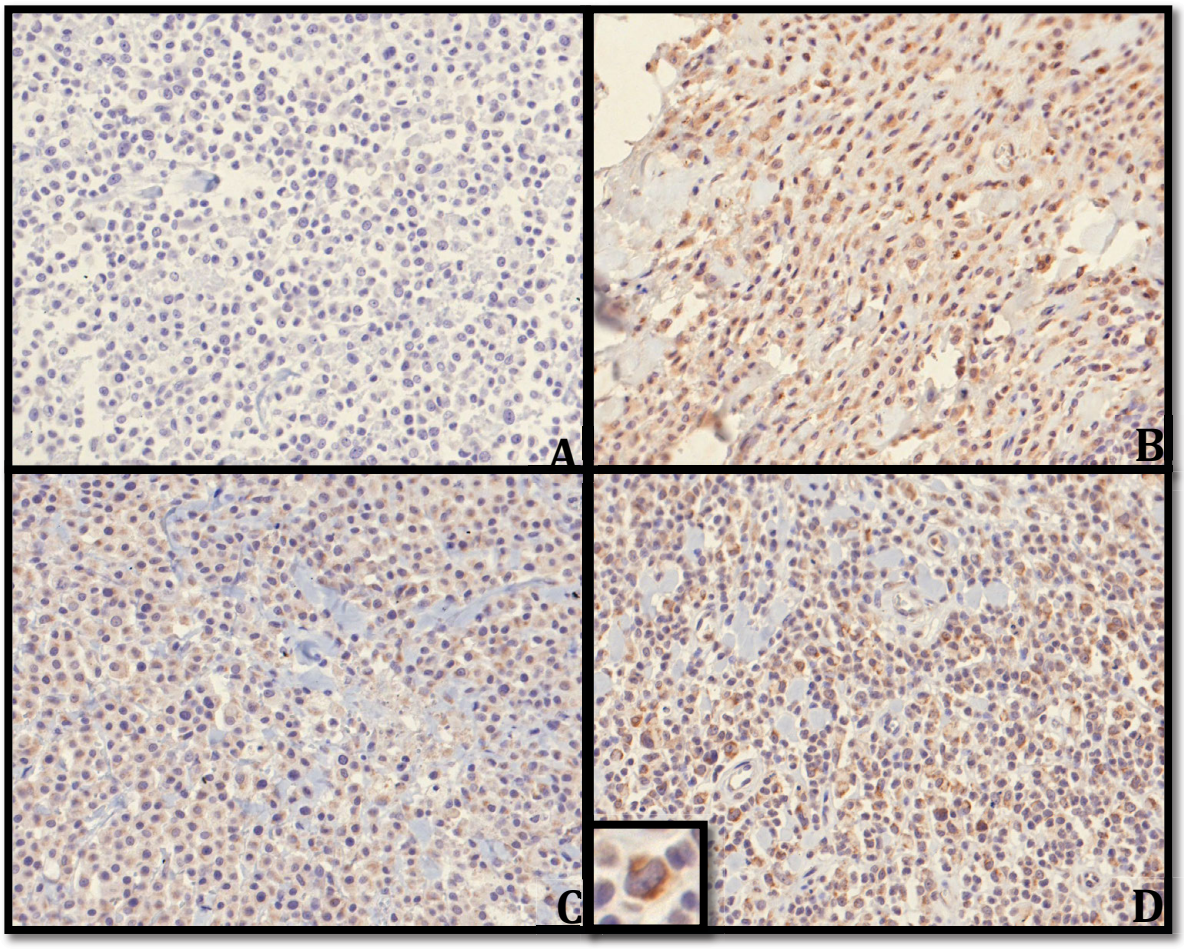


**Figure 4.4:** Phosphorylated KIT staining patterns. A-0; B-1, C-2, D-3. DAB; Hematoxylin counterstain.

**Phospho-KIT expression correlates with mitotic index, Ki67 staining, mutations in exons 8 or 11, and grading by 2-tier.**

To determine if direct measurement of the activated form of the KIT receptor correlated with grade and other known prognostic factors for MCT, we examined 34 archived canine MCTs for pKIT expression with IHC. Correlation coefficients for the MCT pKIT scores and MCT profile parameters are summarized in **Table 4.3**. pKIT immunoreactivity correlated significantly with grade by the 2-tiered grading system ($r=0.3265$; $p<0.05$), mitotic index as described by Romansik and co-workers [16] ($r=0.2880$; $p<0.05$), Ki67 score ($r=0.2880$; $p<0.05$), and *c-kit* mutation status in exons 8 and 11 ($r=0.3142$; $p<0.05$). Surprisingly, KIT localization did not significantly correlate with pKIT staining ($r=0.2714$; $p=0.0602$). Overall, phosphorylated KIT is highly associated with indicators of disease aggressiveness in canine MCT.

**Phospho-KIT as a marker for target modulation.**

The results of target modulation in tumor samples are summarized in **Table 4.2**. Treatment of dogs with MCT with TOC resulted in a decrease in KIT phosphorylation after 6 hours in 5/7 (71.4%) dogs (**Figure 5.4**). The remaining 2 dogs demonstrated either no change (Dog 3) or a slight increase (Dog 1) in pre- and post-TOC pKIT activity by immunohistochemical analysis. MCTs from 4/7 (57.1%) patients (Dogs 1, 2, 5, and 7) demonstrated a partial response to TOC therapy, 2/7 (28.6%) patients (Dogs 3 and 6) showed stable disease, and one patient (Dog 4) demonstrated progressive disease. Of the four patients experiencing PR, 3/4 (75%) demonstrated a reduction in pKIT 6 hours after the first dose of TOC. The fourth patient (Dog 1) received CCNU in addition to TOC, therefore, it is difficult to attribute any reduction of tumor size exclusively to KIT inhibition as CCNU is an effective

cytotoxic therapy for MCT. Of the two patients that were classified with SD, Dog 3 showed no change in pre- and post-TOC pKIT activity while Dog 6 demonstrated a 100% reduction in pKIT activity. Finally, one patient (Dog 4) was classified as having PD despite an initial response to therapy as determined by a decrease in pKIT 6 hours post TOC. However, this patient was removed from the study at the owner's request after two weeks. The patient was diagnosed with multiple cutaneous MCTs. The sum of the diameter of his target lesions at day 0 was 10.95 cm, at 1 week was 12.6 cm, and at week 2 was 13.2 cm, a 20.5% increase compared to baseline. In addition, the patient developed multiple new masses at the 2-week visit. While this patient may have had an initial response to TOC therapy, he later became refractory. Acquisition of relapse biopsies and assessment for pKIT could be an appropriate approach to identifying acquired resistance in these patients.

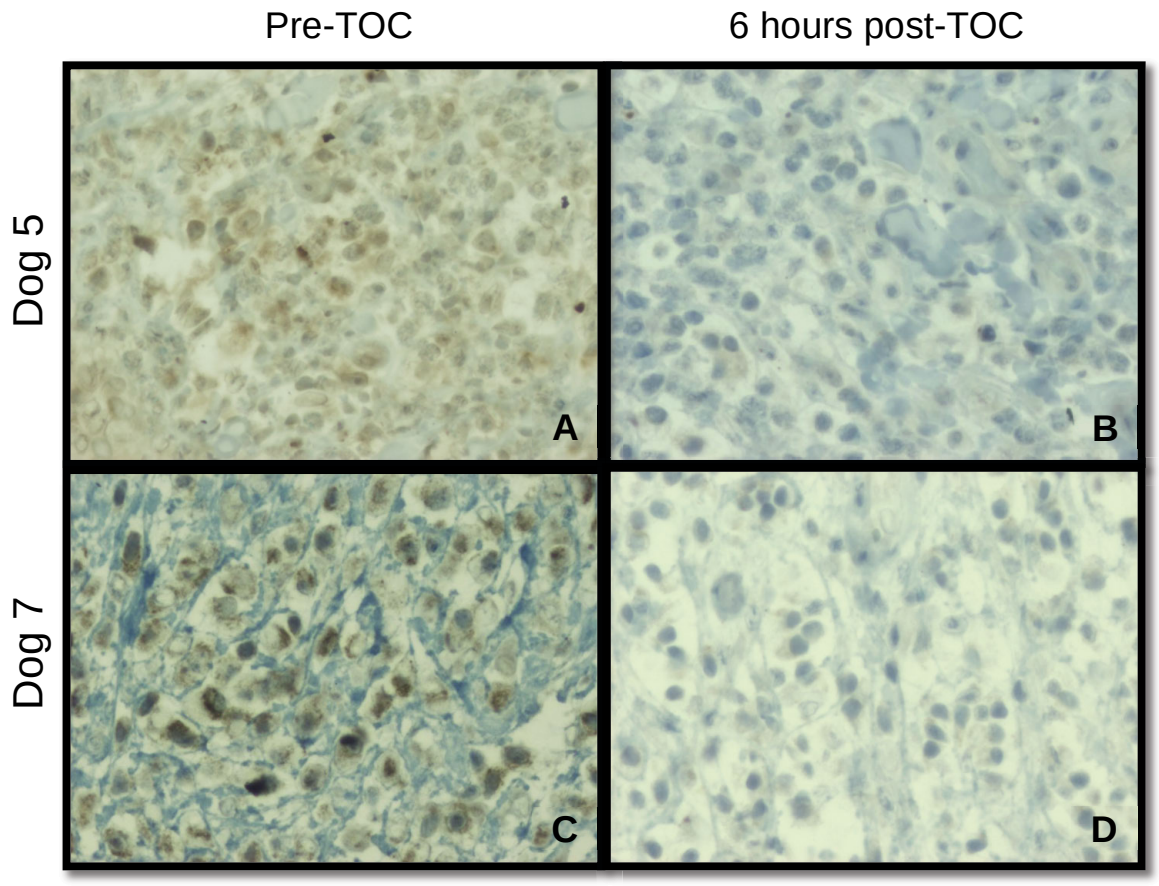


**Figure 4.5:** KIT activation in two patients' MCTs. Pre-TOC (A, C) and 6 post-TOC (B, D); 6mm punch biopsies; DAB; Hematoxylin counterstain.

## DISCUSSION

To the authors' knowledge, this is the first report of the immunohistochemical detection of phosphorylated KIT using a phospho-specific antibody in FFPE canine MCTs. We have applied this IHC-based assay of KIT activation to explore its correlation to other established prognostic parameters in canine MCT as well as monitoring tumor response to inhibitors of KIT.

To validate the specificity of the selected phospho-KIT antibody, we used the previously established C2 mastocytoma cell line. This cell line was established from a spontaneously

occurring canine MCT and harbors the commonly reported internal tandem duplication in exon 11 of the *c-kit* gene [17]. As a result of this mutation, the KIT receptor in C2 cells is constitutively active/phosphorylated. The anti-phospho-KIT antibody demonstrated phosphorylated KIT by both western blot analysis of C2 cell lysates and cytoplasmic immunohistochemical staining of C2 cells embedded in HistoGel. Furthermore, upon treatment of C2 cells with the KIT inhibitor, TOC, pKIT immunoreactivity was decreased by both western blot analysis and IHC. This demonstrated the phospho-specificity and potential applicability of this antibody to investigate KIT activation in canine MCTs. We subsequently used this pKIT antibody for two applications: 1) to retrospectively investigate the correlation of activated KIT in MCT to other established prognostic parameters that comprise the MCT profile offered through the Molecular Pathology Lab at CSU; and 2) to monitor the pharmacodynamic response to TOC in client-owned animals presenting to CSU for the treatment of MCT.

The expression of pKIT was demonstrated in approximately 50% of MCTs investigated. This prevalence of activated KIT closely follows the frequency with which *c-kit* mutations have been reported and reflects the oncogenic role KIT plays in MCT tumorigenesis [4,5,18]. Current prognostic parameters for canine MCT include grade [13,14], mitotic index [16], KIT localization [2,5], Ki67 [10], and *c-kit* mutation status [3,4,7]. A review of these parameters is beyond the scope of this study; however, while they can be used to interpret the activation status of KIT, they do not provide a direct measurement of the activated receptor. In the current study, there was a significant correlation between pKIT staining and MI, Ki67, *c-kit* mutation status, and grade by the 2-tier scheme. Interestingly, a correlation between KIT localization and pKIT staining was not observed. Upon activation, RTKs are rapidly internalized and recycled off of the plasma membrane [19]. Constitutively active KIT due to mutations in *c-kit*, and subsequent rapid

receptor internalization is likely the reason for the loss of membranous staining and increased cytoplasmic staining in biologically aggressive MCTs. Xiang and co-workers eloquently showed that intracellular, not membranous, localization of mutant KIT is responsible for downstream oncogenic signaling [20]. For further scrutiny of these findings, KIT localization was redefined as either inactive KIT (membranous staining) or active (cytoplasmic) since more benign MCT cells demonstrate KIT expression limited to the membrane and malignant MCT cells display a redistribution of KIT to the cytoplasm with loss of membranous staining [2]. Despite this redefinition, correlation between pKIT and KIT redistribution (membranous or cytoplasmic) failed to reach significance ($r=0.2765$; $p=0.0597$).

In addition to biomarkers, histologic grade has been widely and more traditionally used as an indicator of biologic behavior in MCT. Histologic grading by the Patnaik system has been the gold standard and has provided a strong foundation in the grading of canine cutaneous MCTs, however, certain criteria within the grading system require subjective interpretation and significant inter-pathologist variability exists [13]. An additional limitations of the Patnaik grading system has been the frequency at which grade II MCTs are diagnosed and further complicated by the observation that some grade II MCTs are fairly benign while others are biologically aggressive. The 2-tier system attempts to address the predominance of Patnaik grade II MCTs and the ambiguity and biologic variability within this group [14]. Since its introduction, grading by the 2-tier system has been independently validated by several groups [8,10,15]. Results of these studies highlighted the significantly higher intra-observer concordance and prognostication of the 2-tiered system compared to the Patnaik system. Interestingly, in the current study, expression of pKIT was significantly correlated to grade by the 2-tier system while no significant correlation was shown between pKIT and Patnaik grade. However, when Patnaik

grades 1 and 2 were grouped together, there was a highly significant correlation (r=0.41; p=0.007) between pKIT and grades I/II and grade III [8,15]. Recently, two independent studies comparing the utility of Patnaik and two-tiered grading schemes concluded that there were no significant prognostic differences between Patnaik grades I and II. Overall, these results suggest that expression of pKIT correlates significantly with other commonly used indicators of aggressiveness in canine MCT.

The activated KIT receptor represents a viable therapeutic target for the treatment of canine MCT. As such, targeted inhibitors of KIT have been developed for the treatment of recurrent, non-resectable MCTs and have shown clinical efficacy, particularly in tumors demonstrating mutations in the KIT receptor [11,12]. However, *de novo* and acquired resistance to targeted therapy remains a significant clinical challenge [21,22]. Reproducible and clinically relevant tests are needed to identify patients that will respond to targeted therapy and those that are refractory and might benefit from an alternative treatment. We have developed an IHC-based assay to measure changes in activated KIT as an indication of target modulation. Pryer and co-workers similarly measured response to SU11654 (TOC) in dogs with canine MCT by assessing pre- and post-treatment pKIT levels western blot analysis. While this is a reasonable approach, western blot analysis is time consuming and requires adequate tumor tissue sample size collected under specific conditions. In contrast, tissue for immunohistochemical evaluation is collected by routine, clinically relevant procedures and requires less tissue. In addition, any potential contribution of signal from the tumor stroma can be visually excluded by immunohistochemical evaluate. This is in contrast to western blot analysis in which whole tissue lysates are evaluated. Regardless of the method used, valid biomarkers are needed to effectively monitor response to treatment and, more importantly, identify patients unlikely to respond. Early identification of

treatment failure is critical to adjusting the treatment plan so that these patients may benefit from second line therapies. We have shown that immunohistochemical detection of phosphorylated KIT prior to and six hours post-TOC is a practical way by which to monitor response to TOC in canine MCT. Correlation of tumor response and reduction of pKIT was not statistically significant, most likely due to the limited number of patients enrolled. However, the trend suggests that in patients demonstrating a partial response to TOC alone, there is reduction of KIT activation by immunohistochemical analysis of pKIT.

Collectively, these results demonstrate that immunohistochemical detection of pKIT is a clinically relevant assay for and hallmark of the activation status of the major oncogenic pathway in canine MCT. As such, it may serve as an indication of the aggressiveness of the tumor as well as a rapid pharmacodynamic biomarker that demonstrates successful or unsuccessful target modulation. Future studies should be performed to assess the prognostic significance of pKIT expression in a cohort of uniformly treated and systematically evaluated canine MCT patients.

**Table 4.2:** Retrospective study of the relationship between pKIT to grade and other established prognostic parameters for canine MCT.

| Case | pKIT score | pKIT on/off (0 vs 1-3) | Patnaik | 2-tier | mitotic count | MI-<,> 5 | Ki67 | KIT pattern | c-kit mutation |
|---|---|---|---|---|---|---|---|---|---|
| 1 | 0 | off | 2 | hi | 4 | > | hi | 3 | no |
| 2 | 0 | off | 2 | lo | 0 | < | lo | 1 | no |
| 3 | 2 | on | 1 | lo | 0 | < | lo | 1 | yes |
| 4 | 1 | on | 1 | lo | 0 | < | lo | 1 | no |
| 5 | 0 | off | 1 | lo | 0 | < | lo | 1 | no |
| 6 | 1 | on | 2 | hi | 10 | > | hi | 2 | no |
| 7 | 0 | off | 3 | hi | 25 | > | hi | 2 | yes |
| 8 | 1 | on | 2 | lo | 5 | > | hi | 2 | no |
| 9 | 1 | on | 2 | lo | 2 | < | lo | 1 | no |
| 10 | 1 | on | 2 | lo | 0 | < | lo | 1 | no |
| 11 | 0 | off | 2 | lo | 3 | < | lo | 1 | no |
| 12 | 0 | off | 2 | lo | 1 | < | lo | 1 | no |
| 13 | 0 | off | 2 | lo | 0 | < | lo | 1 | no |
| 14 | 2 | on | 2 | lo | 0 | < | lo | 1 | no |
| 15 | 2 | on | 2 | hi | 6 | > | hi | 2 | yes |
| 16 | 2 | on | 2 | lo | 1 | < | lo | 1 | no |
| 17 | 1 | on | 2 | lo | 5 | > | hi | 2 | no |
| 18 | 0 | off | 2 | lo | 0 | < | lo | 1 | no |
| 19 | 3 | on | 3 | hi | 14 | > | hi | 3 | no |
| 20 | 0 | off | 2 | lo | 1 | < | lo | 1 | no |
| 21 | 1 | on | 3 | hi | 20 | > | hi | 2 | yes |
| 22 | 0 | off | 2 | lo | 2 | < | lo | 2 | no |
| 23 | 0 | off | 2 | lo | 1 | < | lo | 2 | no |
| 24 | 2 | on | 2 | lo | 0 | < | lo | 1 | no |
| 25 | 0 | off | 2 | lo | 0 | < | lo | 1 | no |
| 26 | 0 | off | 2 | hi | 20 | > | hi | 1 | no |
| 27 | 0 | off | 2 | lo | 6 | > | hi | 1 | no |
| 28 | 0 | off | 2 | lo | 0 | < | lo | 1 | no |
| 29 | 0 | off | 2 | lo | 0 | < | lo | 1 | no |
| 30 | 0 | off | 2 | lo | 0 | < | lo | 2 | yes |
| 31 | 0 | off | 2 | lo | 0 | < | lo | 1 | no |
| 32 | 1 | on | 1 | lo | 1 | < | lo | 1 | no |
| 33 | 3 | on | 3 | hi | 17 | > | hi | 2 | yes |
| 34 | 0 | off | 2 | lo | 1 | < | lo | 1 | no |
| | | | | | | | | | |
| **Correlation** | | pKIT score: pKIT on/off | pKIT: Patnaik | pKIT: 2-tier | pKIT: mitotic count | pKIT:MI >/< 5 | pKIT:Ki67 | pKIT:KIT | pKIT:*c-kit* mutation |
| **R-score** | | 0.7385 | 0.1968 | 0.3265 | 0.2123 | 0.288 | 0.288 | 0.2714 | 0.3142 |
| **p-value** | | p<0.05 | p=0.1324 | p<0.05 | p=0.114 | p<0.05 | p<0.05 | p=0.0602 | p<0.05 |

**Table 4.3:** Pre and six hours post-TOC tumor response, pKIT grade and percent positive, KIT localization, and *c-kit* mutation status for seven dogs enrolled in clinical trial.

| Dog | Pre-TOC (cm) | Best Response (cm) | % reduction | Response | Pre- pKit grade | Pre- pKit % | Post- pKit grade | Post- pKit % | % pKIT reduction | KIT | *c-kit* |
|---|---|---|---|---|---|---|---|---|---|---|---|
| 1 | 17.8 | 12.2 | -31.46067416 | PR | 3 | 30 | 3 | 40 | 33.33333333 | N/A | N/A |
| 2 | 5.87 | 2.67 | -54.51448041 | PR | 3 | 90 | 2 | 80 | -11.11111111 | 2 | no |
| 3 | 7.2 | 5.1 | -29.16666667 | SD | 1 | 90 | 2 | 90 | 0 | 1 | no |
| 4 | 10.95 | | | PD | 1 | 20 | 0 | 0 | -100 | 3 | no |
| 5 | 3.6 | 1.5 | -58.33333333 | PR | 3 | 90 | 1 | 40 | -55.55555556 | 2 | no |
| 6 | 1.53 | 1.08 | -29.41176471 | SD | 0-1 | 80 | 0 | 0 | -100 | 1 | no |
| 7 | 17.6 | 6.9 | -60.79545455 | PR | 3 | 60 | 0-1 | 25 | -58.33333333 | 2 | ITD exon 11 |

## References


1. Zemke D, Yamini B, Yuzbasiyan-Gurkan V (2002) Mutations in the juxtamembrane domain of c-KIT are associated with higher grade mast cell tumors in dogs. Vet Pathol 39: 529-535.
2. Kiupel M, Webster JD, Kaneene JB, Miller R, Yuzbasiyan-Gurkan V (2004) The use of KIT and tryptase expression patterns as prognostic tools for canine cutaneous mast cell tumors. Vet Pathol 41: 371-377.
3. London CA, Galli SJ, Yuuki T, Hu ZQ, Helfand SC, et al. (1999) Spontaneous canine mast cell tumors express tandem duplications in the proto-oncogene c-kit. Exp Hematol 27: 689-697.
4. Downing S, Chien MB, Kass PH, Moore PE, London CA (2002) Prevalence and importance of internal tandem duplications in exons 11 and 12 of c-kit in mast cell tumors of dogs. Am J Vet Res 63: 1718-1723.
5. Webster JD, Yuzbasiyan-Gurkan V, Kaneene JB, Miller R, Resau JH, et al. (2006) The role of c-KIT in tumorigenesis: evaluation in canine cutaneous mast cell tumors. Neoplasia 8: 104-111.
6. Letard S, Yang Y, Hanssens K, Palmerini F, Leventhal PS, et al. (2008) Gain-of-function mutations in the extracellular domain of KIT are common in canine mast cell tumors. Mol Cancer Res 6: 1137-1145.
7. Avery AC (2012) Molecular diagnostics of hematologic malignancies in small animals. Vet Clin North Am Small Anim Pract 42: 97-110.
8. Takeuchi Y, Fujino Y, Watanabe M, Takahashi M, Nakagawa T, et al. (2013) Validation of the prognostic value of histopathological grading or c-kit mutation in canine cutaneous mast cell tumours: a retrospective cohort study. Vet J 196: 492-498.
9. Webster JD, Yuzbasiyan-Gurkan V, Miller RA, Kaneene JB, Kiupel M (2007) Cellular proliferation in canine cutaneous mast cell tumors: associations with c-KIT and its role in prognostication. Vet Pathol 44: 298-308.
10. Vascellari M, Giantin M, Capello K, Carminato A, Morello EM, et al. (2013) Expression of Ki67, BCL-2, and COX-2 in canine cutaneous mast cell tumors: association with grading and prognosis. Vet Pathol 50: 110-121.
11. Pryer NK, Lee LB, Zadovaskaya R, Yu X, Sukbuntherng J, et al. (2003) Proof of target for SU11654: inhibition of KIT phosphorylation in canine mast cell tumors. Clin Cancer Res 9: 5729-5734.
12. London CA, Malpas PB, Wood-Follis SL, Boucher JF, Rusk AW, et al. (2009) Multi-center, placebo-controlled, double-blind, randomized study of oral toceranib phosphate (SU11654), a receptor tyrosine kinase inhibitor, for the treatment of dogs with recurrent (either local or distant) mast cell tumor following surgical excision. Clin Cancer Res 15: 3856-3865.
13. Patnaik AK, Ehler WJ, MacEwen EG (1984) Canine cutaneous mast cell tumor: morphologic grading and survival time in 83 dogs. Vet Pathol 21: 469-474.
14. Kiupel M, Webster JD, Bailey KL, Best S, DeLay J, et al. (2011) Proposal of a 2-tier histologic grading system for canine cutaneous mast cell tumors to more accurately predict biological behavior. Vet Pathol 48: 147-155.

15. Sabattini S, Scarpa F, Berlato D, Bettini G (2014) Histologic Grading of Canine Mast Cell Tumor: Is 2 Better Than 3? Vet Pathol.
16. Romansik EM, Reilly CM, Kass PH, Moore PF, London CA (2007) Mitotic index is predictive for survival for canine cutaneous mast cell tumors. Vet Pathol 44: 335-341.
17. DeVinney R, Gold WM (1990) Establishment of two dog mastocytoma cell lines in continuous culture. Am J Respir Cell Mol Biol 3: 413-420.
18. Jones CL, Grahn RA, Chien MB, Lyons LA, London CA (2004) Detection of c-kit mutations in canine mast cell tumors using fluorescent polyacrylamide gel electrophoresis. J Vet Diagn Invest 16: 95-100.
19. Wiley HS, Burke PM (2001) Regulation of receptor tyrosine kinase signaling by endocytic trafficking. Traffic 2: 12-18.
20. Xiang Z, Kreisel F, Cain J, Colson A, Tomasson MH (2007) Neoplasia driven by mutant c-KIT is mediated by intracellular, not plasma membrane, receptor signaling. Mol Cell Biol 27: 267-282.
21. Ellis LM, Hicklin DJ (2009) Resistance to Targeted Therapies: Refining Anticancer Therapy in the Era of Molecular Oncology. Clin Cancer Res 15: 7471-7478.
22. Barouch-Bentov R, Sauer K (2011) Mechanisms of drug resistance in kinases. Expert Opin Investig Drugs 20: 153-208.

# Chapter 5

## General Conclusions

The development of drugs that precisely target genetic susceptibilities in tumors have shown great promise and expanded the repertoire of effective cancer treatments. However, virtually all tumors eventually develop resistance to targeted therapy, largely limiting their long-term use. MCT is the most common skin tumor in dogs and one of the only malignancies in veterinary medicine for which targeted therapy is approved. TOC resistance in MCT offers an excellent spontaneous tumor model with which to study mechanisms of acquired resistance to targeted therapy. The molecular mechanisms driving the tumorigenesis of MCT have been well characterized, with constitutively activated, mutant KIT contributing a significant role in the majority of MCTs. As such, inhibitors of KIT have offered a rational therapeutic option. Nevertheless, analogous to other targeted therapies, resistance ultimately develops. The studies contained within this dissertation describe the elucidation of molecular mechanisms of resistance to TOC in the context of its use in the treatment of canine cutaneous mast cell tumors.

We chose the C2 canine MCT cell line as the parental line from which to generate the three resistant lines. The clinical relevance of this line is reinforced by the internal tandem duplication in exon 11 of *c-kit,* an activating mutation reported in 30-50% of canine MCTs. Moreover, MCTs harboring this mutation demonstrate a better response to TOC therapy than those with wild-type KIT. By chronically exposing C2 cells to increasing concentrations of TOC, three TOC-resistant sublines emerged. These sublines were expanded and further characterized. All resistant sublines showed strong resistance to TOC, in addition to three other KIT kinase

inhibitors. Western blot analysis of phosphorylated KIT revealed reactivation of the target protein in the resistant sublines. From this observation, coupled with the knowledge of one the most common mechanisms of resistant to targeted therapy, we hypothesized that acquisition of secondary mutation in the *c-kit* gene was likely responsible for the resistant phenotype. To test this hypothesis, we sequenced full-length *c-kit*. All resistant sublines retained the original activating mutation in exon 11 in addition to the acquisition of several point mutations located exclusively in the juxtamembrane and kinase domains of *c-kit*.

Tyrosine kinase inhibitors exert their effect by binding in a competitive manner to the ATP-binding site of the activation domains of receptor tyrosine kinases. Interestingly, the point mutations identified by the sequencing of *c-kit* were located in and around these domains in all three drug-resistant KIT proteins. We hypothesized that these mutations impede the effects of the inhibitors by either inducing a conformational change in the drug binding site or altering the amino acids that serve as contact points between the inhibitor and target. To explore this, homology models were generated *in silico* for the cytoplasmic domains of the TOC-sensitive and TOC-resistant KIT proteins. Indeed, the reported mutations were predicted to alter the entrance to the drug-binding site in all TOC-resistant proteins to various degrees. In addition, amino acid substitutions in two of the resistant KIT proteins disrupted key hydrogen bonding interactions within the ATP-binding and allosteric sites of the activation domains. Inhibitor docking and predicted binding energy calculations were performed on 16 energy minimized drug-target combinations. All four KIT inhibitors were predicted to bind with reduced affinity to the TOC-resistant KIT proteins compared to TOC-sensitive KIT. We concluded that the mutations observed in the TOC-resistant KIT proteins altered the structure of the drug-binding pocket causing significant steric hindrance, precluding binding and effective inhibition of the target. The

validity of this model was demonstrated in its use in predicting binding of another KIT TKI that inhibits its target by similar modes. We demonstrated this predictive power by calculating the predicted binding energy for the novel KIT inhibitor, ponatinib. Similar to the other KIT inhibitors, ponatinib was predicted to bind with favorable affinity to TOC-sensitive KIT but with decreased affinity to all three TOC-resistant KIT proteins. This was recapitulated following growth inhibition assays, demonstrating inhibition of cell growth of parental C2 cells in a dose-dependent manner while failure to inhibit growth in all three TOC-resistant sublines. Therefore, this model may serve as a structural-based method to predicting KIT TKI response *a priori* as well as help guide rational drug design to overcome resistance to KIT inhibitors.

Two basic strategies are employed to study drug resistance: preclinically, through the generation of isogenic cell lines as described above, and clinically, by monitoring response to therapy and collecting tumor samples at the time of relapse. This latter approach requires the use of sensitive and specific biomarkers in order to monitor response to therapy. The final aim of this dissertation was pursued with this in mind. As TOC is an inhibitor of KIT, monitoring KIT activation is a reasonable method by which to detect a modulation in the target and potential tumor response. As such, we validated and optimized an immunohistochemical assay for phosphorylated (activated) KIT. This clinically relevant assay facilitates the ability to quickly measure changes in KIT activation status in response to treatment and identify those patients that are responding and those that become resistant. A measurable decrease in pKIT labeling in pre-TOC versus post-TOC MCT biopsy samples were identified in the majority patients with tumors that exhibited a reduction in size in response to TOC. We extended the use of this novel marker to a series of archived MCT samples to investigate the relationship of pKIT to other established prognostic parameters in MCT. These included mitotic index, Ki67, KIT localization, *c-kit*

mutation status, and grade by both Patnaik and the more recent 2-tiered systems. pKIT correlated significantly with MI, Ki67, *c-kit* mutation status and grade by the 2-tier scheme. These studies demonstrate the usefulness of pKIT as a direct measure of KIT activation.

In conclusion, we have successfully established *in vitro* and *in silico* models of acquired resistance to TOC in canine MCT. We used these models to identify and characterize the acquisition of secondary mutations in *c-kit*. These models may be used to assist in the rational design of novel treatment strategies to overcome TOC resistance in canine MCT.

## Future Directions

There are a number of additional studies that could be performed to complement and further validate the findings presented herein. Perhaps the most crucial question to answer is whether or not the secondary *c-kit* mutations identified and described herein *in vitro* are clinically-relevant. That is, are these mutations responsible for TOC in patient tumor samples. Genomic and molecular analysis of tumor samples from patients that develop resistance to TOC will answer this question. These studies could be performed either in a non-bias approach by sequencing full-length canine *c-kit* as we did *in vitro* or by hypothesis-driven analysis of the same regions of *c-kit* in which we identified the mutations *in vitro*.

In Chapter 1, we explored a number of different pathway-dependent and pathway-independent mechanisms of acquired resistance. These included sequencing for secondary *c-kit* mutations, analysis of target gene and protein overexpression, and analysis of P-gp expression and function. While the acquisition of secondary mutations in *c-kit* presented here likely play a significant role in the observed TOC resistance, other mechanisms may contribute to the resistant phenotype. Indeed, it is not uncommon for multiple resistant mechnisms to occur concurrently in

the same patient. Other mechanisms not explored in these studies include alternative signaling pathways that bypass KIT, such as the MAPK and PI3K/AKT pathways. Additionally, downstream pathway analysis might highlight alternative drug targets independent of KIT. Indeed, more durable remissions may be achieved by treating resistant MCT with combination regimens that target anticipated resistance mechanisms. This could include trials investigating the utility of sequential administration of inhibitors in response to the development of resistance, or initial treatment with multiple inhibitors of the same target, with the goal of potentially preventing the development of resistance.

The Ba/F3 cell line is a murine pro-B line that is dependent on interleukin-3 (IL-3) for growth and survival. Upon withdrawal of IL-3, these cells undergo apoptosis. Growth-promoting oncogenes, however, can substitute for the dependence of Ba/F3 cells on IL-3. To further validate the secondary mutations identified in *c-kit*, resistance screens using mouse IL-3-dependent Ba/F3 cells transfected with the *c-kit* mutant constructs might serve as an excellent model system for characterizing the TOC-resistant mutations.

We concluded that the described mutations are responsible for the altered binding affinities. While the trend suggests that these observations largely correlate to growth inhibition *in vitro*, there are many other factors not controlled for in a cell culture system. To make a more direct comparison between drug binding and inhibition of KIT activity, further *in vitro* confirmation by binding assays or activity assays using purified protein is warranted. Finally, pKIT was shown to be a practical biomarker of target modulation for KIT TKIs. This is a rational marker by which to identify resistance in relapse biopsies in order to investigate mechanisms of resistance in tumor samples and compare the clinical relevance of the mechanisms described in these preclinical studies. Moreover, serial pharmacodynamic

assessment of patient samples while on treatment will allow better monitoring of patient response and early identification of acquired resistance so that selection of the most appropriate second line therapy can be made.